ASSESSING FLOODING AND RAINWATER HARVESTING IN KAIAKA BAY WATERSHED, OʻAHU, HAWAIʻI

A THESIS SUBMITTED TO
THE GLOBAL ENVIRONMENTAL SCIENCE
UNDERGRADUATE DIVISION IN PARTIAL FULFILLMENT
OF THE REQUIREMENTS FOR THE DEGREE OF

BACHELOR OF SCIENCE

IN

GLOBAL ENVIRONMENTAL SCIENCE

MAY 2013

By
Kelly-Rose L. Lariosa

Thesis Advisor

Dr. Aly El-Kadi

I certify that I have read this thesis and that, in my opinion, it is satisfactory in scope and quality as a thesis for the degree of Bachelor of Science in Global Environmental Science.

THESIS ADVISOR

____

Aly El-Kadi
Department of Geology & Geophysics

ACKNOWLEDGEMENTS

I would like to express my deepest thanks to my thesis advisor, Dr. Aly El-Kadi for his direction, patience, and support. This opportunity and his expertise in hydraulic and hydrologic modeling have helped me to improve my research and scientific writing skills, as well as prepare me for other challenges. I would also like to extend my thanks to Dr. Russell Yost for his guidance and assistance with an important portion of this project.

I am grateful and fortunate to receive the constant support and encouragement from my family and friends throughout this journey, which has helped me to successfully complete my project work.

ABSTRACT

The purpose of this project was to assess potential flood control through water harvesting in Kaiaka Bay Watershed (KBW) located in north central O‘ahu, Hawai‘i. Rainwater harvesting not only provides the benefit of helping to meet the fresh water demand through periods of drought or summer seasons, but the system also diminishes the downstream energy from surface runoff during extreme precipitation events.

Water harvesting can be achieved through the implementation of flood retention basins and groundwater-recharge injection wells. Modeling was used in the analysis by two software programs, the Watershed Modeling System (WMS), a model user interface combining a number of watershed models, and WELL, a simple groundwater analytical model. Within WMS, the watershed models used were HEC-1, for flood simulations, and HEC-RAS for flood zone delineations. Site models were developed to test the success of the harvesting system. First, HEC-1 was calibrated through comparing observed and simulated streamflow from five dates of precipitation—3/2/12, 3/4/12, 3/24/12, 4/27/12, and 1/5/13. Two different data sets of rain distributions were employed and compared. Values for HEC-1 model-parameters were initially attained based on reviewed literature of a 2008 storm calibration. The parameters were then adjusted to achieve the best fit between observed and simulated data. Next, the model HEC-RAS was used in assessing flooding zones based on streamflows estimated by HEC-1 under a number of scenarios. Cases with and without harvesting were compared. The assessment included delineating floodplains and estimating flood levels. Each delineated floodplain was compared to areas delineated by the Federal Emergency Management Agency (FEMA), based on a 100-year flood analysis. Finally, the WELL model was

used to determine how water table levels could be affected through artificial groundwater recharge from ten injection wells in each of four hypothetical flood basins.

Modeling results showed inaccuracies regarding streamflow, and when compared to FEMA's zones, seemed to overestimate flood depths produced from surface runoff under conditions of heavy rainfall. With the application of the harvesting system, the model showed a depth reduction of nearly seven feet in areas of the floodplain that generally exhibit the greatest impact from flooding. One third of streamflow predicted by HEC-1 showed the best match with the FEMA flood zones.

Inaccuracies were due to the lack of data and accurate parameters, but the results were acceptable for an initial assessment of water harvesting in KBW. In addition to watershed parameters, the results were sensitive to rainfall data, including amounts and distribution, which requires site rain gauges. The results generated from the WELL model showed an increase of up to about 7 feet in the water table level, a welcome contribution to water resource sustainability. A detailed and site-specific groundwater model should be used in future assessments.

TABLE OF CONTENTS

.

LIST OF TABLES

LIST OF FIGURES

LIST OF ABREVIATIONS AND SYMBOLS

Agencies

USGS	United States Geographical Survey
FEMA	Federal Emergency Management Agency

Project Site & Other Descriptions

KBW	Kaiaka Bay Watershed
BMP	Best Management Practices

Models & Other Data Acronyms

GIS	Geographic Information Systems
WMS	Watershed Modeling System
HEC-RAS	Hydrologic Engineering Centers River Analysis System
HEC-1	Hydrologic Engineering System-1
DEM	Digital Elevation Model
NAD83	North American Datum 1983
CN	Curve Number
SCS	Soil Conservation Service
TOPAZ	Topographic Parameterization Program
RS	Storage Routing
RSVRIC	Reservoir Initial Condition
SQ	Known Outflow
SV	Known Volume
SE	Known Elevation

United States Customary Units

cfs	cubic feet per second
ft	feet
ft^3	cubic feet
km	kilometer
m	meter
mm	millimeter
s or sec	seconds
min	minutes
mi^2	square miles

1 INTRODUCTION

1.1 KAIAKA BAY WATERHSED & FLOODING

Watersheds are vital and resourceful landforms—not only do they sustain life, but they can also be aesthetically pleasing. The health and quality of a watershed are fundamental to maintain for these reasons. Studies regarding the components of watersheds and factors that affect them have stimulated the finding of ways in which they can be best maintained.

The particular geography of a watershed consists of an area of land that obtains water in any form and ultimately drains into a common water body, such as a stream, lake, or ocean (Yost et al., 2009). In Hawai‘i, some of the same general concepts of watersheds are also applied to the ahupua‘a system—a land division that extends from the mountains to the sea. Throughout ancient Hawai‘i, an ahupua‘a usually held all the natural resources that the island populations relied on for subsistence.

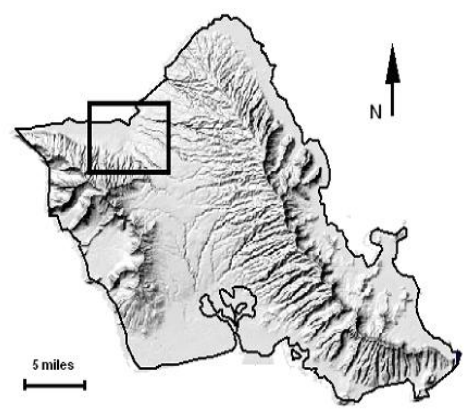

Figure 1.1 Project location: 21° 33' 8” N 158° 7' 44” W NAD 83 west (USGS seamless data distribution system, April 13, 2005)

The specific site for this project, Kaiaka Bay Watershed (KBW) is located in north-central O‘ahu, Hawa‘i (**Figure 1.1**) and is bounded by two mountain ranges—the Wai‘anae Range on the west and the Ko‘olau Range on its east periphery (Yost et al., 2009). The 20,800-hectare watershed is subdivided into four main sub-watersheds—Opaeula, which resides the furthest to the north, Kaukonahua, which is situated at the southernmost end, and Helemano and Poamoho, which are located Poamoho, which are located in between these regions (**Figure 1.2**).

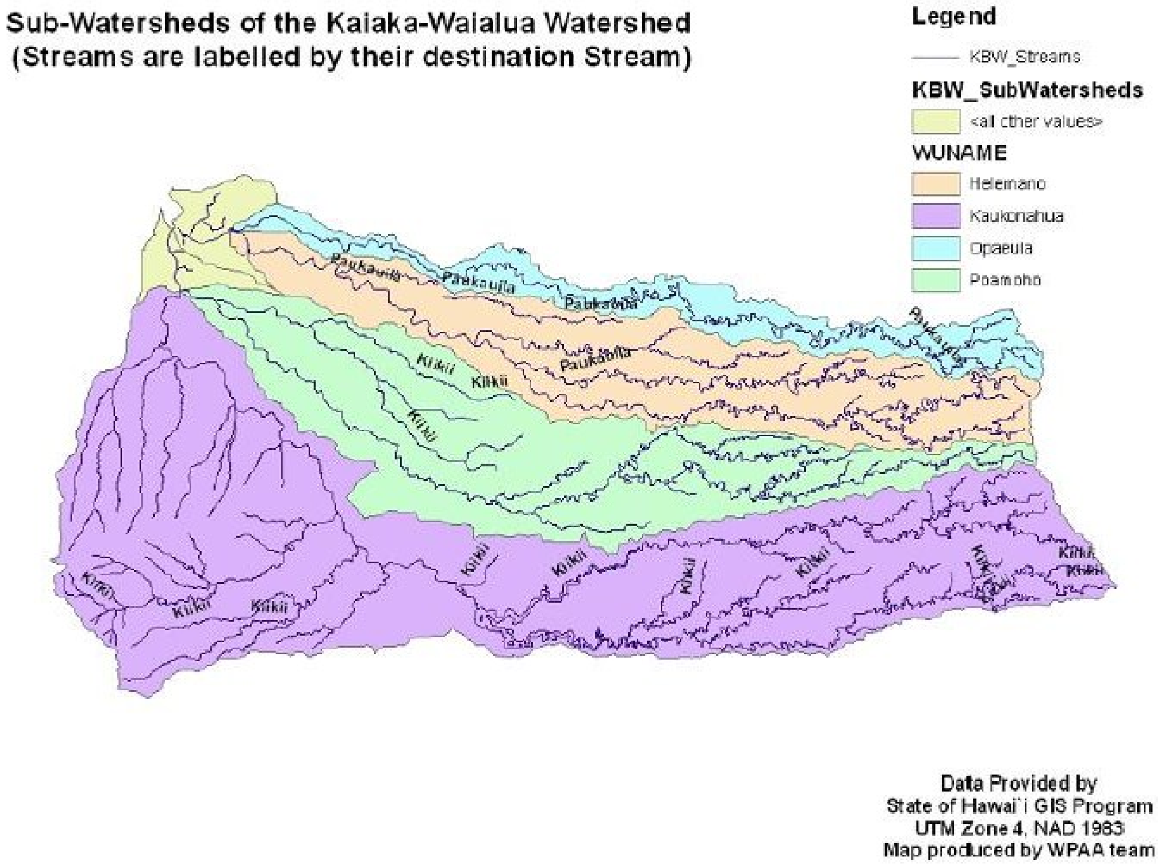

Figure 1.2 Sub-watersheds of KBW, whose streams drain into Kaiaka Bay (from Yost et al., 2009)

Kaiaka Bay Watershed is diversified in land use—most of the land (56%), is allocated for agriculture, 37% is preserved for conservation, and the remaining 6% is urban land (Yost et al., 2009). Approximately 45,000 people reside in the urban regions of KBW. Most of this population is located within the areas of Wahiawa-Schofield Barracks and Waialua-Haleiwa (Hawai‘i Dept. of Business and Economic Development, 2000). The bay area is a popular site for many recreational activities such as boating, fishing, crabbing, surfing, and swimming (DeVito et al., 1995).

Over time, occurrences of strong storms and hurricanes have generated several events of severe flooding which have greatly affected the residents of this area and the overall quality and health of the watershed. Given its proximity to the coastline, many residents of KBW are situated in an environment with a high risk of sea level rise, tsunamis, and floods. During past heavy precipitation events, flooding in KBW has caused insurmountable property damage and a few fatalities.

In the Waialua-Haleiwa district, flooding usually occurs in areas with low-elevations, generally less than 30 feet (Yost, et al., 2009). Furthermore, the steep terrain in the upper portion of the watershed generates turbid storm runoff and short concentration periods. Kaiaka Bay receives a substantial 86% of runoff from four drainage areas of the entire hydrologic unit's surface area, while the remaining 14% flows into Waialua Bay (Giambelluca et al., 1986). **Figure 1.3** encompasses these two bays and the Haleiwa and Waialua districts.

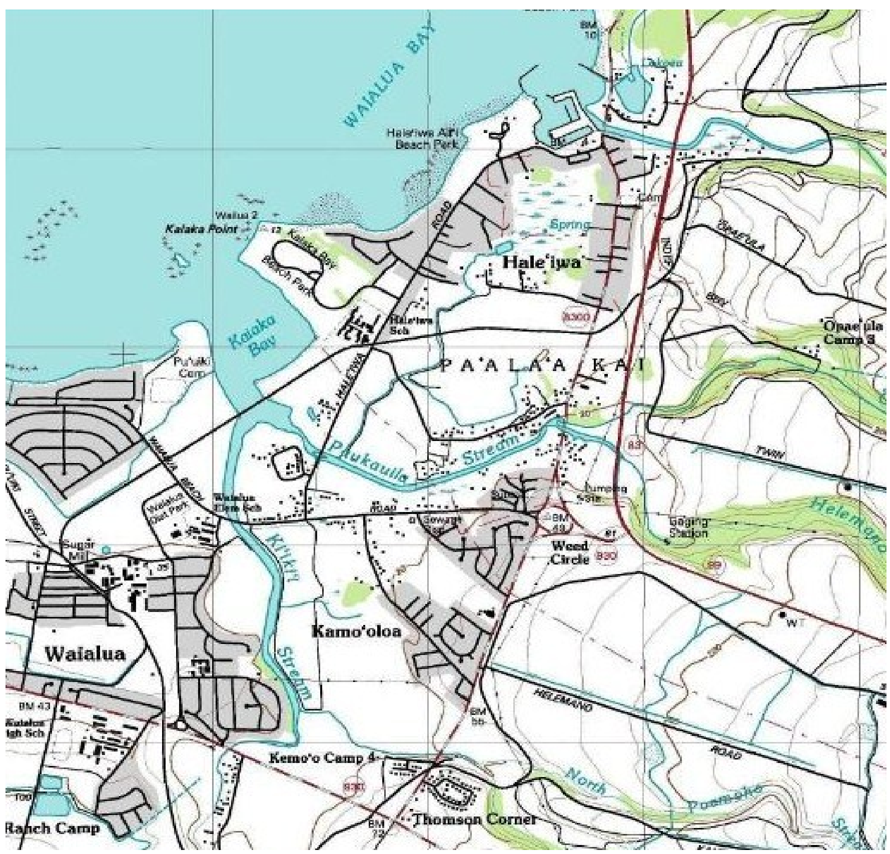

Figure 1.3 Waialua-Haleiwa district & bays

On O‘ahu, storms that often bring very aggressive winds and torrential rains are most prevalent from October through March. Annually, anywhere from two to seven of storms in this category will occur (Blumenstock & Saul, 1967). Near Kaiaka Bay, the median annual rainfall is approximately 30 inches. As you move leeward towards the crest of the Ko‘olau mountain range, rainfall can exceed 275 inches (Giambelluca et al., 1986).

1.1.1 FLOODPLAINS

Comparable to many communities, the districts that are situated closest to Kaiaka Bay—Waialua and Haleiwa, are built on a floodplain, defined to be generally a flat area of land neighboring a river, stream, or ocean. Hence, they are very prone to flooding events. Historically, although flooding in communities built on such land types has posed an obstacle, societies are constructed upon floodplains for many reasons: development on flat land is far less complicated than building on any other type of terrain, there is an ease of transportation and access to freshwater, and floodplains are proficient in facilitating agriculture (Powell, 2009). With proper management, extreme flood events can be moderated. However, high costs associated with land prices and construction expenses can be a major hurdle.

1.1.2 COMPONENTS OF FLOOD MANAGEMENT

Managing flooding is necessary for communities built on flood prone regions, and there are many variables that need to be taken into account when employing such management. Efficacy requires examining elements that reach further than the applications of technology and engineering.

One of the variables linked to flood management includes understanding people's influence on flood prone environments and ecosystems. For instance, traditional river management has generally aimed towards reducing natural irregularities in flows in order to regulate extreme conditions such as droughts and floods. When this variability in river flow is altered excessively, changes in the biogeochemical conditions and functions of an ecosystem can be expected to ensue, causing the degradation of that ecosystem, consequently having a detrimental effect to both society and biodiversity (Richter et al., 2003). Such practices are not expected to be effective in KBW due to land use, land cover, and topography.

An additional component that facilitates effective flood management is community involvement. Collaborative exchanges among the participants involved in making water management decisions and the community members who are affected make it easier to reach the consensus required for the development of sustainable water management. Throughout this discourse, needs, preferences, regulations, and limitations should be expressed in order for goals to be set and reached (Richter et al., 2003). An understanding of the aspects tied to flooding by these parties can bring about the greatest potential in best management practices (BMP's). The study by Yost et al. (2009) documents efforts adopted in integrating community's activities into managing floods and other water problems for the KBW.

1.2 FLOOD RETENTION BASINS & GROUNDWATER RECHARGE INJECTION WELLS

Flood retention basins and groundwater-recharge injection wells have been utilized in efforts to manage and minimize flooding and sustain groundwater levels. This water harvesting system functions as a single unit and is operated to efficiently manage runoff. As a recent development towards flood management, this artificial recharge technology has presented many benefits. (For brevity, the term flood basin will be used throughout the report to describe the whole harvesting system).

This facility essentially allows water to be collected and routed. The flood retention basin is positioned upstream of a dam which extends to the terminus of the dam's spillway. The flood basin serves the purpose of collecting and storing water, as well as to exhaust downstream energy from surface runoff. A spillway near the top of the dam permits the controlled outflow of water from the basin when water volume exceeds the basin's capacity. This overflow then gets routed to an area downstream. At the bottom of each basin, injection wells are assembled to inject the stored water into the ground, hence recharging the groundwater aquifer. **Figure 1.4** illustrates a cross-sectional sketch of a flood retention basin, the spillway crest, and injection wells.

Comparable to any technology being introduced into a new environment, this implementation faces challenges. A few of these drawbacks are related to finding ideal locations within the watershed and the high costs of implementation, which can be prohibitive, as will be shown later in this study. However, the benefits are ultimately invaluable reduction of property damage, injuries, and fatalities.

It is crucial to assess the total expenses involved in implementing harvesting systems in KBW. The overall price can be expected to be very high. The cost of land on O'ahu is fairly expensive and availability is limited. Regarding construction, contractor prices vary in different areas but costs depend heavily on the site's conditions. Terrain characteristics determine the amount of land needed to be excavated. Excavation is usually the next largest cost factor involved after the price of land. Other expenses of water harvesting to be considered are the costs of land surveyance, labor, grading, associated equipment and materials, and maintenance (Curtis, Nelson, & Oakes, 2001).

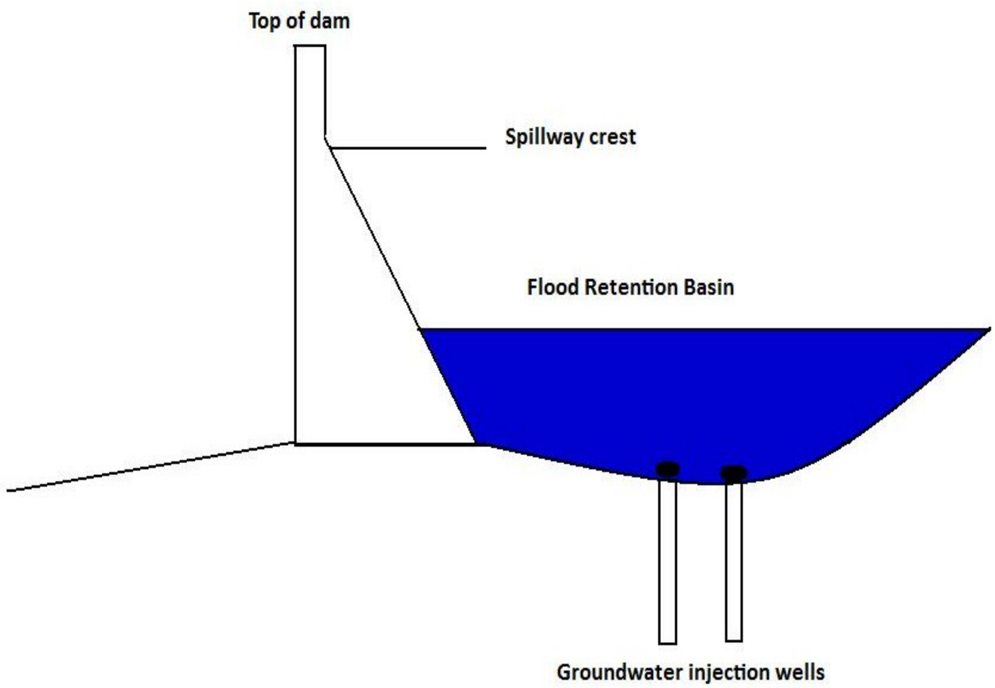

Figure 1.4 Schematic of flood retention basin system

1.2.2 CRITERIA TO CONSIDER FOR LOCATIONS OF STORAGE BASINS

A vital component of this project pertained to the quantity and locations of the proposed flood basins, where a considerable amount of factors needed to be taken into account. Components included the topography analysis of KBW, as well as the implementation of soil and land use coverage of the project site area. Factors that were contemplated regarding the most viable locations for the basins were as follows:

- Locations that would best minimize the risk of flooding,
- Areas of the watershed that receive the highest amount of rainfall, and consequently where the greatest catchment of surface runoff would occur,

- Locations with land coverage that would facilitate the implementation of retention basins,
- Type of soil, and
- Depth to the water table.

In addition, availability of land at the chosen locations is an important controlling factor.

1.3 PURPOSE

The objective of this project was to assess the feasibility of floodwater harvesting systems for use in minimizing flooding in KBW's floodplain region, as well as to analyze the expected level of groundwater replenishment. The design and potential efficiency of these structures was tested using the software programs Watershed Modeling System (WMS) and WELL. Hydrologic models of the area were developed with main tasks that included model calibration, delineating flood areas and flooding depth, as well as analyzing and interpreting the results. Both cases with and without harvesting were also compared. These results will help to assess if this technology has the ability to significantly reduce the risk of major flood events in KBW, and will also assist in estimating the costs and benefits of this development.

1.4 JEJU ISLAND & AQUIFER RECHARGE TECHNOLOGY

A working example of this proposed project for KBW has been developed in one of the nine provinces of South Korea—Jeju Island. With a length of 32 km and a 74 km width, Jeju Island is the largest volcanic island off the Korean peninsula, located 450 km south of Seoul. This island contains no perennial streams; hence its only source of freshwater is groundwater, which provides 95% of the water supply, making the conservation of this source for sustainable development on the island a necessity (Choi &

Lee, 2012). Hawai‘i is made up of a series of volcanic islands whose geological conditions are comparable to those of Jeju Island, with 80% of Hawai‘i's residents rely on groundwater for drinking (Muirhead, 2008). The population on O‘ahu is much greater and denser than that of Jeju Province, exemplifying that freshwater conservation efforts are even more crucial.

In 2007, the installation of ten artificial groundwater recharge injection wells (each with a 50 m depth and 400 mm diameter) on Jeju Island have shown the implementation of this modern technology to be a beneficial product of freshwater management. Before the implementation of these injection wells, the supply of fresh water was made available mainly through other methods of harvested rainwater, wells dug out by hand, and naturally flowing springs (Lee et al., 2007a). The establishment of this system has helped to meet the increasing freshwater demand on Jeju Island (Kim et al., 2008). With the facilitation of these injection wells, 695,000 m^3 of rainwater was injected into 81 of these types of wells as of 2009. This volume is equal to the annual water use of 5,600 people (Choi & Lee, 2012). These outcomes from Jeju Province establish the potential that this artificial recharge technology has for Hawai‘i.

1.5 WATERSHED MODELING SYSTEM & WELL

The Watershed Modeling System (WMS) is a model user-interface built to support elements of hydrologic modeling needed for this study. This software provides tools to conduct various modeling processes, which include automated watershed delineations, geometric parameter calculations, floodplain mapping, and storm drain modeling (Scientific Software Group, 1998). WMS supports many computational numerical models. For this project, the HEC-1and HEC-RAS models within WMS were used for the purpose of delineating the sub-basins, calibrating HEC-1, estimating streamflows, simulating retention basins, and demarcating the final floodplain. Details of WMS can be viewed at http://www.aquaveo.com/wms.

HEC-1 is a watershed model designed to simulate surface runoff of a river basin from a single storm event. It includes several options for modeling rainfall, unit hydrographs, stream routing, and losses. The results of the HEC-1 modeling process mainly include streamflow hydrographs at specified locations within river basins (Scientific Software Group, 1998).

HEC-RAS is a model designed by the U.S. Army Corps of Engineers Hydrologic Engineering Center and is a one-dimensional model designed to compute steady flow water surface profiles, unsteady flow simulations, and movable boundary sediment transport (Aquaveo, LLC, 2012). HEC-RAS also analyzes step backwater curves for steady state or ephemeral conditions in order to determine water surface velocities and elevations (Brigham Young University – Environmental Modeling Research Laboratory, 2006).

WELL is a simple groundwater model, based on the Theis (1935) analytical solution that is used to estimate aquifer response to well pumping or injection under ideal conditions. With the utilization of such a model, the impact on groundwater in KBW from the injection wells can be determined. The model's input information includes transmissivity, storativity, number of pumping or injection wells and observation points, and the flux rate from the wells. The model predicts water levels at different times after the start of pumping or injection at selected observation points and on a grid for plotting purposes. In the current study, the plots illustrate the spatial rise in the groundwater aquifer in response to injection.

1.5.1 OTHER APPROACHES TO HYDROLOGIC MODELING

There are various software programs other than those within WMS that exist for hydrologic modeling and can also be used to carry out the same functions as the ones used in this project. Hydrologic simulation models can differ depending on the specific hydrologic components being simulated in the model. There are a number of alternative programs that can be utilized to examine the elements of flooding given that they have the commonality of being able to assess potential impacts of all water resources in different environments. These include ArcView Generalized Watershed Loading Function (AVGWLF) (Evans et al., 2002; Haith & Shoemaker, 1987), Nonpoint Source Pollution and Erosion Comparison Tool (N-SPECT) (Climate Adaptation Knowledge Exchange, 2013), Soil and Water Assessment Tool (SWAT) 2000 (Council for Regulatory Environmental Modeling, 2009), and MIKE FLOOD (MIKE by DHI, 2011).

For groundwater modeling to assess aquifer response, and in addition to analytical solutions, numerical models, such as WellFlo (Weatherford, 2013) and MODFLOW (Aquaveo, LLC, 2012), can be used to model, characterize, and predict different scenarios pertaining to wells. However, site specific data are needed for such analyses. An actual design plan for water harvesting should implement such models.

2 METHODS

2.1 SETTING UP A HYDROLOGIC MODEL OF KBW & IMPORTING DATA

The initial step of the project was to set up a hydrologic model of KBW using WMS. A shapefile, or geospatial vector storage format of KBW, was imported into WMS, and with GIS software, was superimposed onto a geographical map of the area. Other physical attributes of the model that would affect stormflow were also mapped onto the project area and consisted of terrain data, such as a digital elevation model (DEM) of KBW, and soil type and land-use coverage shapefiles.

Once pertinent data and terrain coverage had been entered into the model, flow accumulations and flow directions were computed in order to create streams by using the DEM. The program within WMS that carries out this specific computation is called the Topographic Parameterization Program (TOPAZ).

2.1.1 DELINEATING RIVER BASINS IN KBW

Following setting up the KBW hydrologic model, the model HEC-1 was calibrated by fitting observed and simulated hydrographs for a number of stream basins within KBW where measured streamflow data are available. Each of these basins is monitored by the U.S. Geological Survey (USGS), is given a station number, and is named according to the stream or reservoir it encompasses. Each station provides continuous measurements. For this calibration, stream discharge data (measured in cubic feet per second every 15 minutes) were acquired for several different dates of precipitation. **Table 2.1** summarizes the physical properties of each of these basins.

Table 2.1 Summary of physical properties of river basin stations monitored in KBW

Station Number	KBW River Basin/Station Name	Coordinates (Latitude, Longitude) (NAD83)
16200000	North Fork Kaukonahua Stream above Right Branch, near Wahiawa	21°30'58.6", 157°56'43.1"
16345000	Opaeula Stream near Wahiawa	21°33'44.4", 158°00'00.9"

Each stream basin needed to be delineated before the calibrations could be performed. A separate model for each basin was created so that certain parameters could be input individually. For each individual model, outlets were placed at each stream node, located just below the stream junction for that basin. **Figures 2.1** and **2.2** illustrate the delineations of the two river basins in KBW.

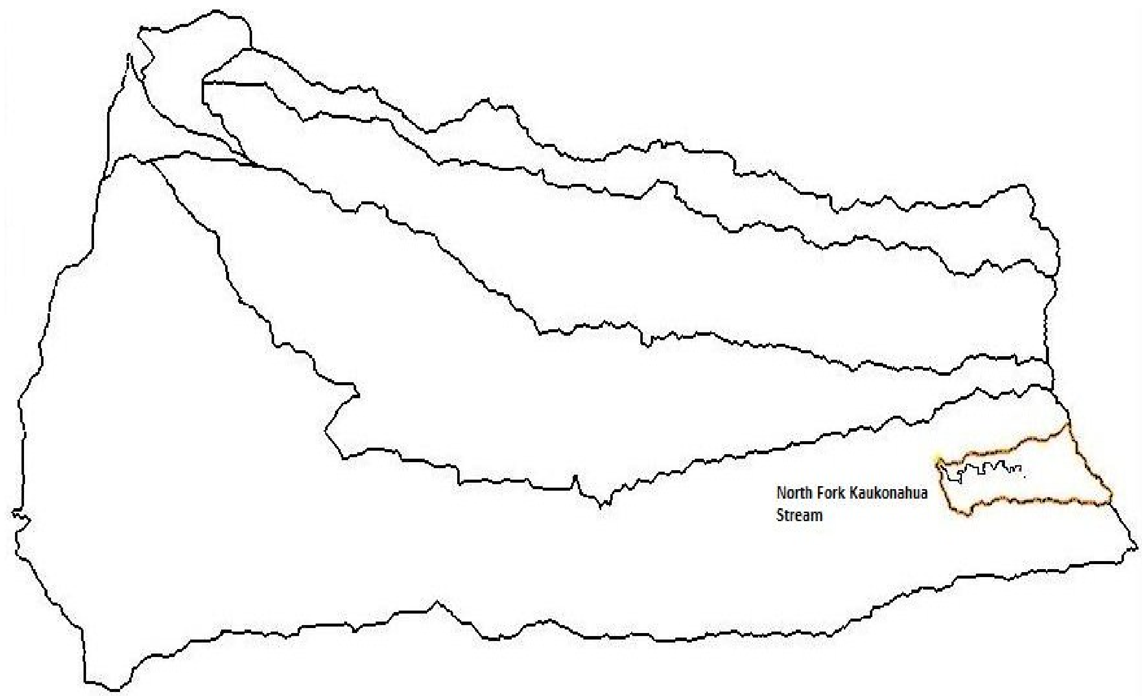

Figure 2.1 Delineated basin of North Fork Kaukonahua Stream above Right Branch, near Wahiawa

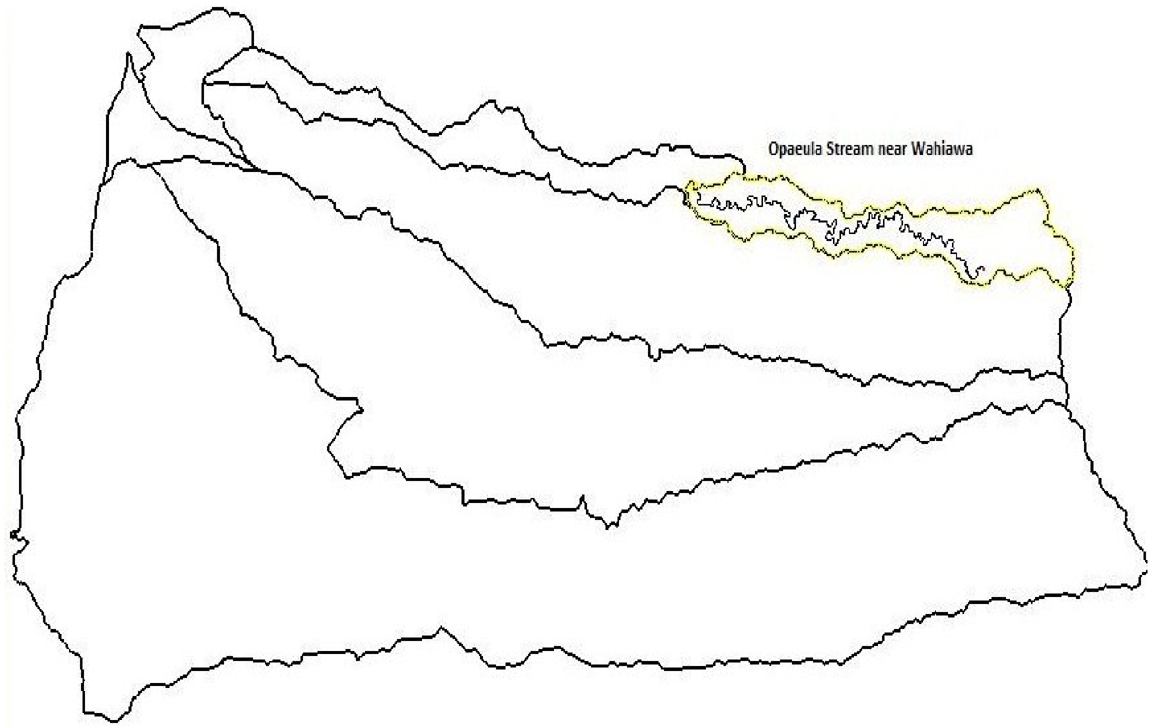

Figure 2.2 Delineated basin of Opaeula Stream near Wahiawa

2.1.2 ESTIMATING BASIN PARAMETERS & MODEL CALIBRATION

Subsequent to the basin delineations, their individual parameters could be estimated and assimilated into the model. A HEC-1 method called *Compute GIS Attributes* uses land and soil type terrain coverage, as well as a Soil Conservation Service Curve Number (SCS CN) to compute composite loss values of precipitation for each of the basins. A curve number is a coefficient that controls runoff potential after factors such as evaporation, infiltration, transpiration, and surface storage have been incorporated (United States Department of Agriculture, 1986). Curve numbers typically range from 30 to 100, where values in the lower range denote low runoff and higher numbers signify increasing runoff potential. Details and values of the SCS CN values can be viewed in Appendix A, **Table A-1**.

Some of the other basin information required for HEC-1 were *Basin Data, Loss Method, Unit Hydrograph Method*, and *Precipitation*. Relevant data for these were estimated through the process of the basin delineation. *Basin Data* included the area of each basin, and the *Loss Method* consisted of a surface runoff CN, which was estimated by using the land use/cover and soil type. Appendix A, **Table A-2** contains values for these calculated parameters.

Precipitation was one of the parameters that had the greatest influence on simulated discharge. Average precipitation for each basin was entered based on a 2008 calibration study (Yost et. al, 2009), and adjusted accordingly to obtain the best "fit" between observed and simulated data. Five days of precipitation were selected for the calibration process and were obtained from the USGS Hawai'i Streamflow data (http://waterdata.usgs.gov/hi/nwis/current). Measurements were acquired from the dates: 3/2/12, 3/4/12, 3/24/12, 4/27/12, and 1/5/13. These dates were selected because data prior to 2012 were not available for each of the basins. Furthermore, certain dates available for 2012 only provided daily mean discharge values.

A temporal distribution series was also required for HEC-1 to generate hydrographs. Measurements for each date were taken from the rain gage station/river basin 213215157552800/883.12 Poamoho Rain Gage No 1, near Wahiawa, O'ahu, HI; located at Latitude 21°32'01.9", Longitude 157°55' 17.0" NAD83. The distribution curves were expressed in time steps of 15 minutes, for a duration of 1425 minutes (23.75 hours). **Figures 2.3** to **2.7** show the temporal distribution curves for the dates used for the calibration.

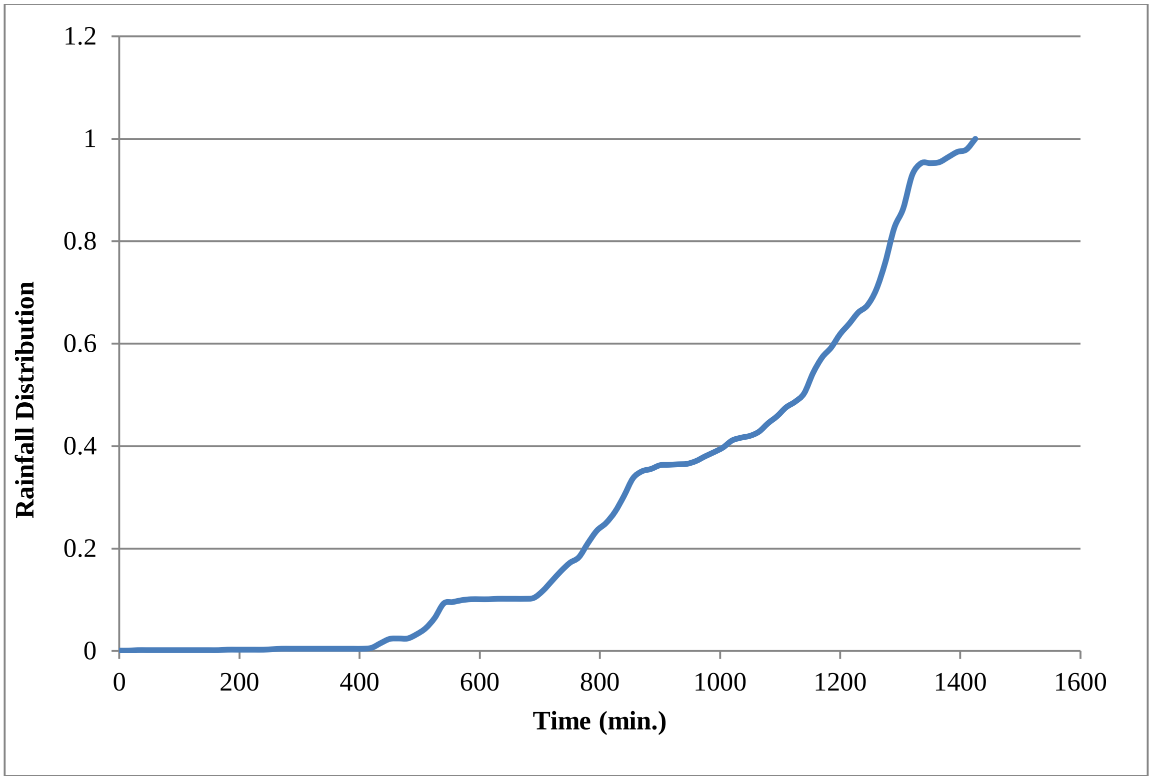

Figure 2.3 Distribution curve for 3/2/12

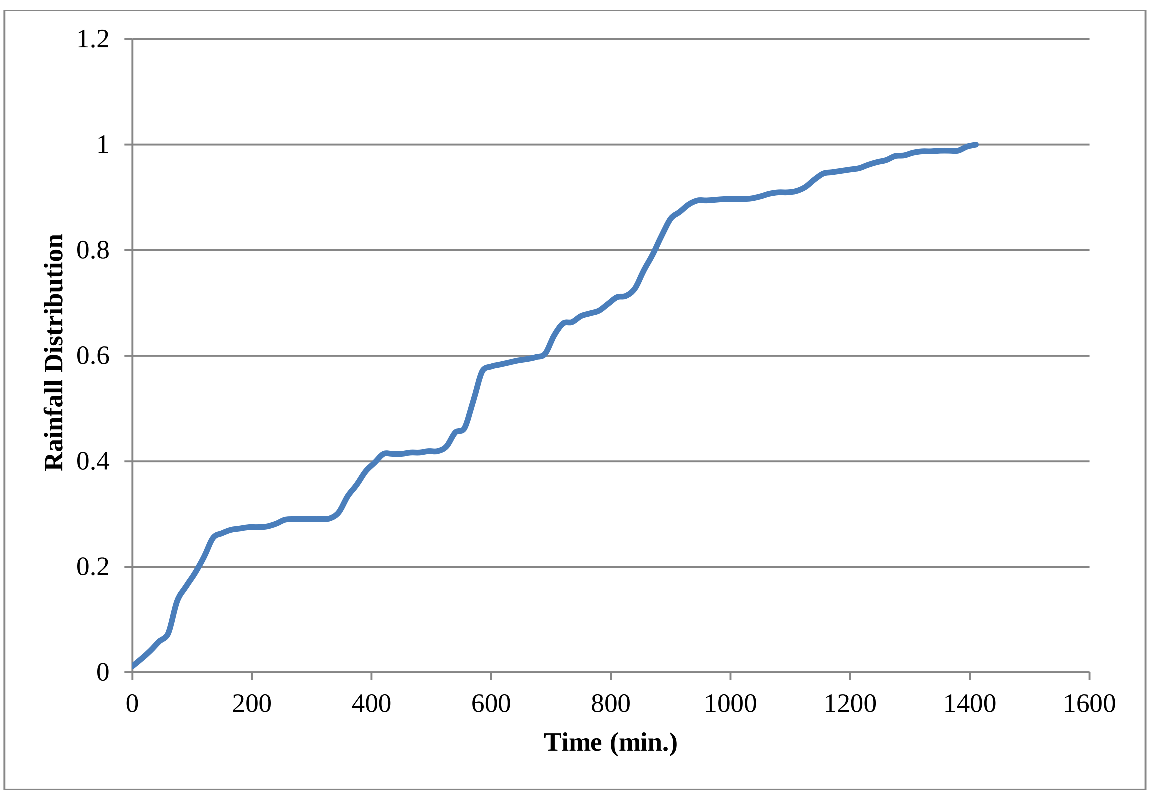

Figure 2.4 Distribution curve for 3/4/12

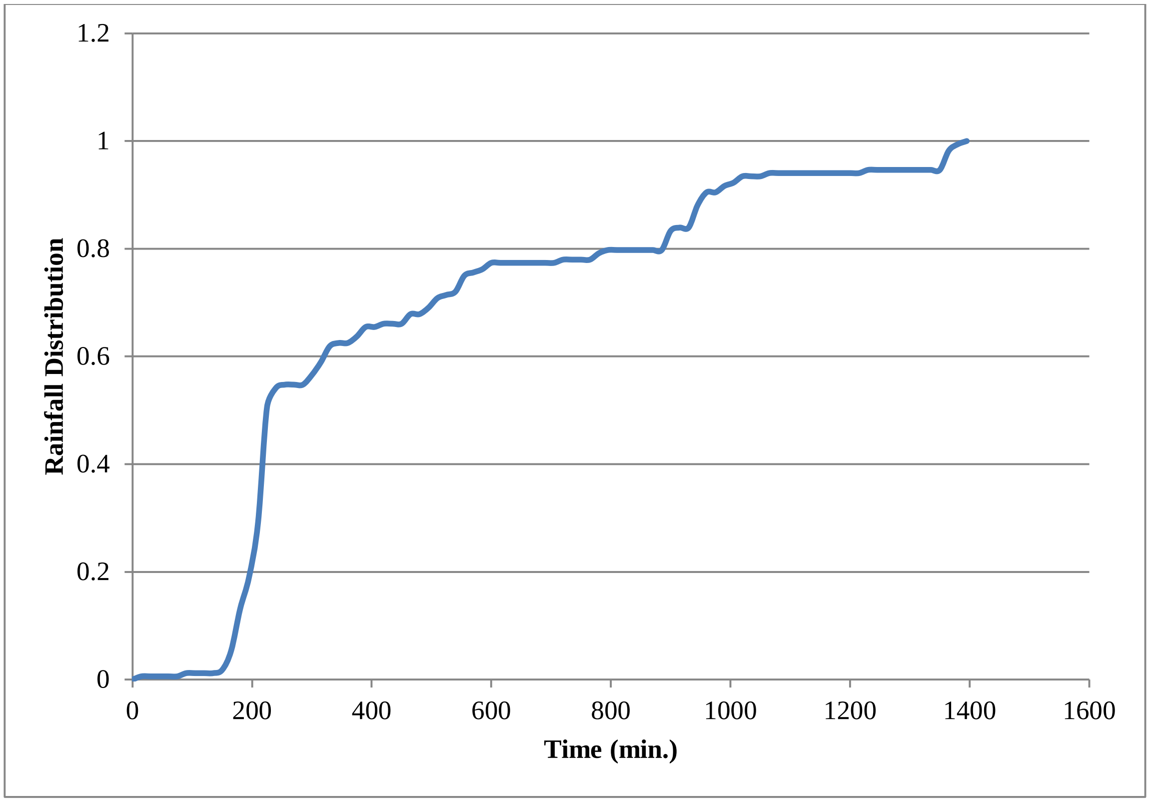

Figure 2.5 Distribution curve for 3/24/12

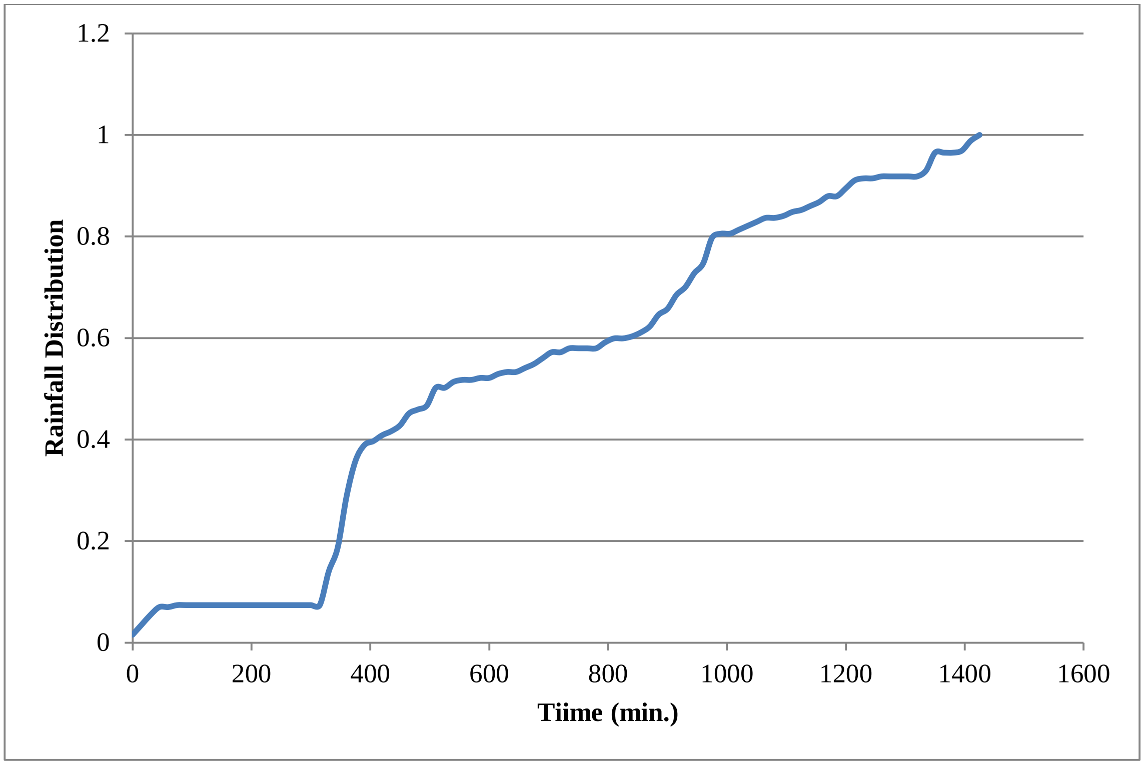

Figure 2.6 Distribution curve for 4/27/12

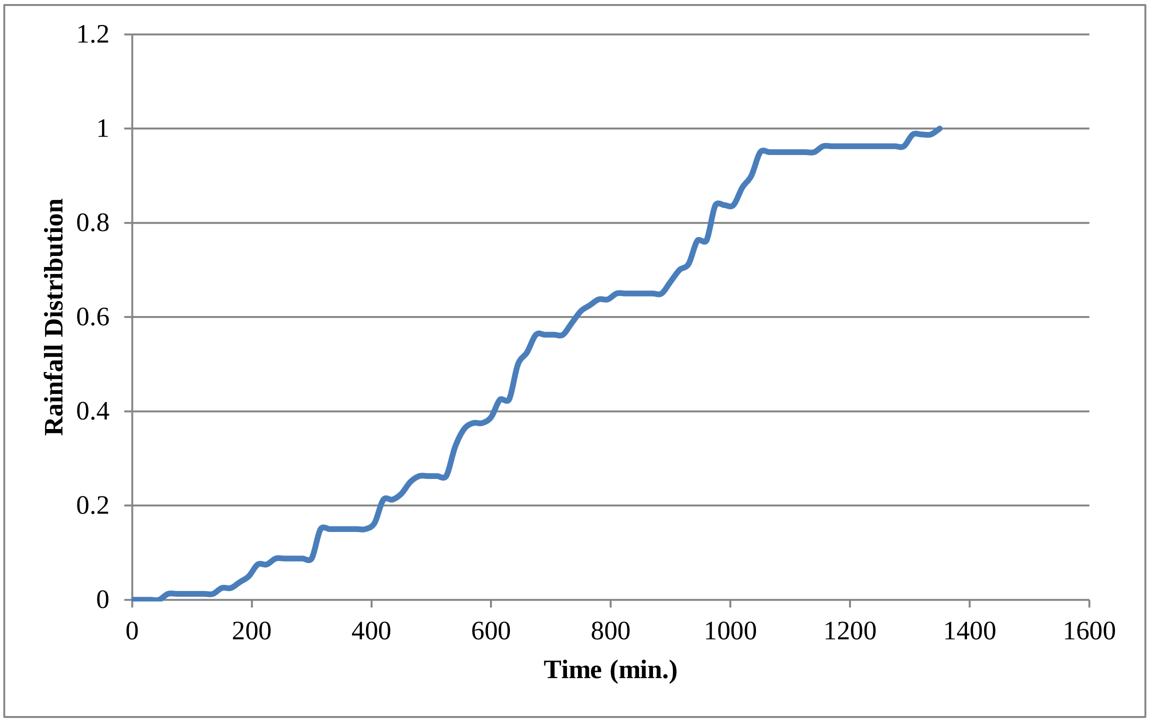

Figure 2.7 Distribution curve for 1/5/13

Simulation results were sensitive to the shape of the distribution curve. Unfortunately, only one rain gage was available, so the exact distribution over the calibration sub-basins was unknown. As an alternative, the available streamflow data for each sub-basin were used to derive new distributions that can be more representative of the actual distribution. That can be a reasonable assumption due to the expected linear behavior of the basins to rain storms because of the relatively small size of the sub-basins and the relatively short residence time. The distributions (**Figures 2.8** through **2.17**) were estimated by normalizing the accumulated streamflows relative to the total sum at the end of the storm. For both sets of rain distributions, parameters for base flow (occurs in the stream between storms when no rain occurs; without that, the stream flow is zero) were applied. Parameters of base flow include STRTQ, which indicates discharge at the beginning of the storm, while QRCSN denotes discharge below which base flow recession occurs. Different values for these parameters were used for each date in both distributions to obtain the best fit possible.

The final phase of the calibration was to generate the hydrographs by HEC-1, utilizing various data, which were then compared to observed hydrographs for stream discharge data. The goodness of fit was then assessed by calculating the root mean square error (RMSE) using the following equation:

Root Mean Square Error = $\sqrt{\frac{\sum_{i=1}^{n}(\hat{y}i - yi)^2}{n}}$

as well as the percent coefficient of variation: (Root Mean Square Error/average)*100.

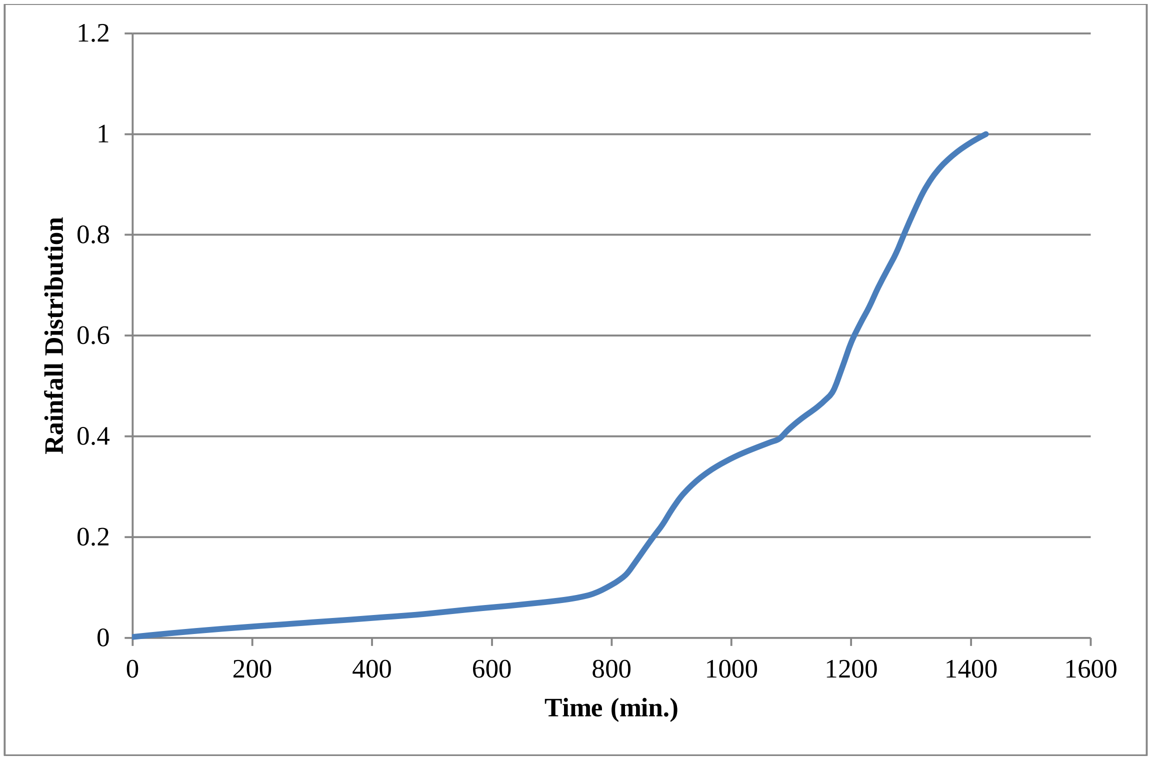

Figure 3.8 Rainfall Distribution for 3/2/12 for station 16200000

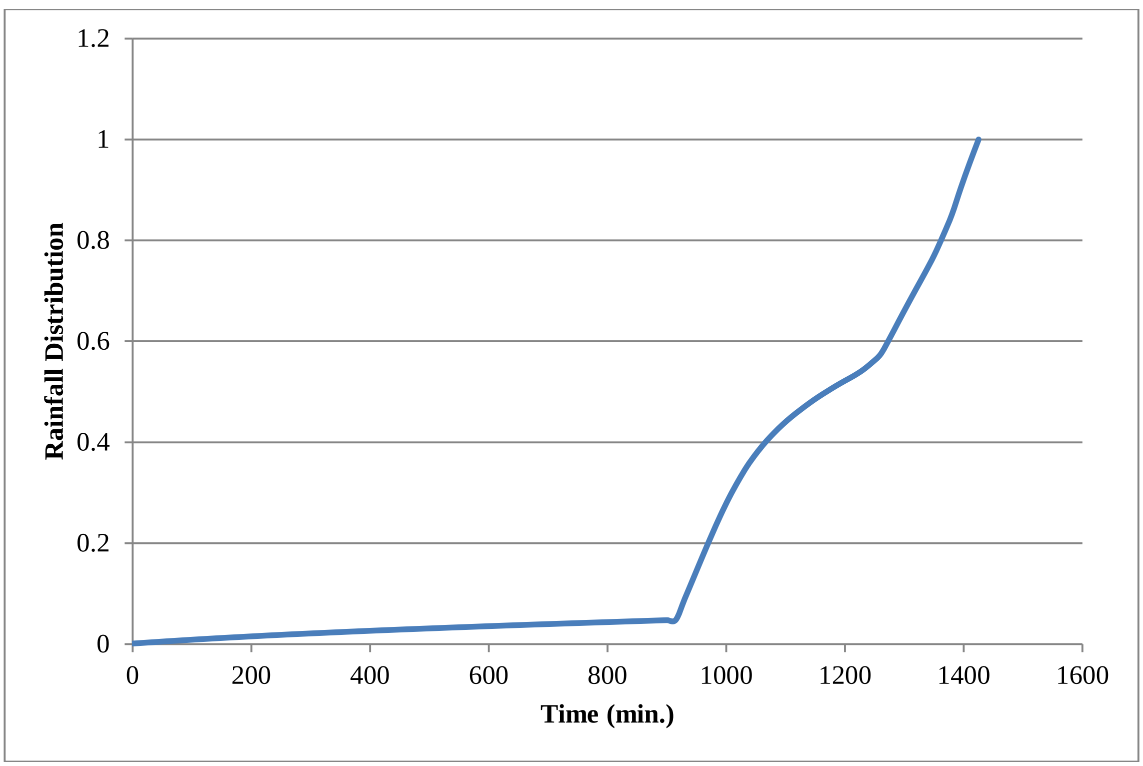

Figure 2.9 Rainfall Distribution for 3/2/12 for station 16345000

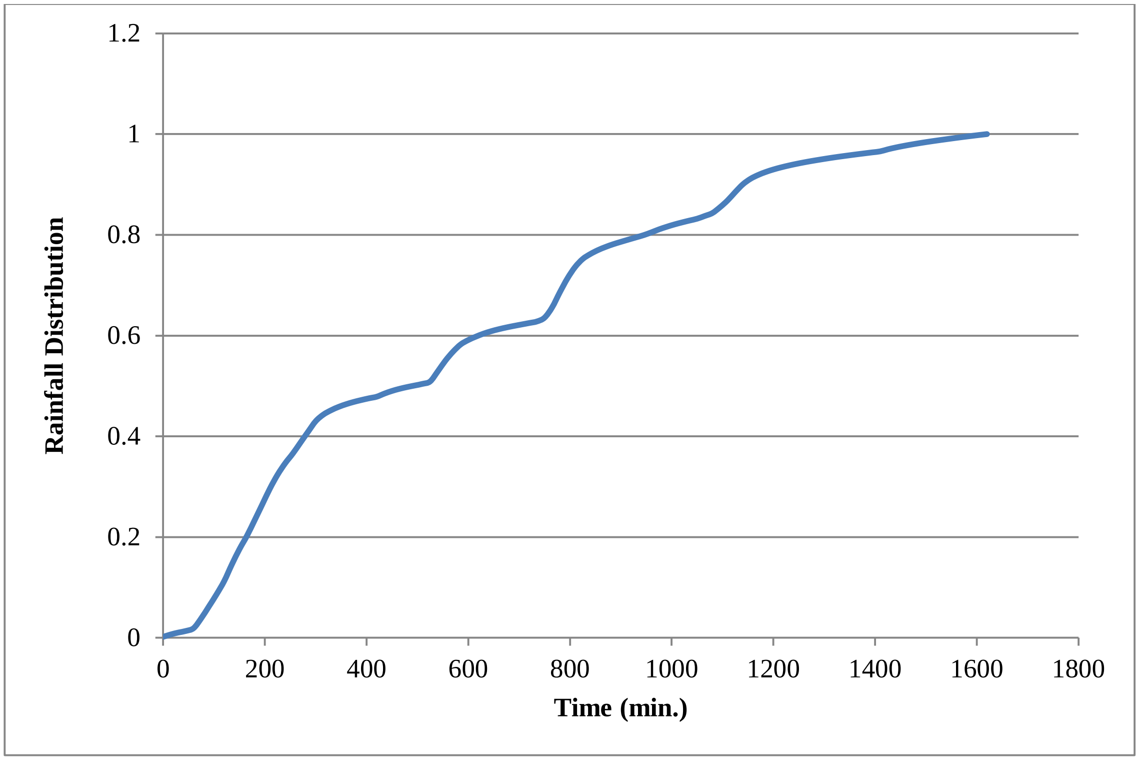

Figure 2.10 Rainfall Distribution for 3/4/12 for station 16200000

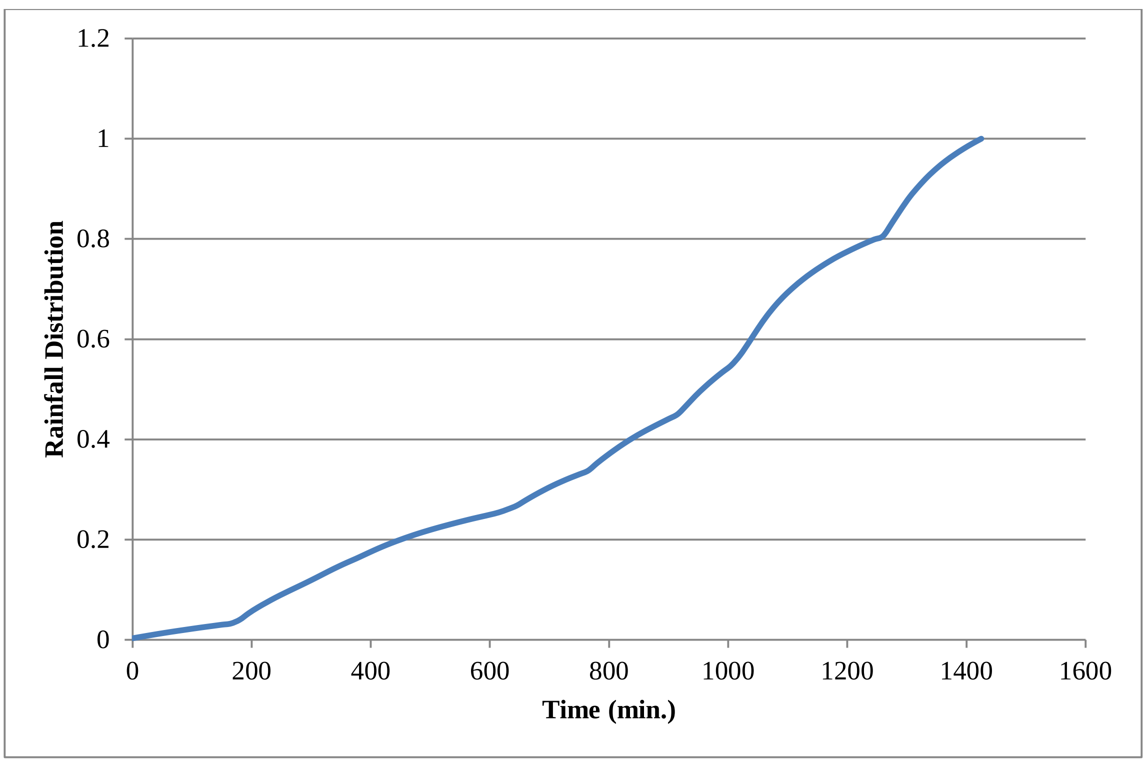

Figure 2.11 Rainfall Distribution for 3/4/12 for station 16345000

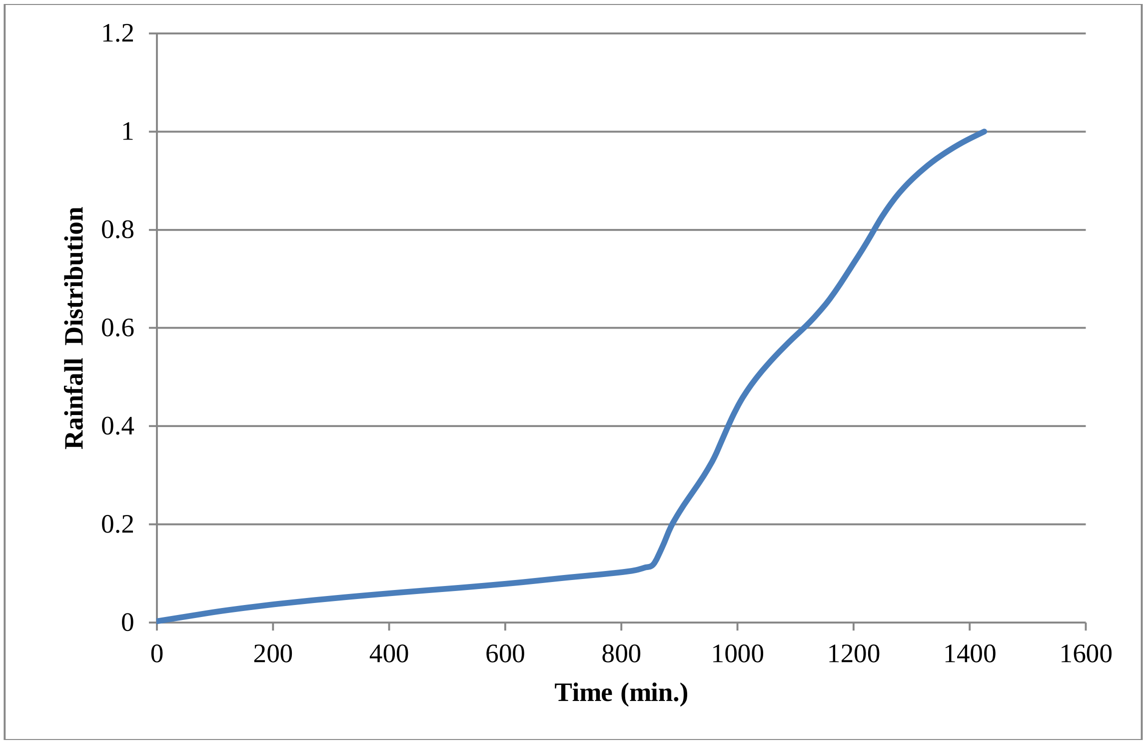

Figure 2.12 Rainfall Distribution for 3/24/12 for station 16200000

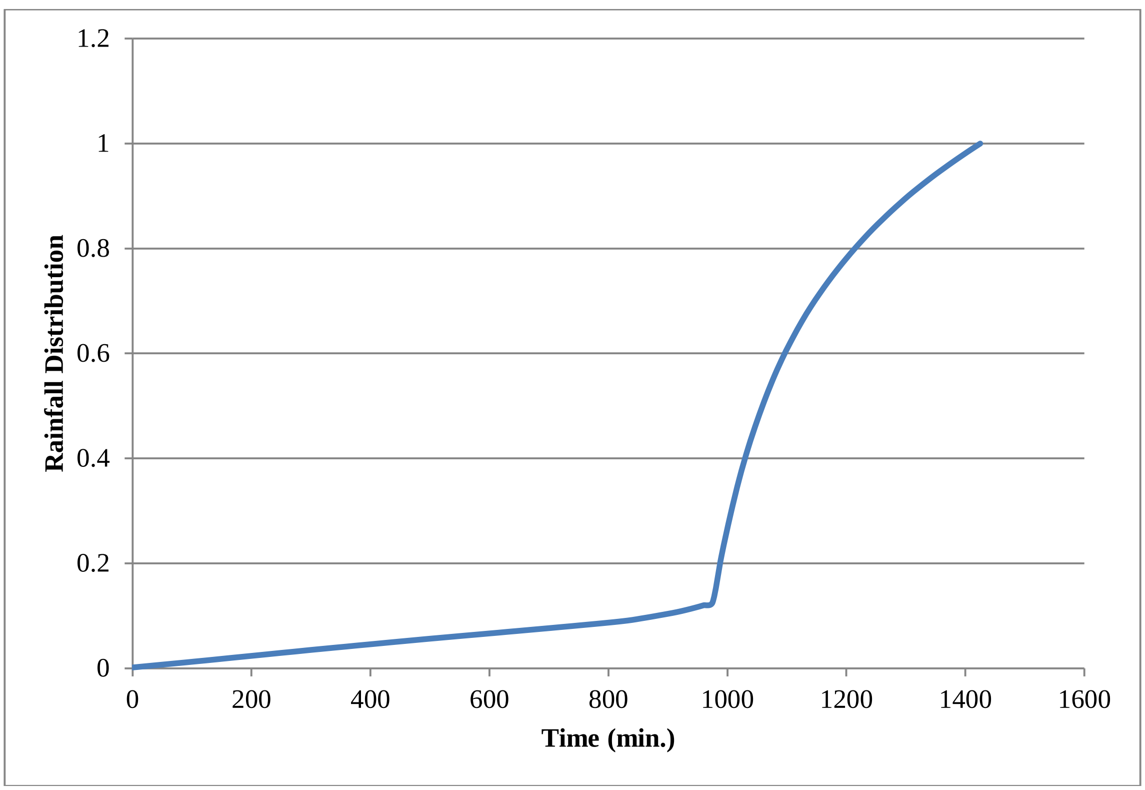

Figure 2.13 Rainfall Distribution for 3/24/12 for station 16345000

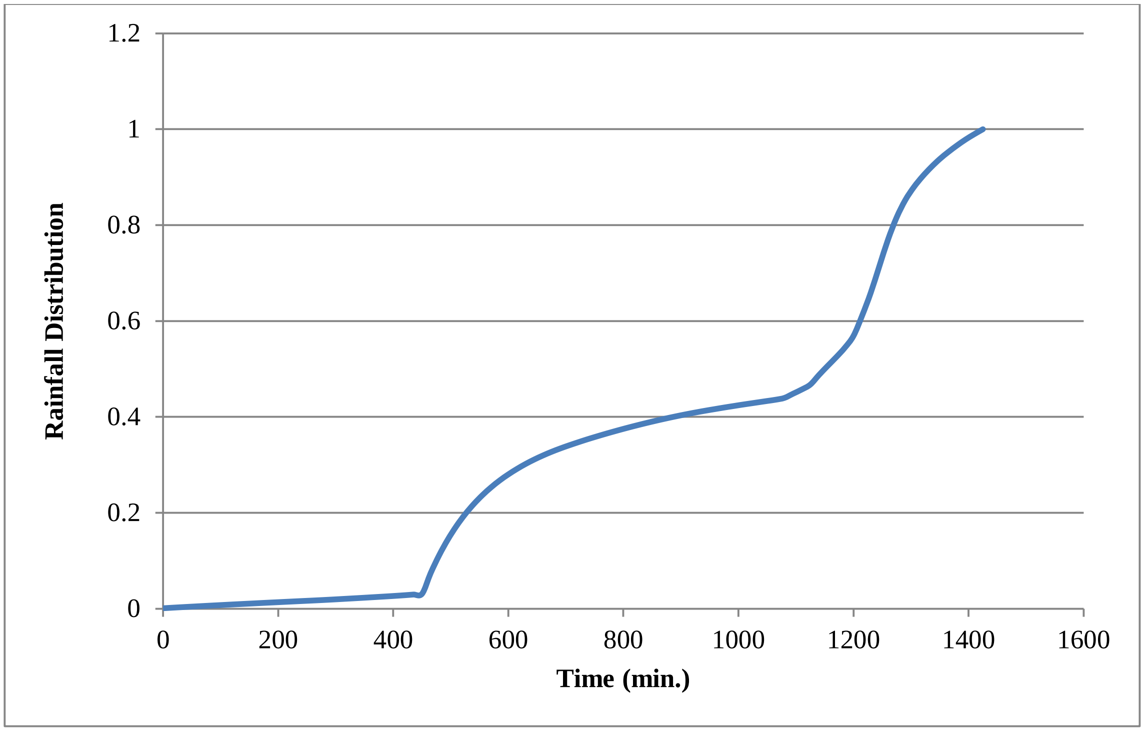

Figure 2.14 Rainfall Distribution for 3/24/12 for station 16200000

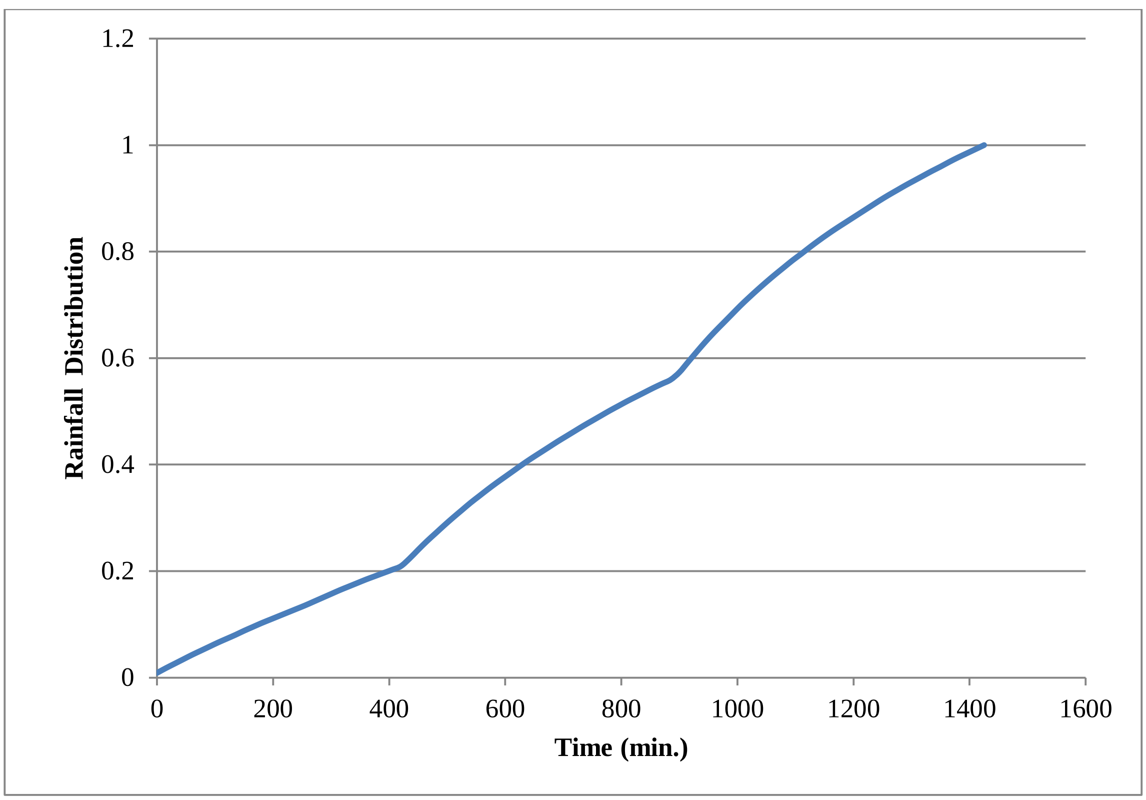

Figure 2.15 Rainfall Distribution for 3/24/12 for station 16345000

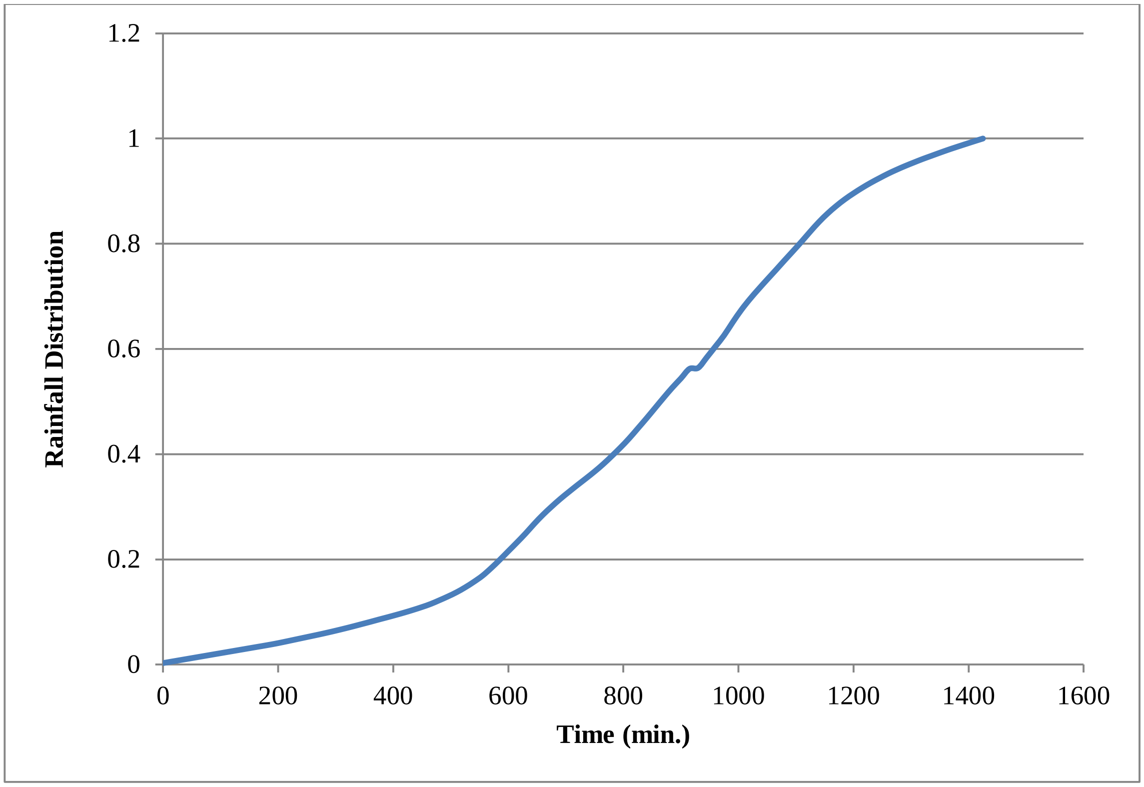

Figure 2.16 Rainfall Distribution for 1/5/13 for station 16200000

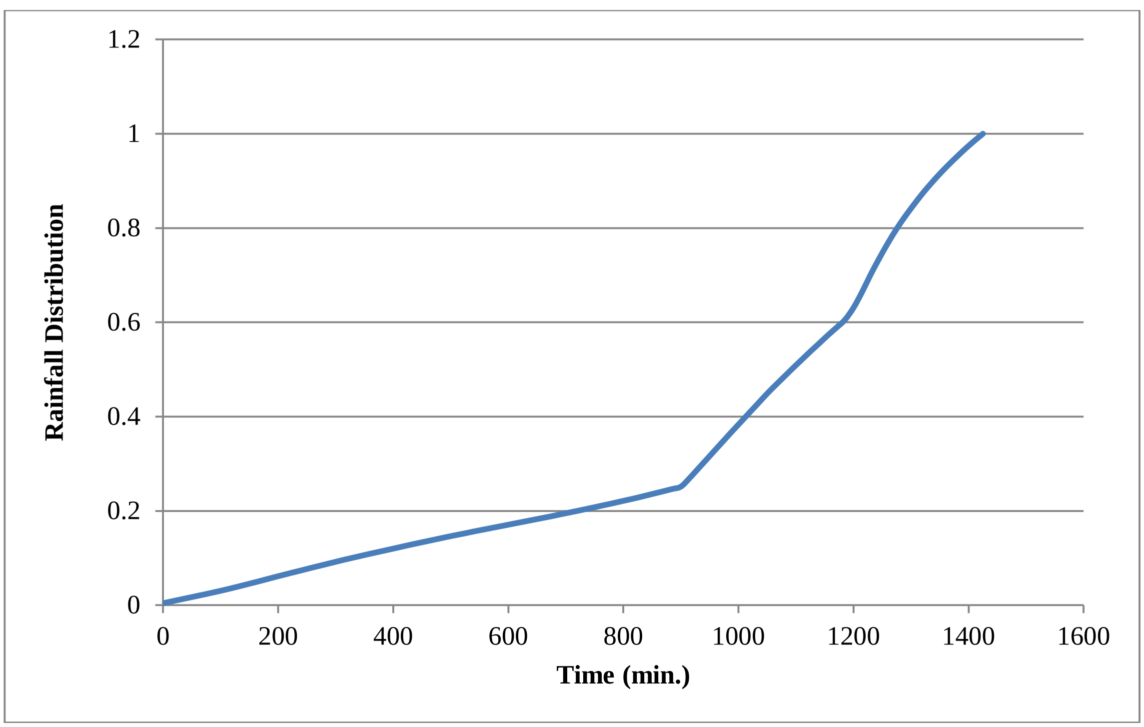

Figure 47 Rainfall Distribution for 1/5/13 for station 16345000

2.2 DESIGN OF FLOOD RETENTION BASINS

HEC-1 was also used in the second stage of the model in the design of hypothetical flood retention basins that were added to KBW. The objective was to assess streamflow in the watershed by comparing cases with and without the basins and the resulting flooding patterns. After considering the factors outlined above (Section 1.2.2), it was determined that four basins would be placed in the two inner sub-watersheds of KBW—Helemano and Poamoho. Two flood retention basins were designated to each sub-watershed (**Figure 2.18**). Locations for the structures were chosen on the geographical map that was superimposed onto the watershed model. These locations were based upon the fact that within KBW, flood basins in these areas would probably have the greatest effect on minimizing storm flow. Additionally, Opaeula is the smallest sub-watershed within KBW and is situated closest to the coast, therefore flood reduction in this sub-watershed is likely to be the least effective. The option of applying a retention basin in the largest sub-watershed, Kaukonahua, was disregarded due to the fact that a flood basin exists within that area—Lake Wilson. Also known as Wahiawa Reservoir, this flood basin was also included in the simulations. The flood basins were labeled as R1, R2, R3, R4, and R5 (**Figure 2.18**).

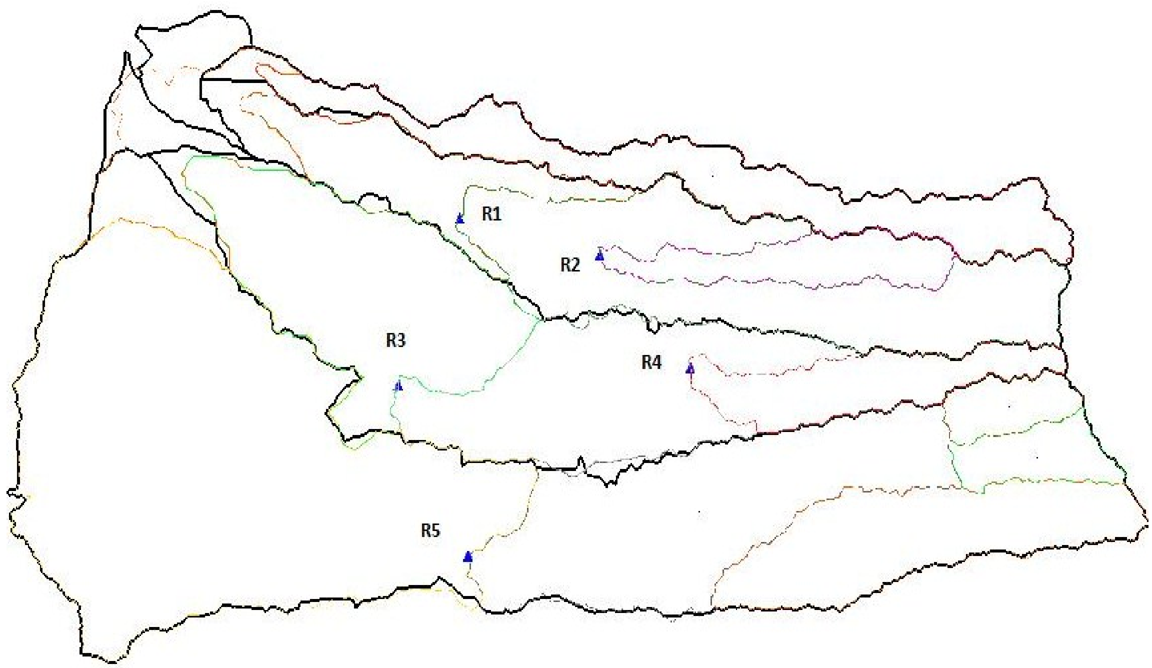

Figure 2.18 R1 through R4 are the locations of the hypothetical flood basins. R5 is the location of the existing Lake Wilson/Wahiawa Reservoir. The lighter line outlines the boundaries of sub-basins served by the flood basins.

The outlet tool in HEC-1 that was used to delineate the various sub-basins in KBW was also used to designate the locations for the four flood retention basins and Wahiawa Reservoir, which allowed HEC-1 to generate hydrographs at those locations through the utilization of pertinent data, similar to what was carried out in the first stage of the model. The generations of these hydrographs were intended to show the difference in streamflows with and without the flood basins. Following the process of adding outlets to the five locations, the *Add Reservoir* tool in HEC-1was used to define each of these locations to designate a reservoir for which relevant parameters could be applied.

2.2.1 PARAMETERS OF FLOOD RETENTION BASINS

Data pertinent to the flood basins were input by utilizing the Reservoir Data command in HEC-1. Information concerns hydrologic reservoir routing, or processes related to water storage in the reservoir and release through the spillway. The calculation method used is called HEC-1 Storage Routing (RS), which can be entered in one of three various ways: STOR-storage in acre-feet, FLOW-discharge in cfs, or ELEV-elevation in feet. For this project, the latter was used to define the *Reservoir Initial Condition* (RSVRIC), which represents the water level in the reservoir before the storm. For example, such a level would be the ground elevation at the bottom of the reservoir under a completely dry condition. This condition, which was assumed in the current treatment, represents an ideal case by allowing the largest possible reservoir-storage capacity. Elevations were assigned to various reservoirs based on local topography. For R5, elevation and additional parameters were based on the actual properties of Wahiawa Reservoir/Lake Wilson in Kaukonahua sub-watershed.

In order to completely define reservoir routing using HEC-1, reservoir volume-elevation data (SV vs. SE) and dam spillway-elevation outflow data (SQ vs. SE) were also needed for each retention basin. The SV-SE curve represents the relationship between the reservoir's volume of water and the water elevation. The SQ-SE curve represents the relationship between the spillway's discharge and the water-elevation. For flood basins R1, R2, R3, and R4, the relations are similar in shape for SV vs. SE by assuming that all the reservoirs have the same dimensions, only differing by the respective (local) elevations. Similarly, the relations SQ-SE are similar in shape by assuming that all the spillways have the same dimensions. The walls for each reservoir were given a 3:2 slope ratio and a total volume of 6.27×10^8 ft^3. The areas at the top and bottom of the reservoir were squares with areas of 7.6729×10^6 ft^2 and 6.25×10^6 ft^2, respectively. Each flood basin was assigned to have a height of 90 ft. **Figure 2.19** shows an illustration for one of the flood basins.

Figure 2.19 Illustration of one of the reservoirs

Just as the reservoirs were quantitatively paired to have the same RSVRIC, the outflow and elevation values used for R1 and R3 were the same, while the values for R2 and R4 were similar. With the parameters defined, HEC-1 was used to run simulations and obtain hydrographs. **Table 2.2** contains values for the physical parameters of the reservoirs. **Figures 2.20**, **2.21**, **2.22**, and **2.23** display SV vs. SE and SQ vs. SE plots for each reservoir. **Figures 2.24** and **2.25** show plots of these same parameters for Wahiawa Reservoir/Lake Wilson.

Table 2.2 Reservoir Data

Reservoir Routing Data			
Initial Condition Type: Elevation			
Type of storage routing: Reservoir			
Reservoir :	R1 & R3	R2 & R4	R5
RSVRIC (ft):	620	1020	830.5

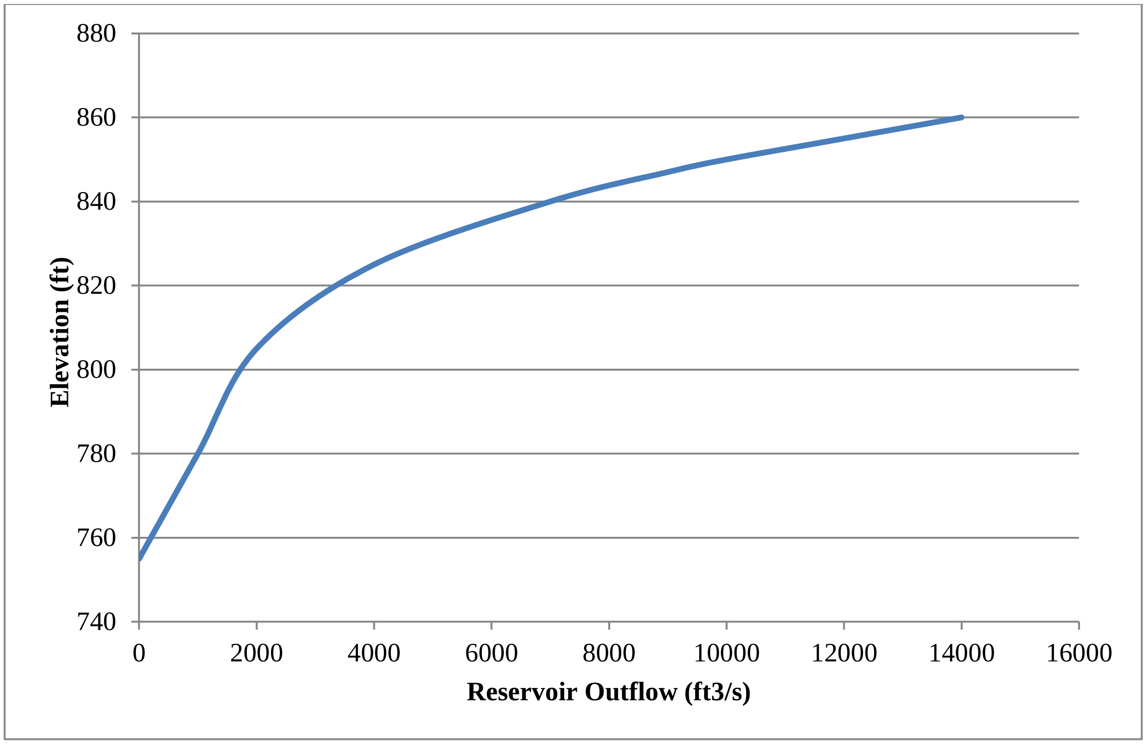

Figure 2.20 SQ vs. SE plot for R1 & R3

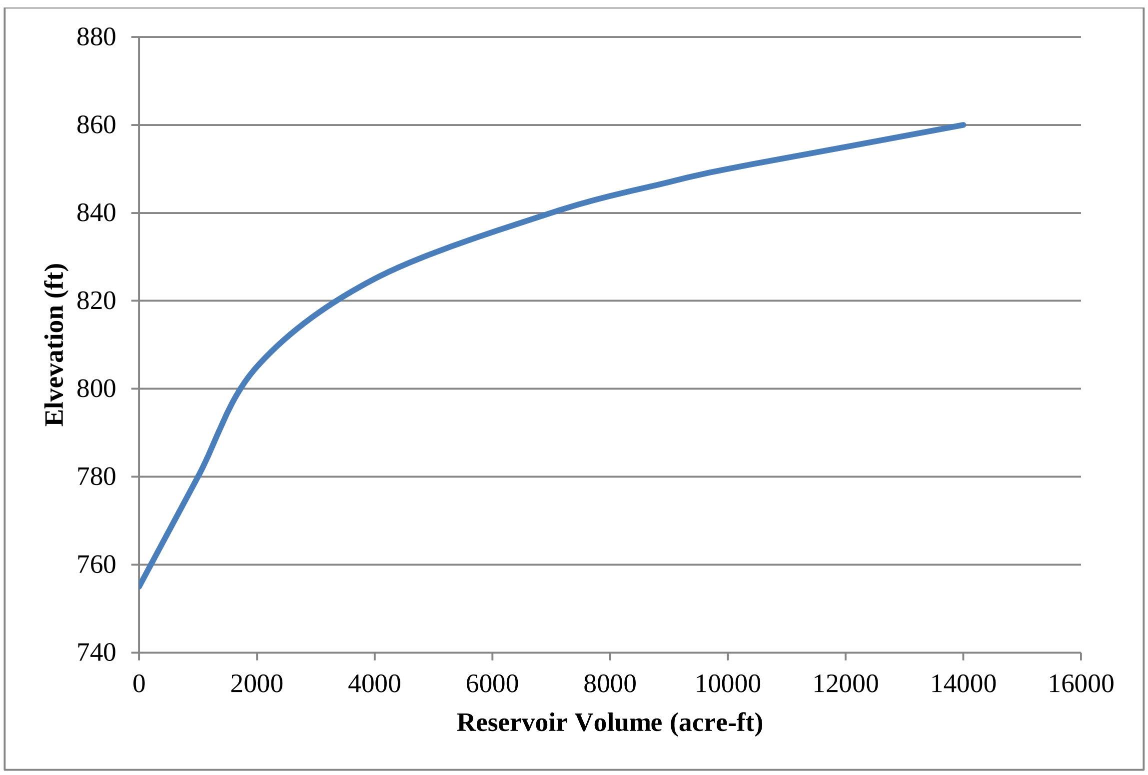

Figure 2.21 SV vs. SE plot for R1 & R3

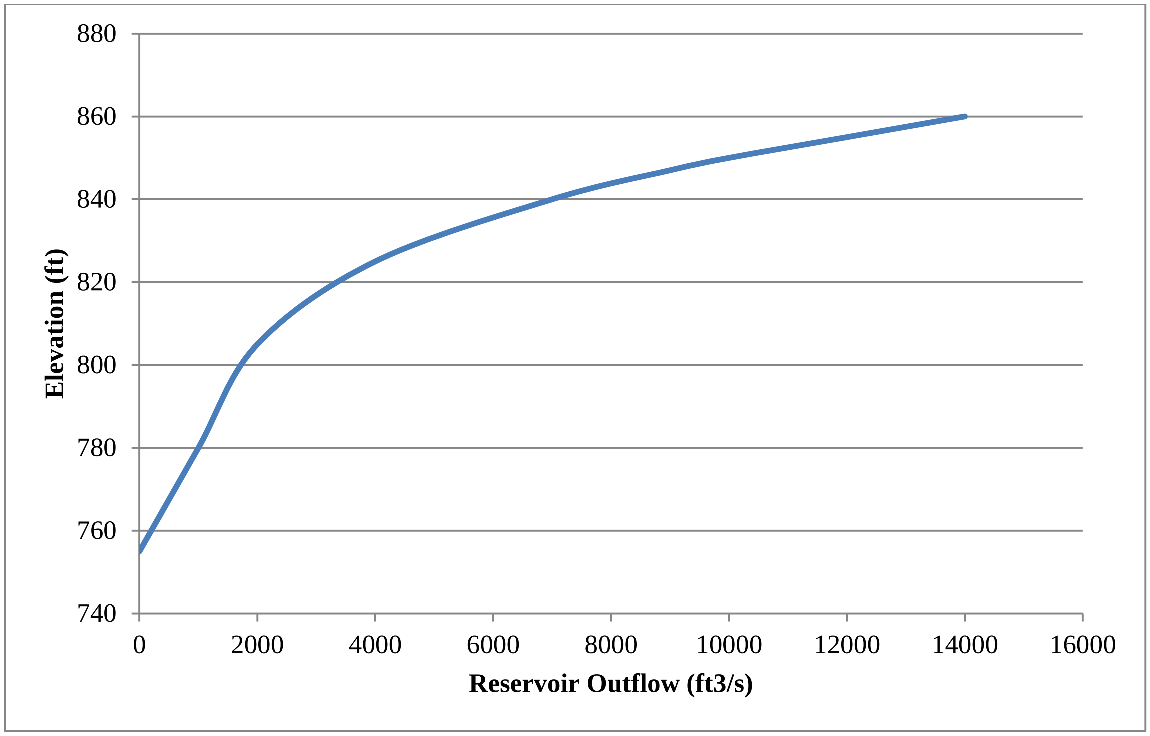

Figure 2.22 SQ vs. SE plot for R2 & R4

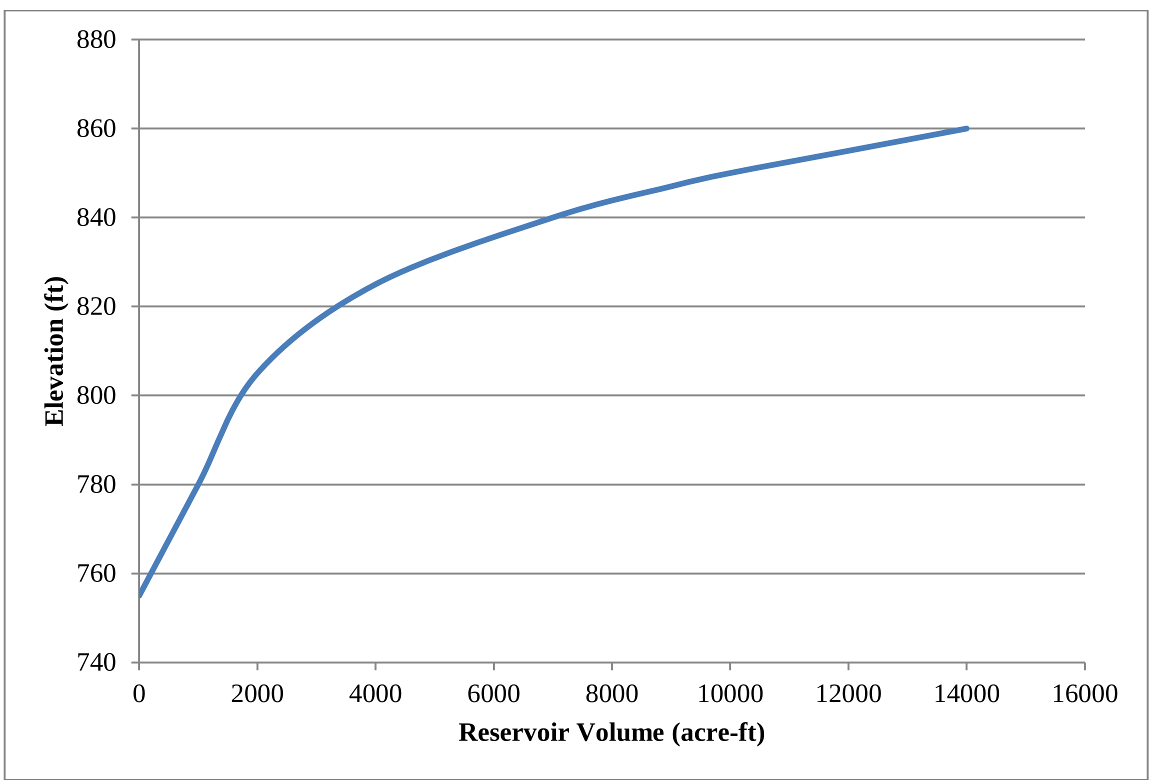

Figure 2.23 SV vs. SE plot for R2 & R4

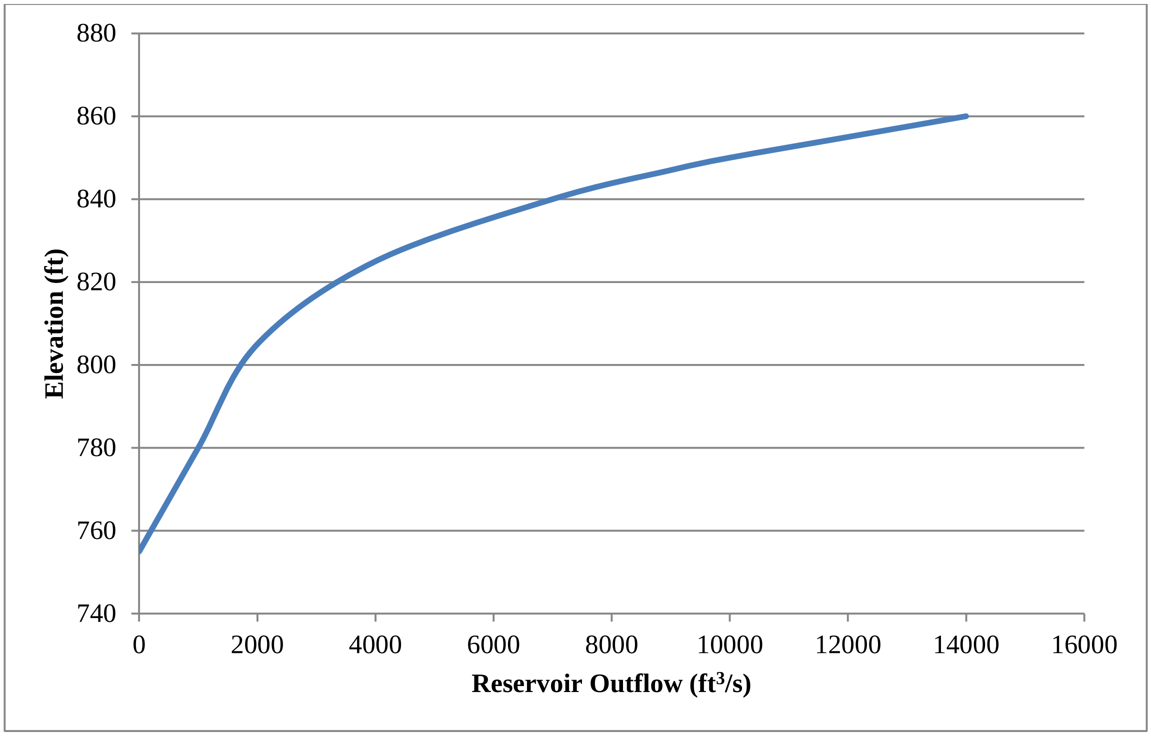

Figure 2.24 SQ vs. SE plot for R5

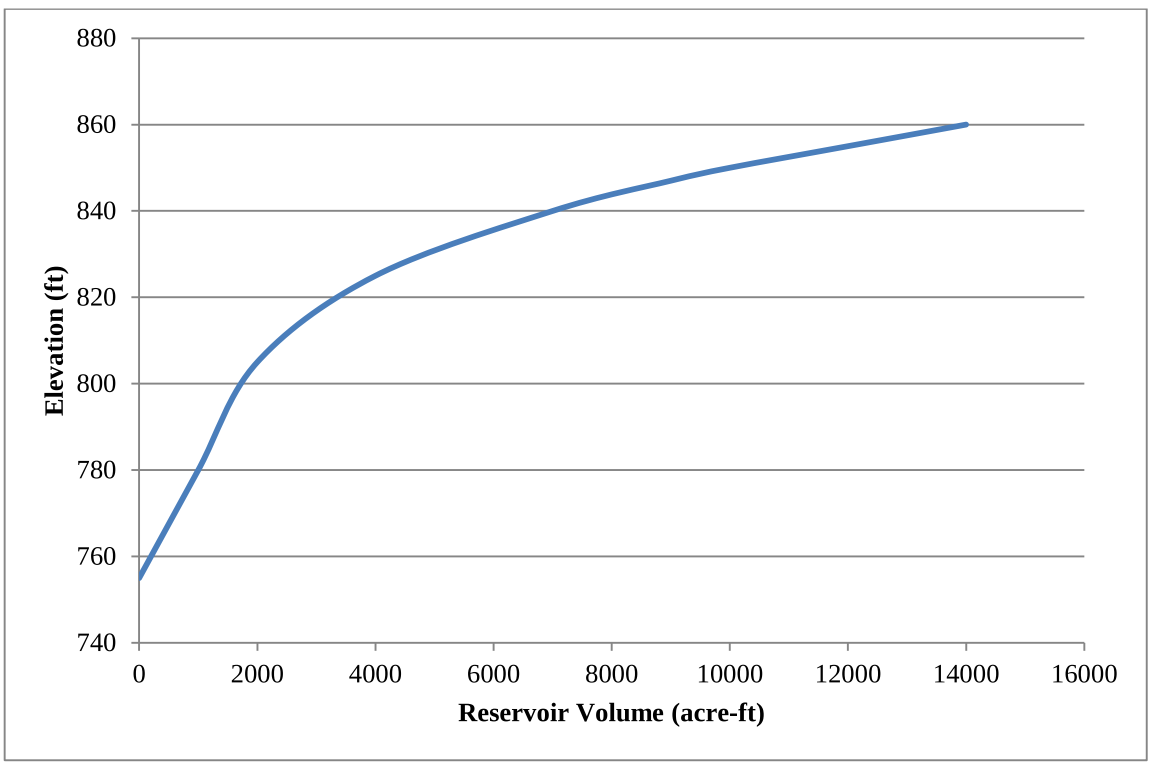

Figure 2.25 SV vs. SE plot for R5

2.3 HEC-RAS & FLOOD DELINEATIONS

In the third stage of the project, the model HEC-RAS was used to define stream cross-sections, which portray channels and surrounding terrain within the KBW floodplain region. The DEM was mainly used in this regard. This modeling system was ultimately used to delineate a floodplain model in WMS. A portion of KBW was trimmed off so that the project area would only include the final floodplain region, which consisted of the vicinities near and within Waialua and Haleiwa.

HEC-RAS was first used to create a conceptual model of the area, which defined stream reaches (layout and attributes and the length of a stream between any two points) based on chosen locations of cross-sections on those reaches. In order to create the conceptual model, HEC-RAS was used to create centerline and bank arcs. Centerline arcs indentified the locations of the study reaches and also defined their properties. The centerline was placed along the main stream channel and tributaries contained in the trimmed project area. Bank arcs were set in order to define locations of the banks and the over-bank distances. **Figure 2.26** shows the trimmed area of KBW and the stream and bank arcs.

In the next step, cross-sectional arcs were extracted for different reaches of the main stream channel and its tributaries. These cross-sections are required given that HEC-RAS computes solutions or output at those locations. **Figure 2.27** shows the different reaches and location of cross-sections, with each cross-section identified by a station number.

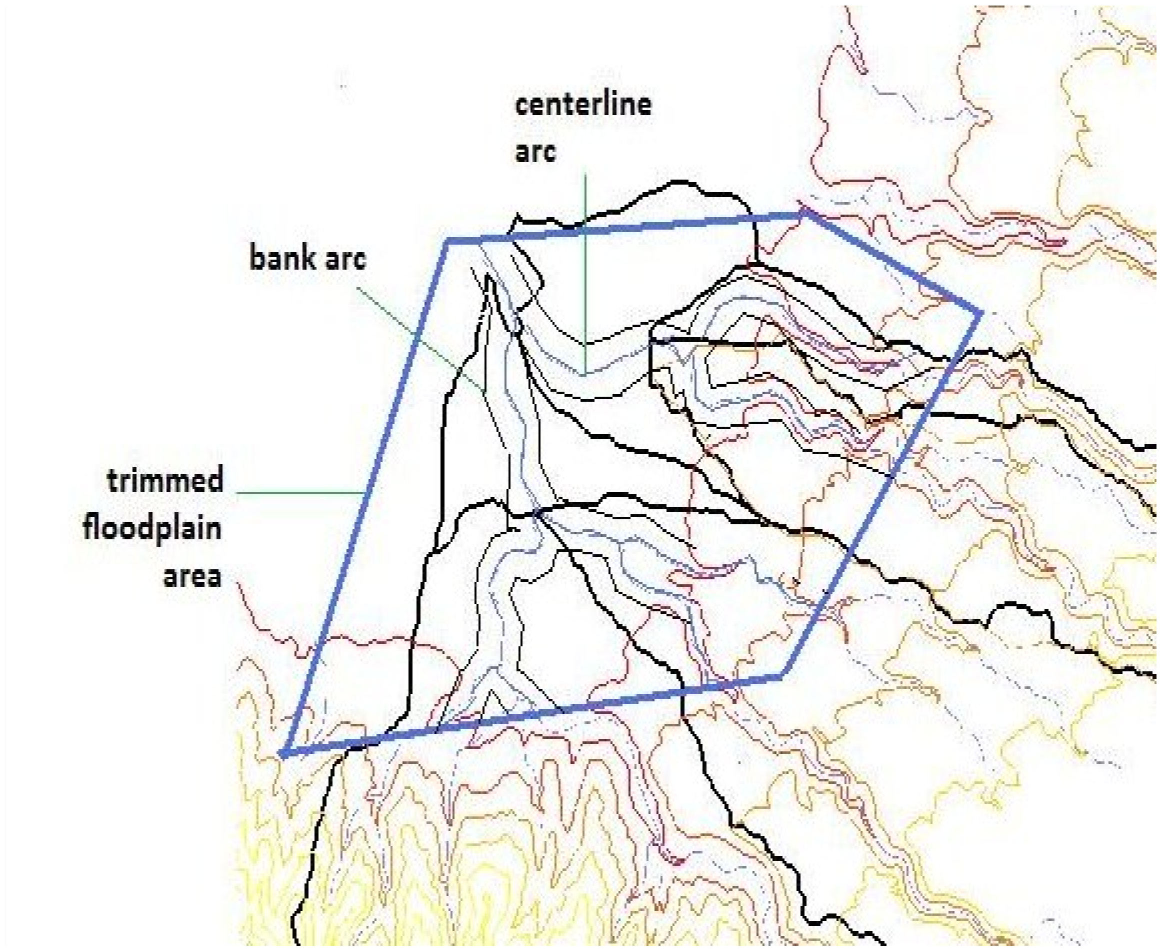

Figure 2.26 A trimmed shapefile of KBW defining the new project flood area. Included are centerline & bank arcs

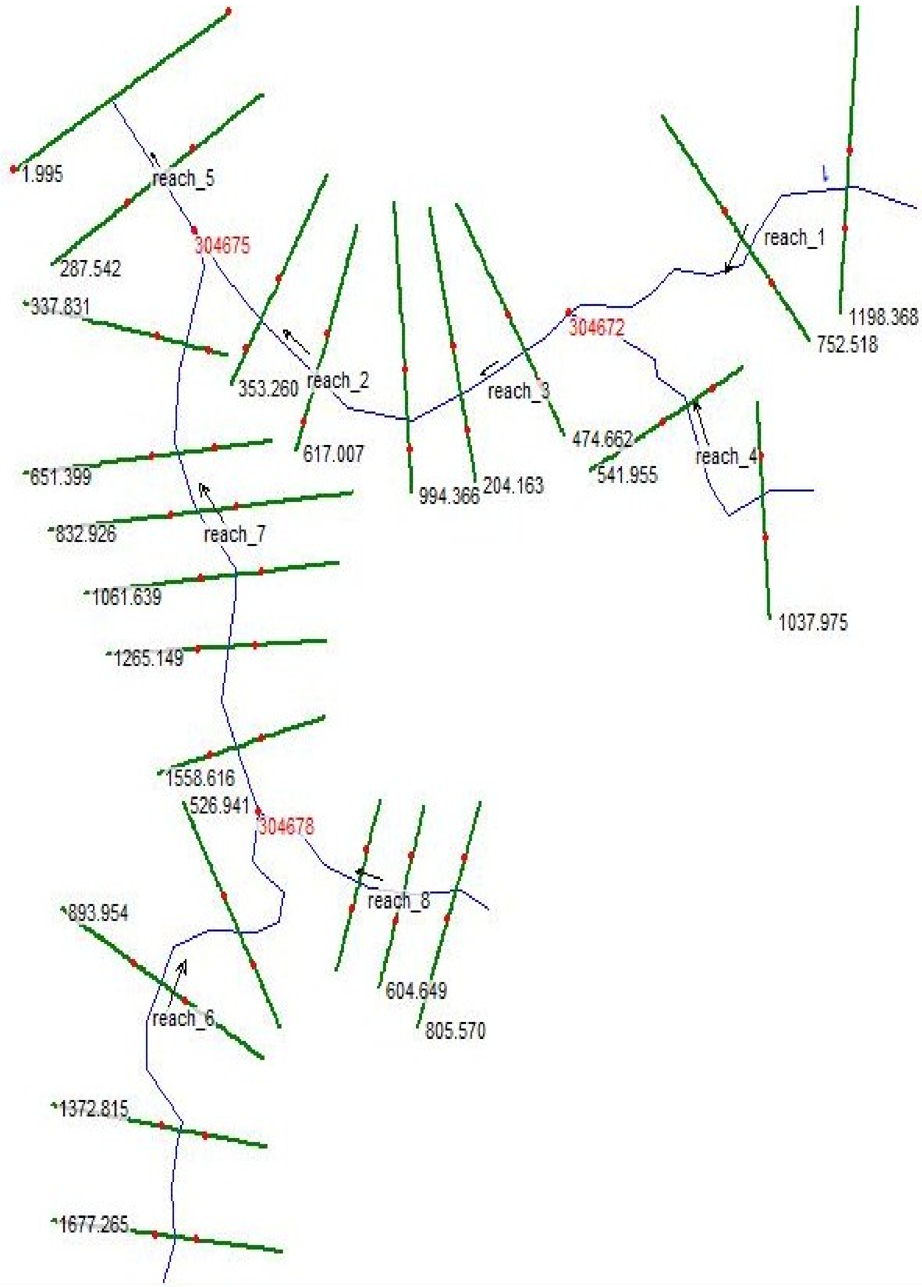

Figure 2.27 Assigned stream reaches and cross sections of the project area

With arcs and reaches delineated, flow and boundary conditions for each reach were applied next by selecting a *Steady Flow Data* option. Data entered include flow for each stream reach, assumed to be uniform through each specific reach, and estimated in this study by HEC-1 as the peak simulated values. Boundary conditions are needed to establish the starting water surface and the ends of a stream reach. Possible conditions include known water elevation, critical depth, normal depth, and rating curve (Brunner, 2010). Each of these options requires specific data, which were not available beforehand. A few options were tried with assumed parameters and the results were not very sensitive to such options. The normal depth option, which requires specifying water surface slope, was used in the final calculations. A constant value of 0.025 was used for this parameter. *Steady Flow Data* was entered several more times into HEC-RAS files with a half, a third, a fourth, and a tenth of the initial peak flow values so that the effect of flooding in different scenarios could be analyzed. These reductions, known as a sensitivity analysis, were used because exact measurements for flood depths were missing. This process demonstrated how water reacts if flow discharges are altered based on the amount of rainfall. The flood basins, excluding Wahiawa Reservoir, were removed to assess the impact on flooding in the study area. The values for several HEC-RAS parameters can be viewed in Appendix B. **Table B-1** contains the junction names and the respective normal depth slopes (slopes at downstream cross-sections). **Table 3.6** contains the reach stations and their respective peak discharge values.

2.3.1 PROCESSING DATA & DELINEATING THE FLOODPLAIN

After HEC-RAS computed water surface elevations, the solution could be analyzed in WMS, which reads water elevations above the surface as 2D-dimensional scatter plots. For this phase of processing, results for the six different discharge-scenarios were analyzed in separate WMS file sets. The points from the scatter plots were used to delineate the flood zone and estimate the flood depths. Each floodplain area was compared with a map provided by FEMA (Flood Emergency Management Agency), which defined different zones for a hundred year flood.

2.4 SIMULATIONS OF THE MODEL WELL

The final step of the study was to evaluate the expected rise in the groundwater table elevation due to injecting captured stream water. The study used the model WELL, which is based on the Theis (1935) analytical solution to assess the response of an ideal aquifer to well injection. Based on the design of the water harvesting system in Jeju Province, it was concluded that ten injection wells would be positioned in a row at the bottom of each basin. Three observation wells that measure water table levels as functions of time were also added within the row of injection wells. **Figure 2.28** displays a schematic aerial view of the well layout at the bottom of one of the flood basins.

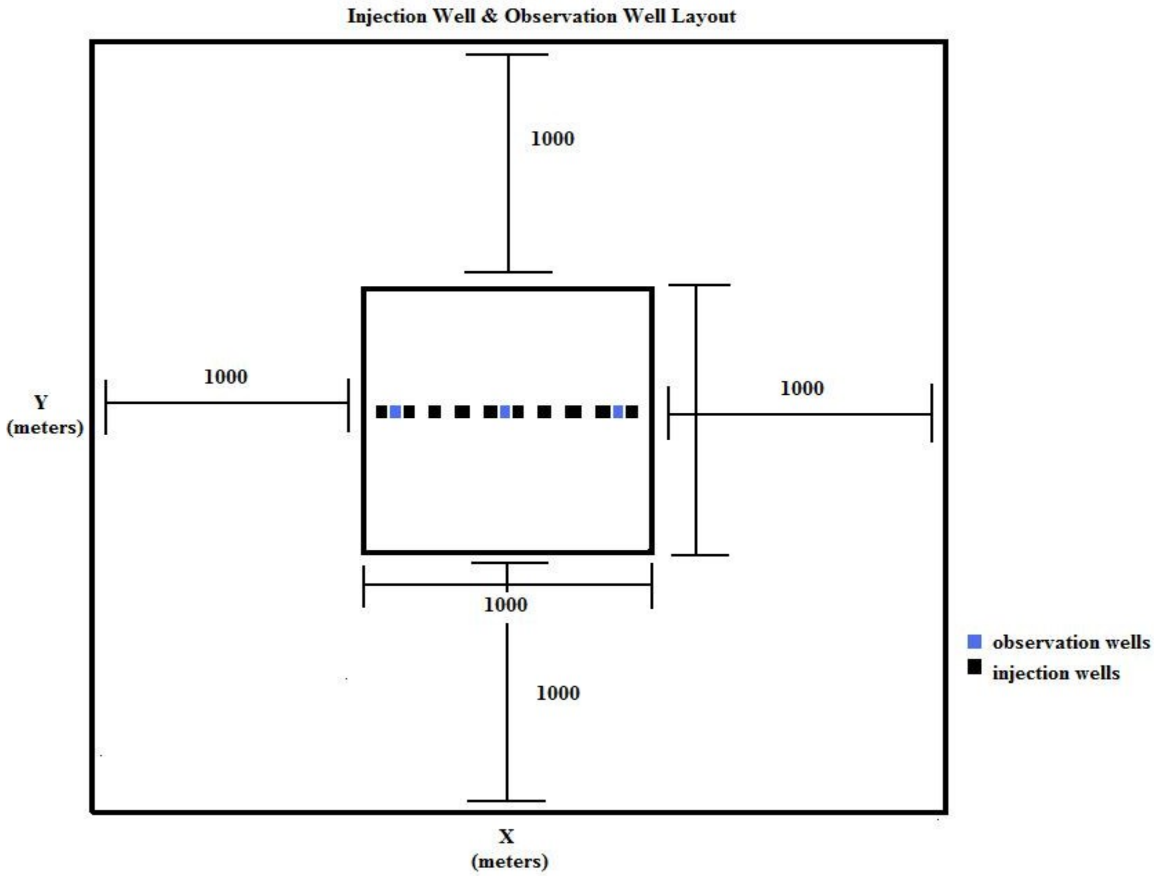

Figure 2.28 A schematic aerial view of well positions within a flood basin

Response of a groundwater aquifer depends on the well injection rate and length of injection period, properties of the aquifer, and the initial water table levels. In this case, it is assumed that other contributions, such as natural groundwater flow and natural recharge due to rain, are insignificant. Under injection, radial outflow from the well occurs, and a buildup cone forms. Water level around the well increases causing an outward gradient. This rise decreases with distance from the well, producing the cone shape. This buildup is the reverse of the cone of depression that forms around a pumping well as water is continuously extracted, also known as the zone of drawdown. Adjacent wells will cause combined effects leading to a higher rise. **Figure 2.29** illustrates an example of build-up surrounding two adjacent injection wells.

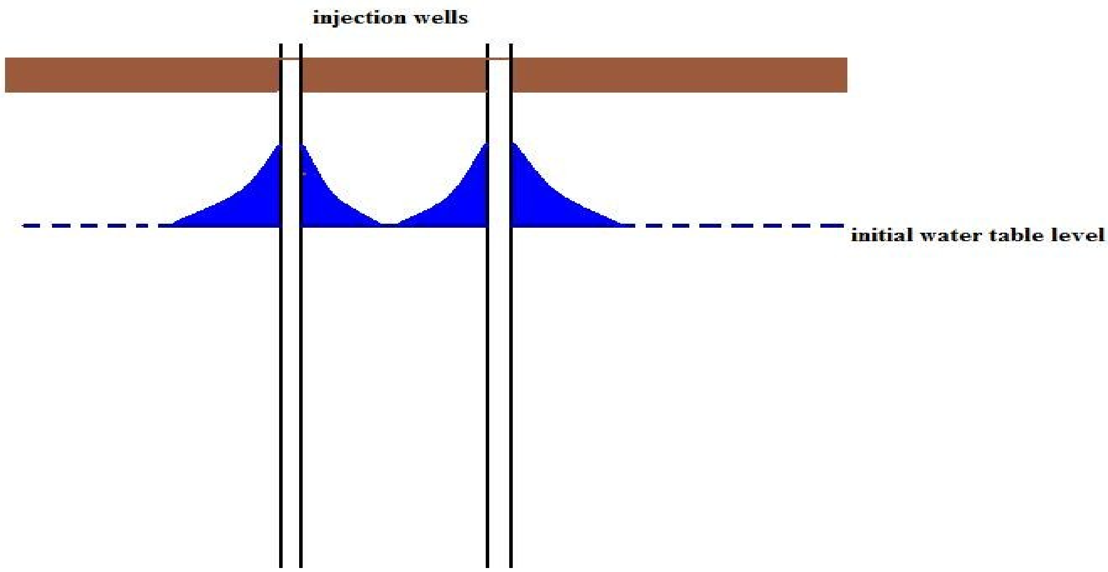

Figure 2.29 Cone of recharge forming around injection wells

For a confined aquifer, the Theis Solution (1935) is written in the form

$$s(r,t) = \frac{Q}{4\pi T}\int_{u}^{\infty}\frac{e^{-u}du}{u}$$

where u = $\frac{r^2 S}{4Tt}$.

In this equation, *s* is the change in the hydraulic head, *r* is the radial distance from the well to where build-up is observed, Q is the constant flow rate from/into the well, *T* is transmissivity, *t* is the duration of injection, and *S* is storativity. The linearity of the equation allows superimposing responses for a group of wells to identify the total response.

The main assumptions included in the solution are: the aquifer is horizontal, homogeneous, isotropic, infinite in horizontal extent, and has a constant thickness. The well would have a constant injection rate and would be fully penetrating, the well diameters would be infinitesimally small, and the initial water table would be flat. For the current study, it is further assumed that the solution is valid for an unconfined aquifer, which is generally valid for relatively small buildup compared to the aquifer thickness. Non- ideal conditions invalidate the Theis equation. For example, properties of the aquifer are generally variable in space and nearby conditions can include certain features that affect response of the aquifer to injection. For instance, the water table would rise faster if the aquifer abruptly ends at an outcrop (or bedrock).

3 RESULTS & DISCUSSION

3.1 HEC-1 MODEL CALIBRATION

Calibration involved testing HEC-1 simulated streamflow values against those observed from the USGS. The analysis used five days of precipitation. For the first set of rainfall distributions, **Table 3.1** and **3.2** list relevant data and the cumulative values of simulated and observed data, as well as the RMSE and resulting percent coefficient of variation. For station number 16345000/sub-basin Opaeula Stream near Wahiawa, the percent coefficient of variation ranged from 12 to 181, while for station 16200000/sub-basin North Fork Kaukonahua Stream above right branch, near Wahiawa, the percent coefficient spanned from 25 to 267.

Most of the simulated and observed data for each figure followed a similar trend from a visual analysis. In **Figure 3.1**, the model underestimated discharge at low values and overestimated them at high values. **Figure 3.2** shows that the simulated and observed hydrographs corresponded at the highest peak. However, the simulated data was more than double the observed data at the lowest peak. **Figure 3.3** had the greatest percent coefficient of variation due to the oscillations in the hydrograph, where the model over or underestimated discharge values along the time series. **Figures 3.4** to **3.7** produced percent coefficients in the mid-range of the results, where simulated and observed data correlated at some points in the time series but varied greatly at others. Although **Figure 3.8** had the lowest percent coefficient of variation due to small variations in discharge, the two hydrographs showed the greatest contrast from a visual perspective. The last precipitation date used for the calibration, 1/15/13 produced the best results for both sub-basins from a visual analysis and from data comparison (see

Figures 3.9 and **3.10**).

Model calibration was also assessed through scatter plots between the simulated and observed data for each case. Amongst the plots, **Figures 3.11** and **3.12,** respectively for data on 3/2/2012 and on 1/5/2013**,** displayed the closest linear relationship between data sets for basin 16200000/North Fork Kaukonahua basin. On the other hand, **Figures 3.13** and **3.14**, respectively for data on 3/2/2012 and on 1/5/2013 exhibited the best fits for basin 16345000/Opaeula Stream near Wahiawa basin. Results show mixed success, most likely due to the absence of accurate rainfall data and to uncertainty in various model data, especially regarding land use and cover. Overall, studies show that models have their limitations in simulating watersheds in Hawaii, due to their special features, especially steep slopes and highly variable conditions (Chu, Chen, & Schroeder, 2010; Murphy & Businger, 2011).

Table 3.1 Cumulative daily streamflow results from the hydrology calibration for station/basin: 16345000/Opaeula Stream near Wahiawa

Precipitation Date	**Observed Flow (cfs)**	**Simulated Flow (cfs)**	**RMSE**	**Percent Coefficient of Variation**	**Base Flow Parameters**	
					STRTQ	**QRCSN**
3/2/2012	13654	11930	173	150	11	600
3/4/2012	17737	14637	130	113	46	171
3/24/2012	4620	26951	208	181	7.5	51
4/27/2012	1807	2203	14	12	12	14
1/5/2013	6415	7571	51	44	26	97
Total	44233	78095	576	500		

Table 3.2 Cumulative daily streamflow results from the hydrology calibration for station/basin: 16200000/North Fork Kaukonahua Stream above Right Branch, near Wahiawa

Precipitation Date	**Observed Flow (cfs)**	**Simulated Flow (cfs)**	**RMSE**	**Percent Coefficient of Variation**	**Base Flow Parameters**	
					STRTQ	**QRCSN**
3/2/2012	8191	5444	76	55	10	78
3/4/2012	33165	22001	368	267	0	0
3/24/2012	5969	11391	110	80	11	51
4/27/2012	5617	9763	100	73	4.9	58
1/5/2013	6029	4261	34	25	17	31
Total	50780	52860	688	500		

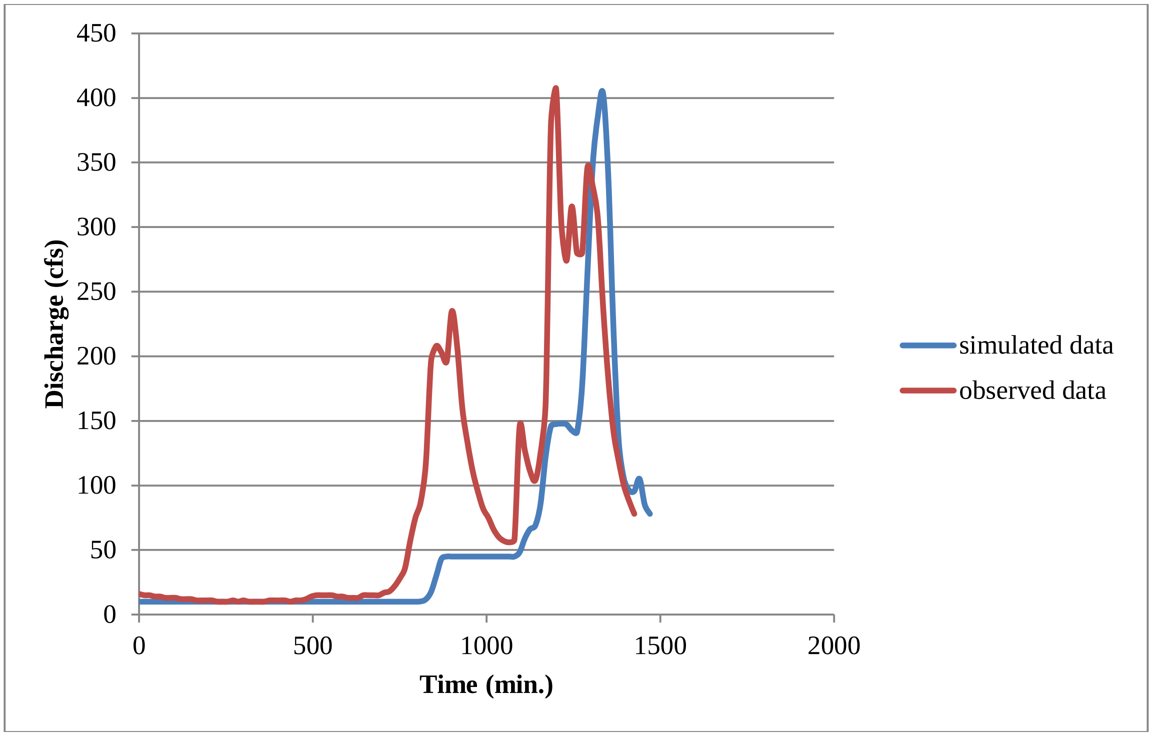

Figure 3.1 Simulated and observed data for basin 16200000 for the precipitation date 3/2/12

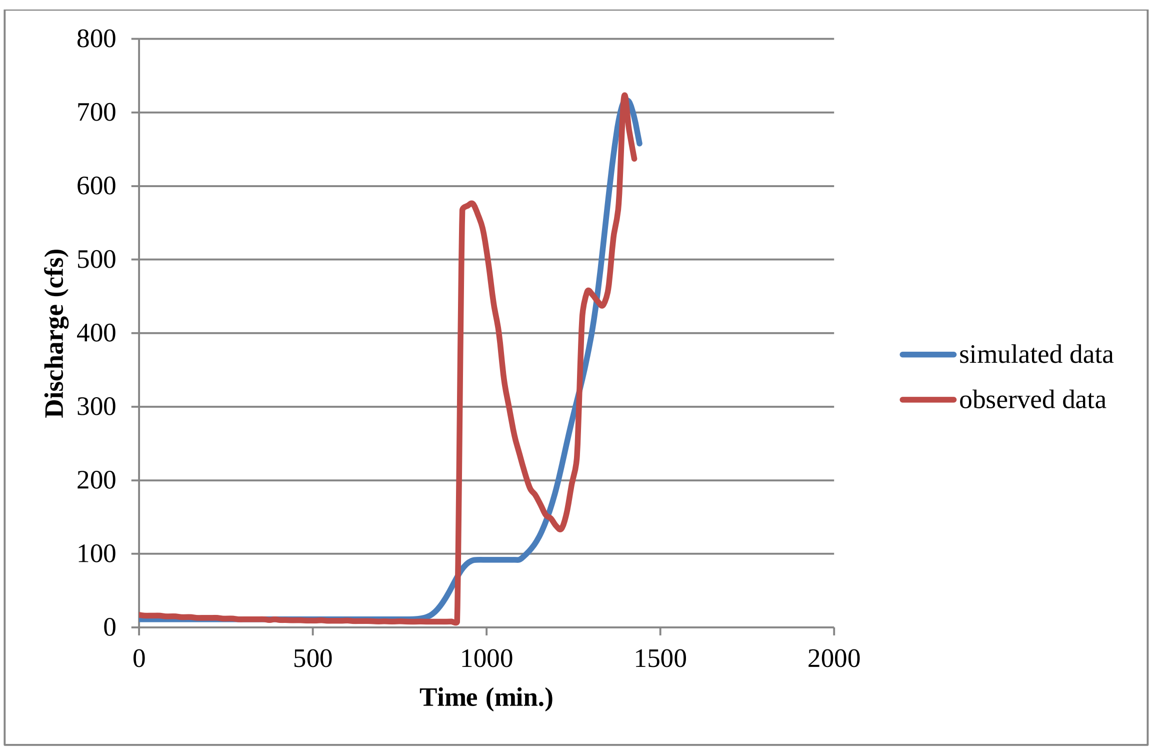

Figure 3.2 Simulated and observed data for basin 16345000 for the precipitation date 3/2/12

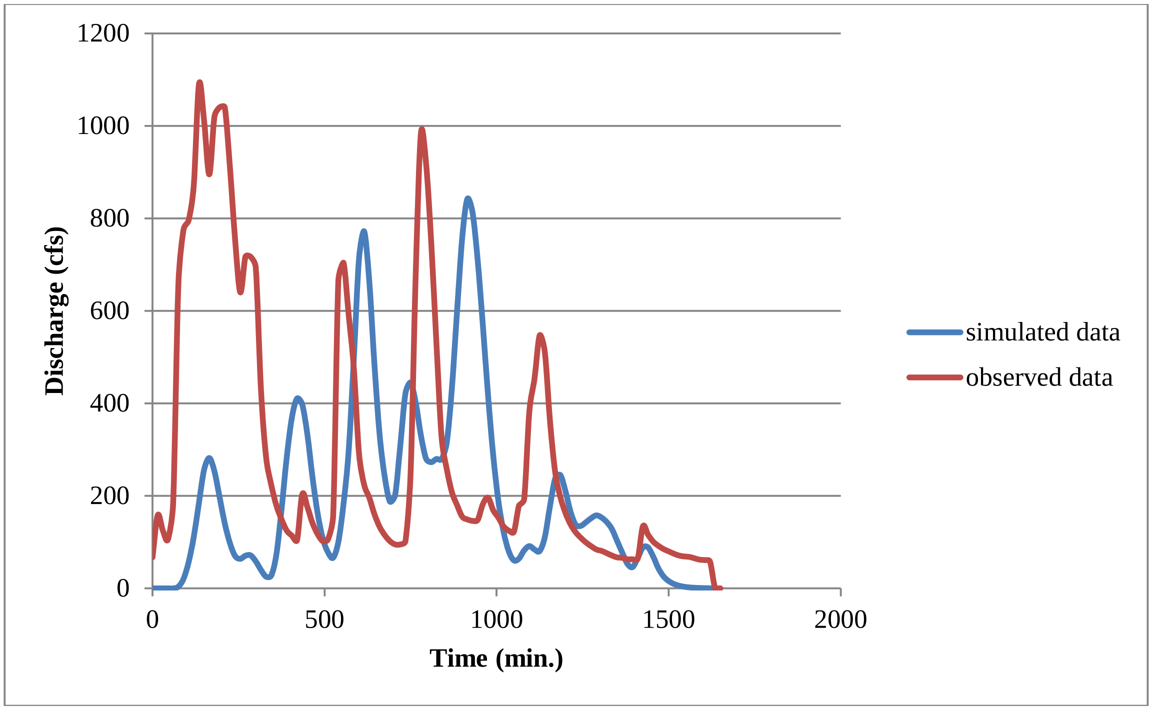

Figure 3.3 Simulated and observed data for basin 16200000 for the precipitation date 3/4/12

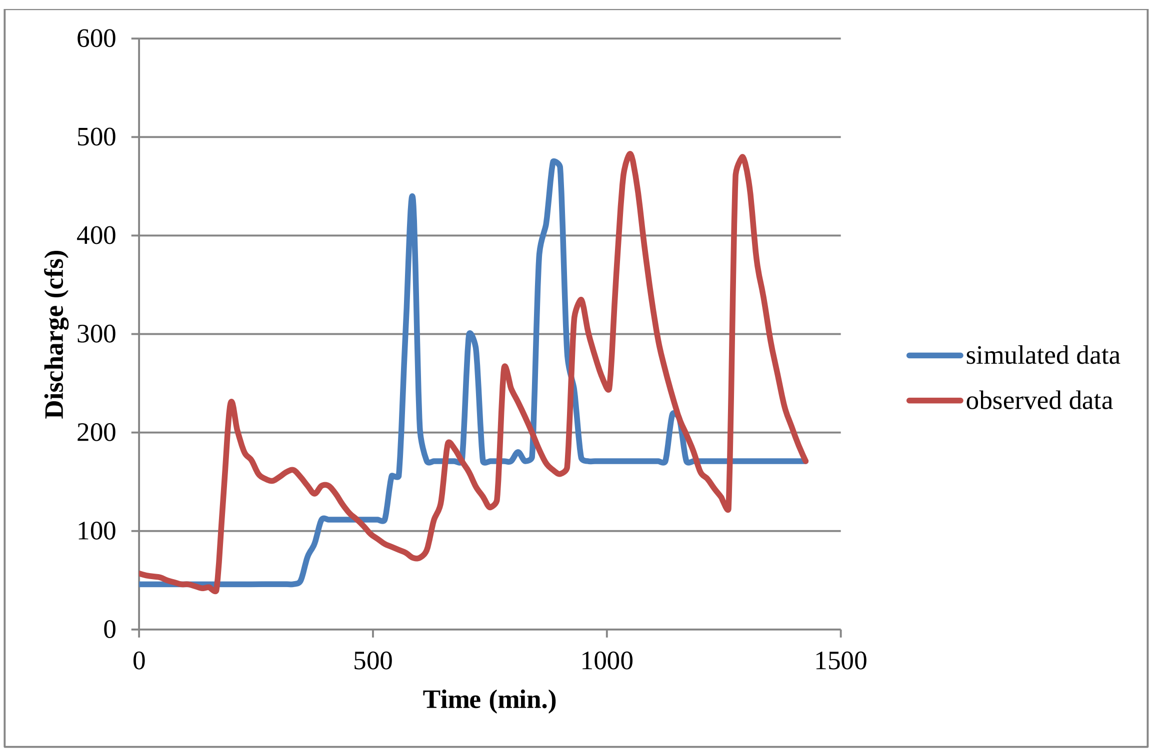

Figure 3.4 Simulated and observed data for basin 16345000 for the precipitation date 3/4/12

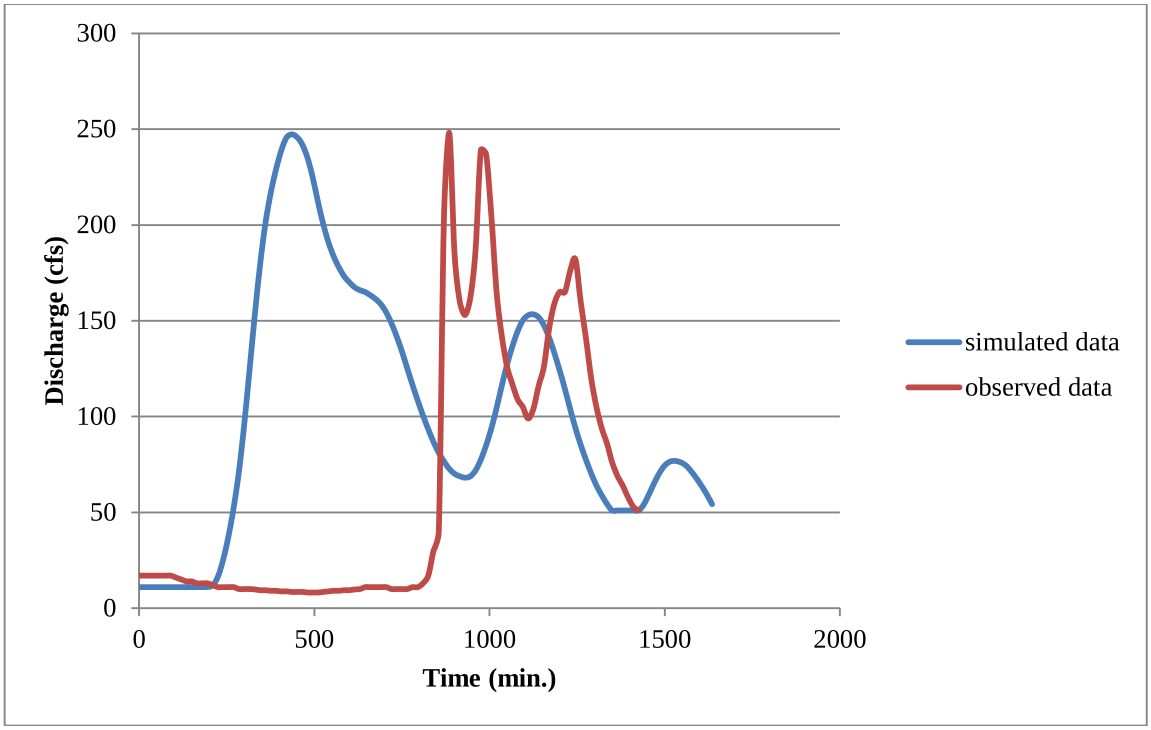

Figure 3.5 Simulated and observed data for basin 16200000 for the precipitation date 3/24/12

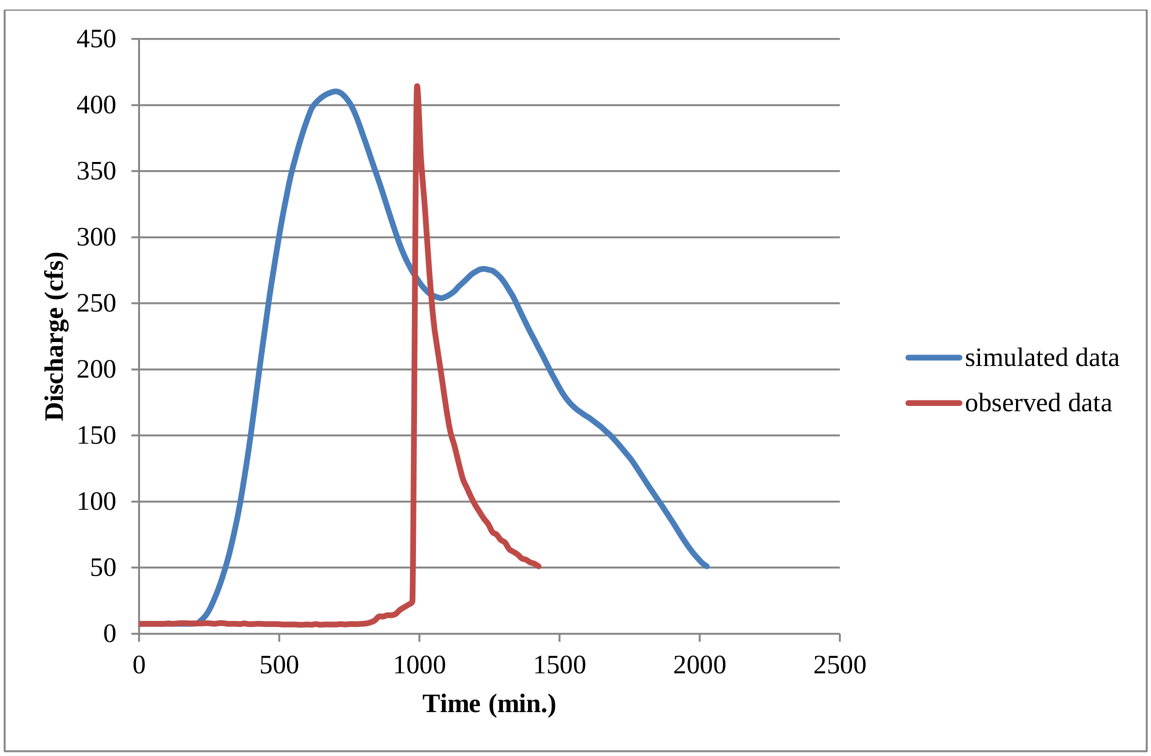

Figure 3.6 Simulated and observed data for basin 16345000 for the precipitation date 3/24/12

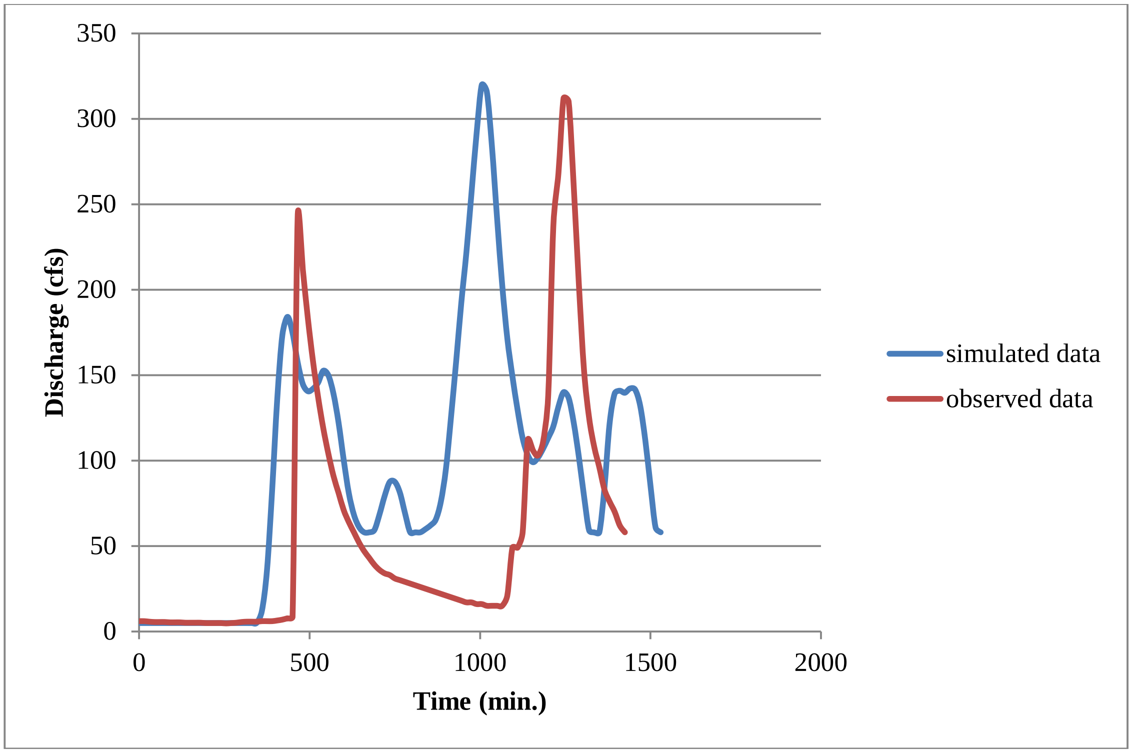

Figure 3.7 Simulated and observed data for basin 16200000 for the precipitation date 4/27/12

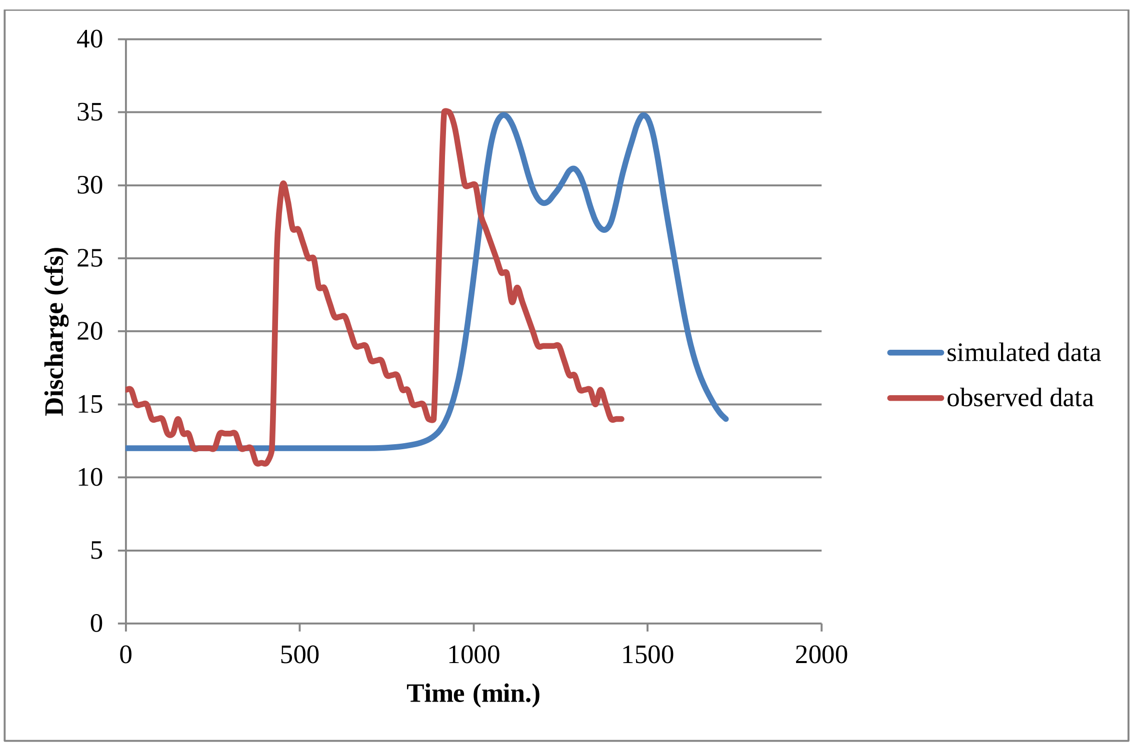

Figure 3.8 Simulated and observed data for basin 16345000 for the precipitation date 4/27/12

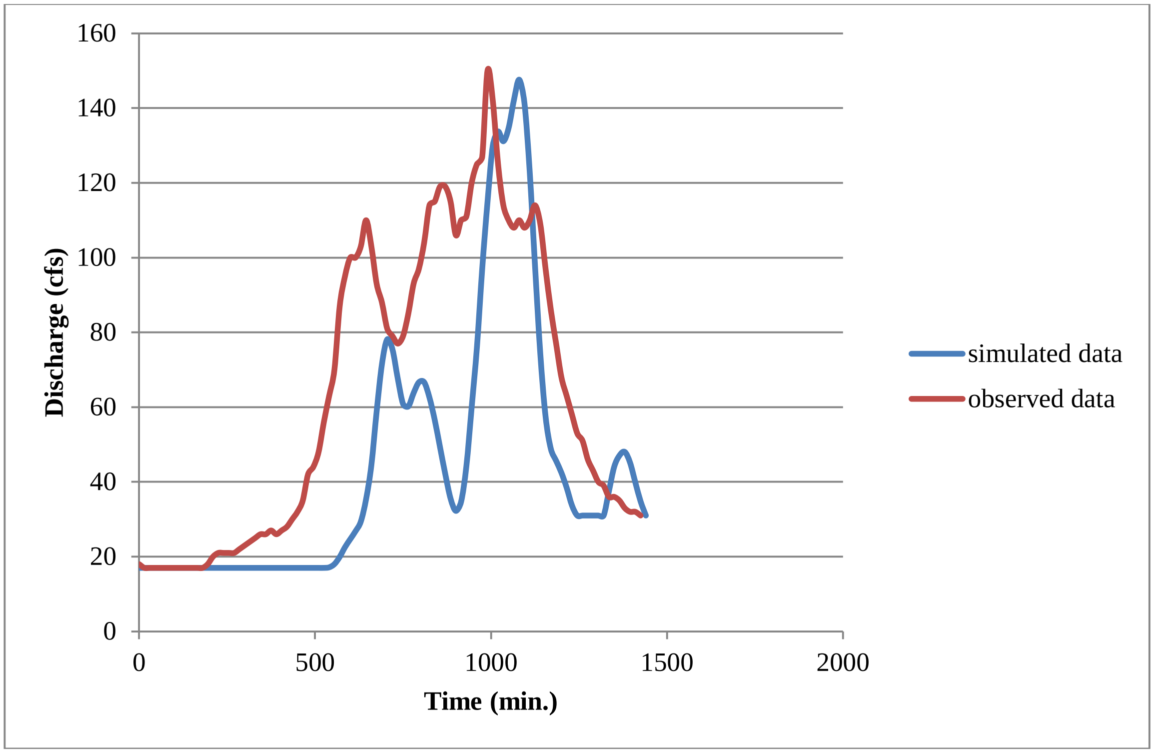

Figure 5.9 Simulated and observed data for basin 16200000 for the precipitation date 1/5/13

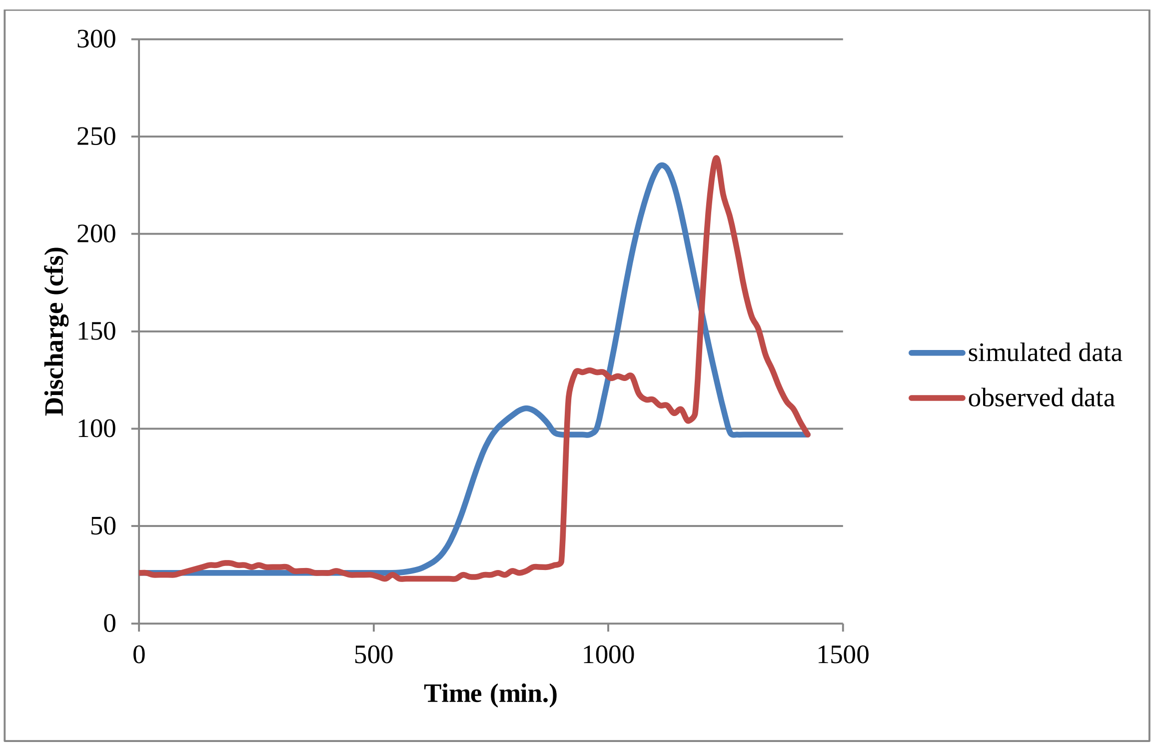

Figure 3.10 Simulated and observed data for basin 16345000 for the precipitation date 1/5/13

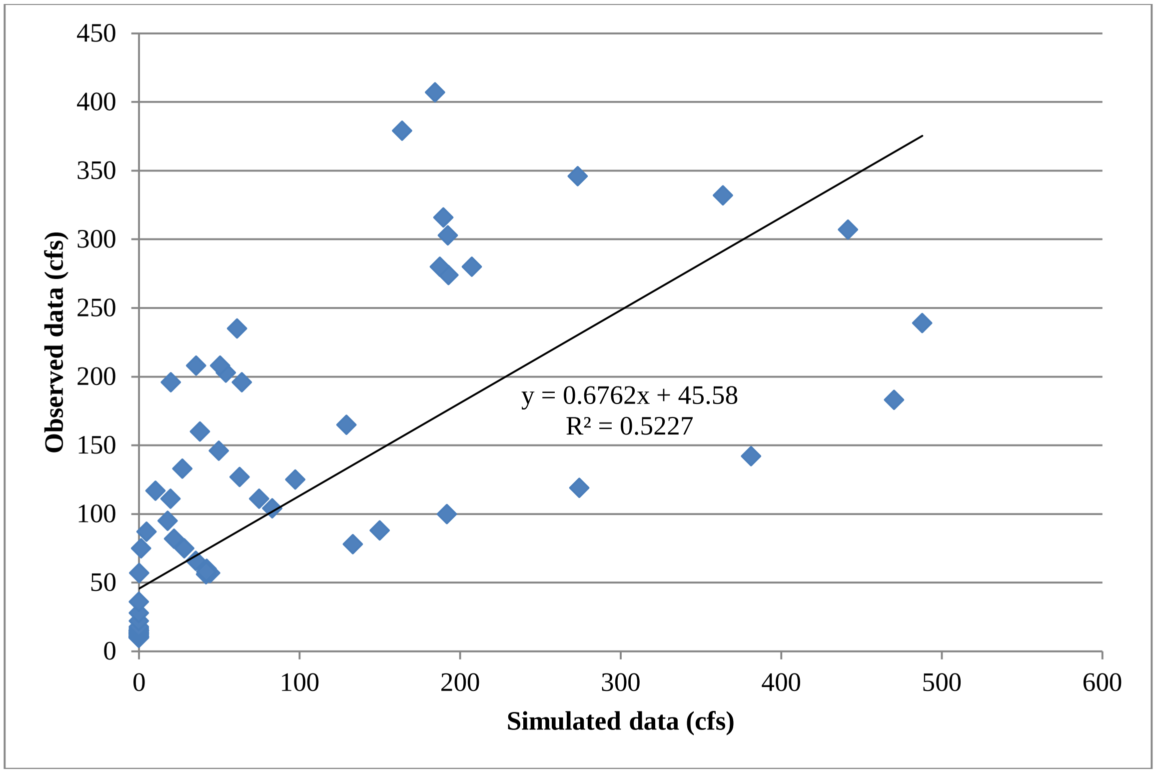

Figure 3.11 Simulated and observed data on 3/2/2012 for basin 16200000

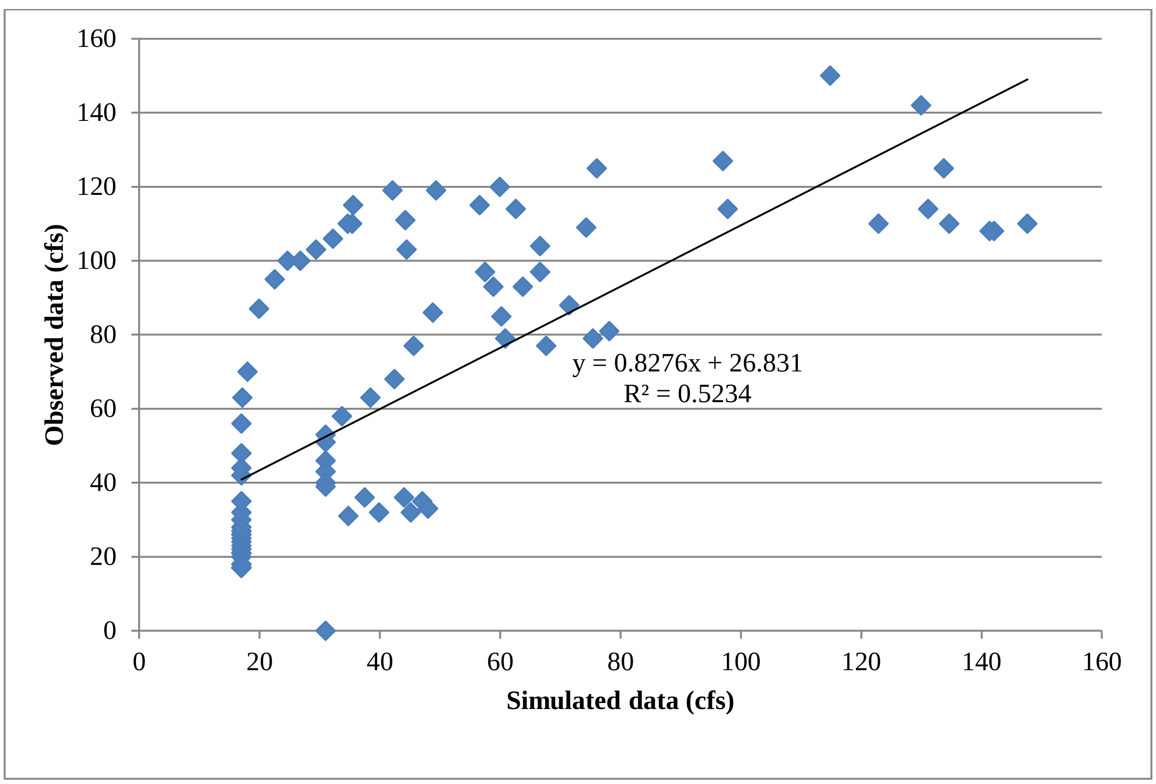

Figure 3.12 Simulated and observed data on 1/5/2013 for basin 16200000

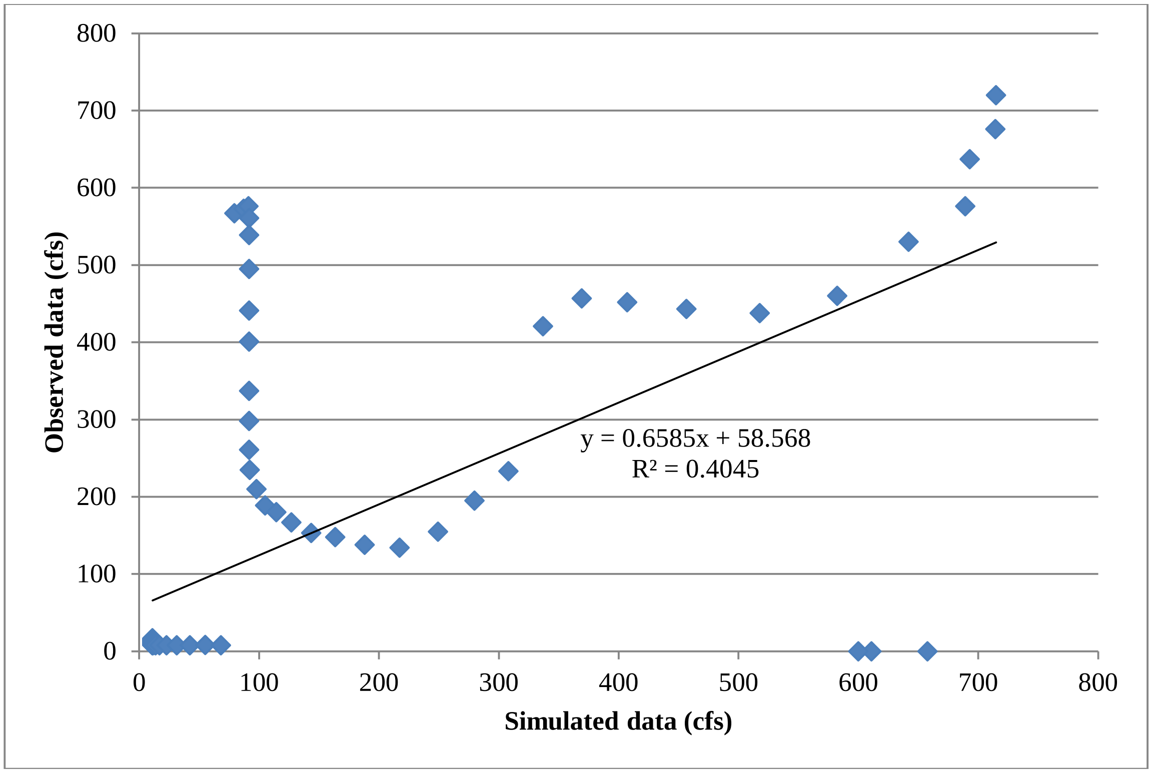

Figure 3.13 Simulated and observed data on 3/2/2012 for basin 16345000

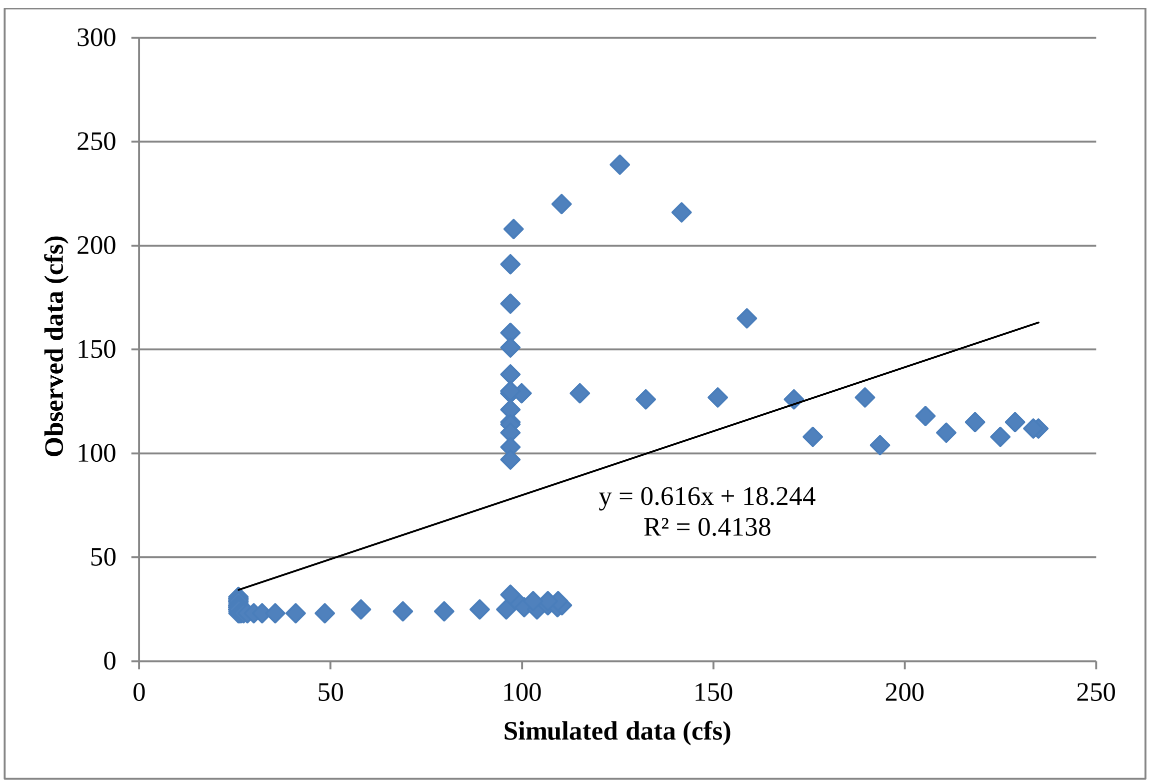

Figure 3.14 Simulated and observed data on 1/5/2013 for basin 16345000

3.1.1 HEC-1 MODEL CALIBRATION FOR ALTERNATIVE RAIN DISTRIBUTIONS

When compared with the HEC-1 calibration results from the previous section, **Tables 3.3** and **3.4** showed that there was a significant improvement in the accuracy of the HEC-1 model, as can be seen for several of the precipitation dates when the alternative rain distributions were used. These improvements were for 3/4/12 and 3/24/12, for basin 16345000/Opaeula Stream near Wahiawa basin, and 3/4/2012, 3/24/2012, and 4/27/2012 for basin 16200000/North Fork Kaukonahua Stream near Wahiawa basin. **Figures 3.15** to **3.24** display the calibration results generated from the alternative rain distributions in chronological order for both basins. The greatest improvement was exhibited in basin 16345000 on 3/24/2012, where the percent coefficient of variation was reduced by 41 percent. From visually observing the new sets of hydrographs, **Figure 3.17** displayed the best match between simulated and observed data. With the exception of discharge in the early stages of stormflow, the remaining observed and simulated values were significantly close. As in the previous section, **Figure 3.22,** which displays results for basin 16345000 on 4/27/2012, produced the greatest deviation from a visual analysis between observed and simulated data with no reduction in the percent coefficient of variation.

Figures 3.25 to **3.28**, for data on 3/2/2012 and 3/4/2012 demonstrated the closest linear relationship between the data sets for both North Fork Kaukonahua and Opaeula Steam basin. Compared with the scatter plots generated from the first set of calibration results, these plots exhibited a much more significant and obvious linear correlation between observed and simulated data.

Table 3.3 Cumulative daily streamflow results from the hydrology calibration for station/basin: 16345000/ Opaeula Stream near Wahiawa

Precipitation Date	**Observed Flow (cfs)**	**Simulated Flow (cfs)**	**RMSE**	**Percent Coefficient of Variation**	**Base Flow Parameters**	
					STRTQ	**QRCSN**
3/2/2012	13654	8222	168	204	7.8	637
3/4/2012	17737	15442	77	94	46	171
3/24/2012	4620	8841	115	140	7.5	51
4/27/2012	1807	1806	11	13	12	14
1/5/2013	6415	5913	40	49	26	97
Total	44233	40012	411	500		

Table 3.4 Cumulative daily streamflow results from the hydrology calibration for station/basin: 16200000/North Fork Kaukonahua Stream near Wahiawa

Precipitation Date	**Observed Flow (cfs)**	**Simulated Flow (cfs)**	**RMSE**	**Percent Coefficient of Variation**	**Base Flow Parameters**	
					STRTQ	**QRCSN**
3/2/2012	8191	6526	59	75	10	78
3/4/2012	33165	28836	193	244	0	0
3/24/2012	5969	4085	57	72	11	51
4/27/2012	5617	3806	52	66	4.9	58
1/5/2013	6129	5363	34	43	17	60
Total	59071	48616	395	500		

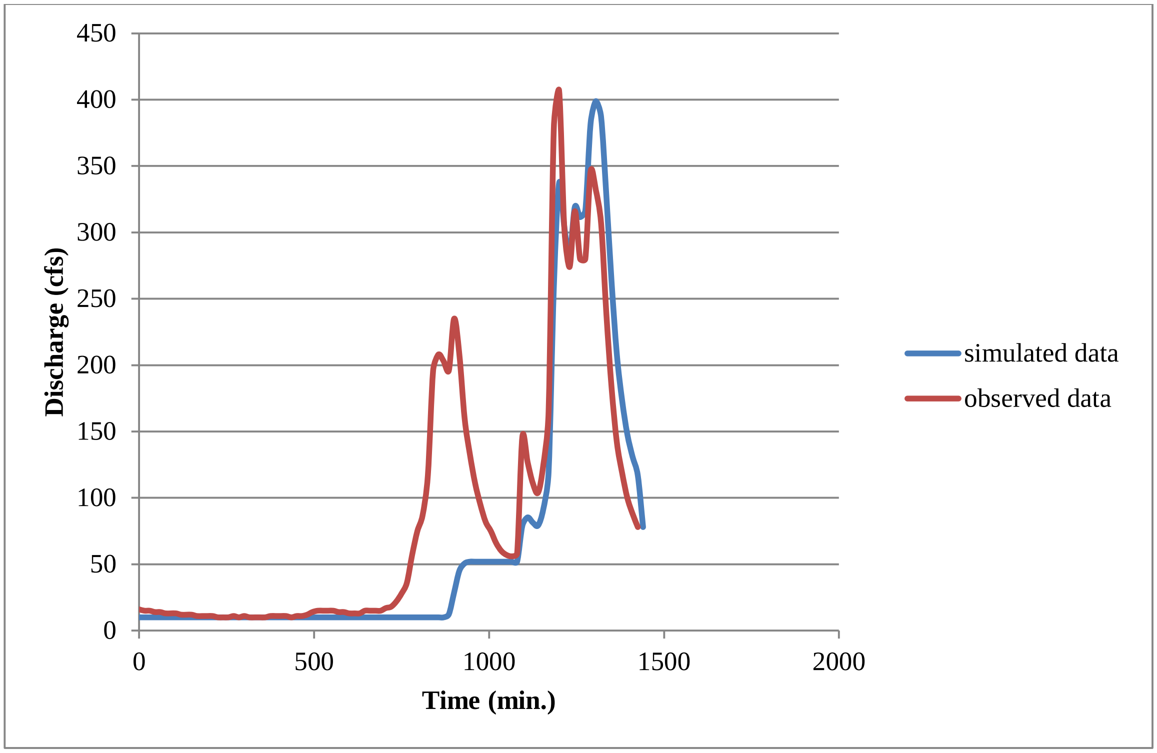

Figure 3.15 Results from new rainfall distribution for 3/2/12 for basin 16200000

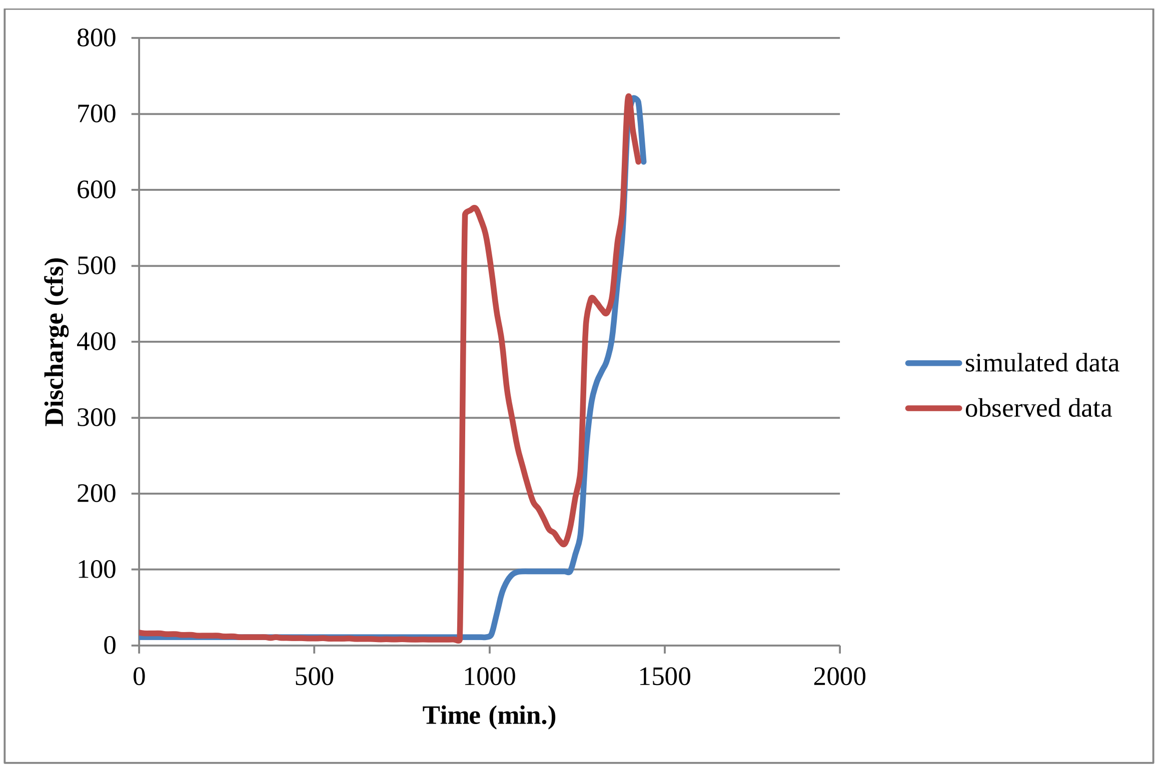

Figure 3.16 Results from new rainfall distribution for 3/2/12 for basin 16345000

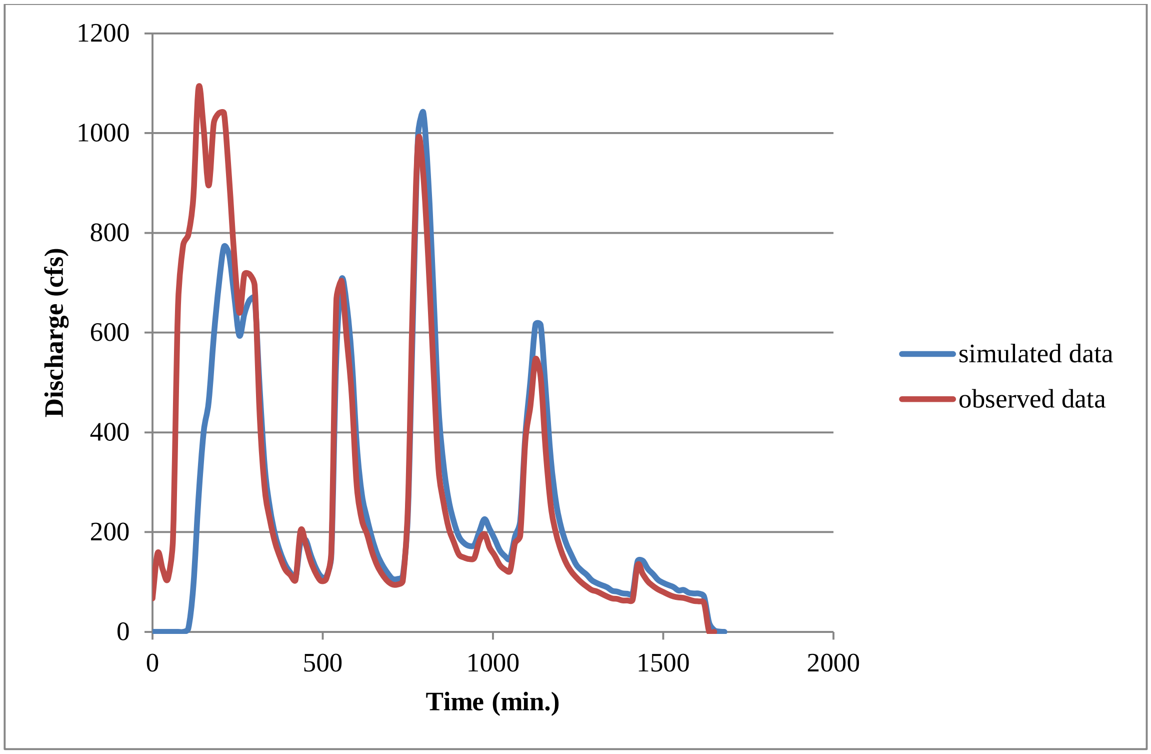

Figure 3.17 Results from new rainfall distribution for 3/4/12 for basin 16200000

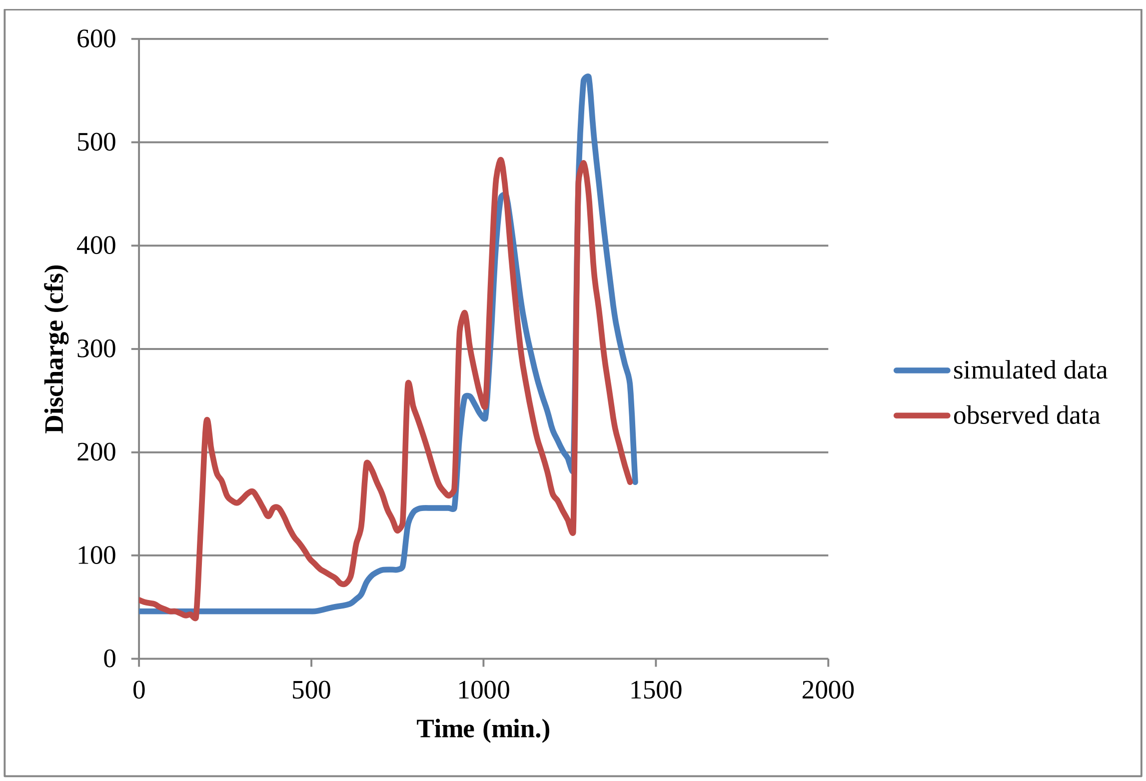

Figure 3.18 Results from new rainfall distribution for 3/4/12 for basin 16345000

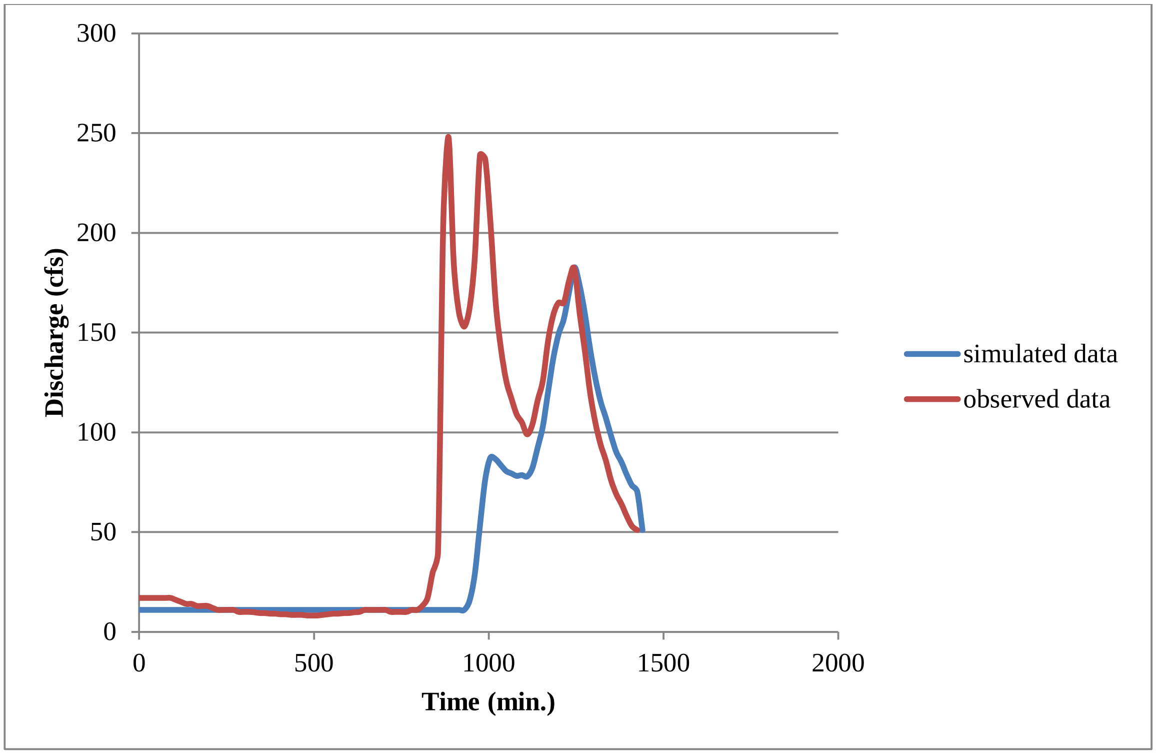

Figure 3.19 Results from new rainfall distribution for 3/24/12 for basin 16200000

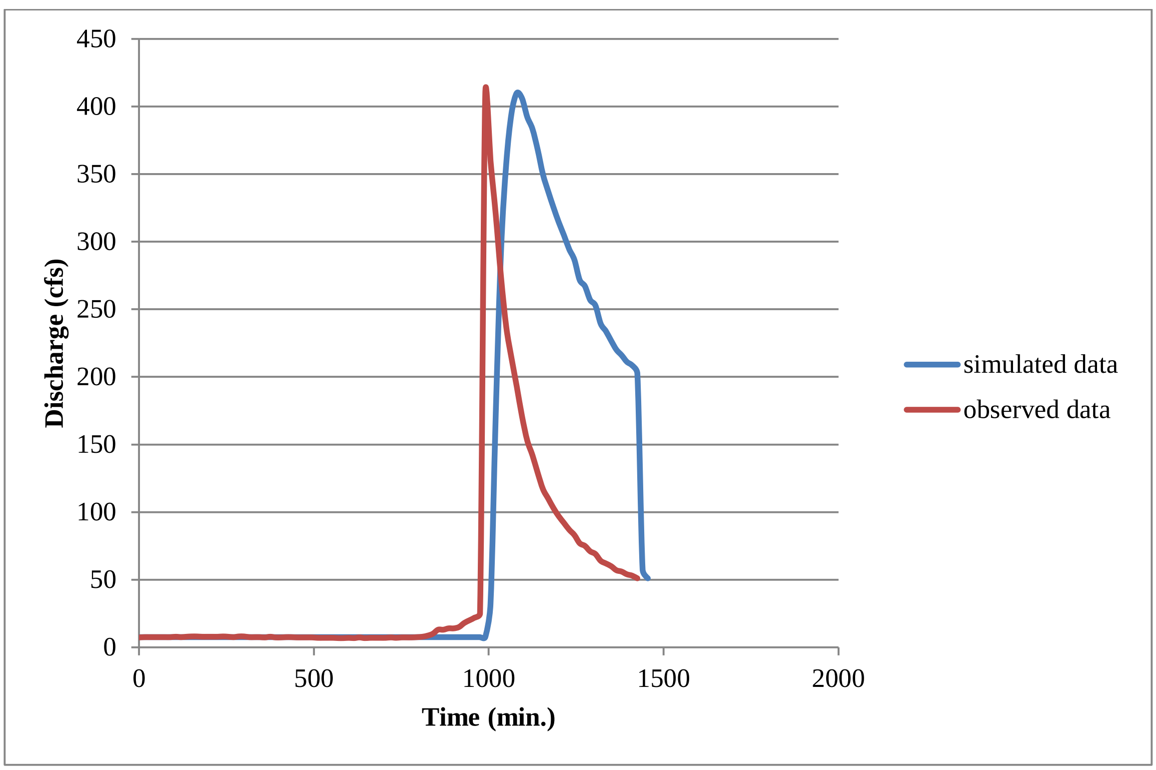

Figure 3.20 Results from new rainfall distribution for 3/24/12 for basin 16345000

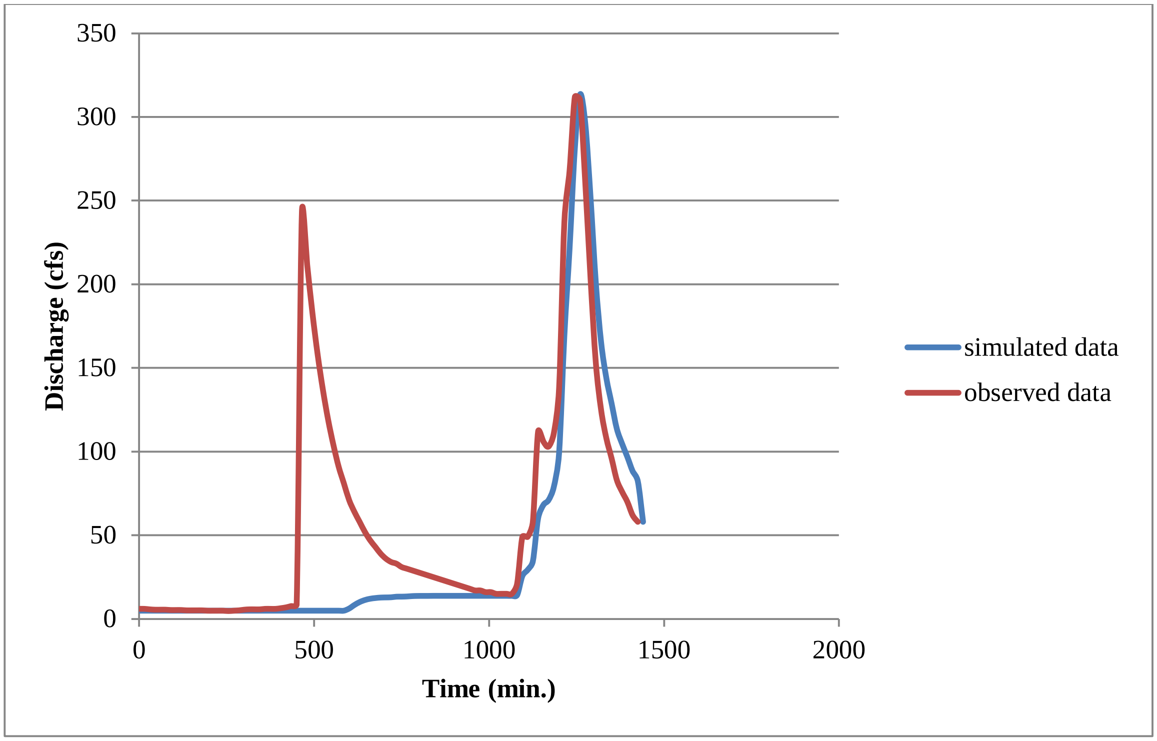

Figure 3.21 Results from new rainfall distribution for 4/27/12 for basin 16200000

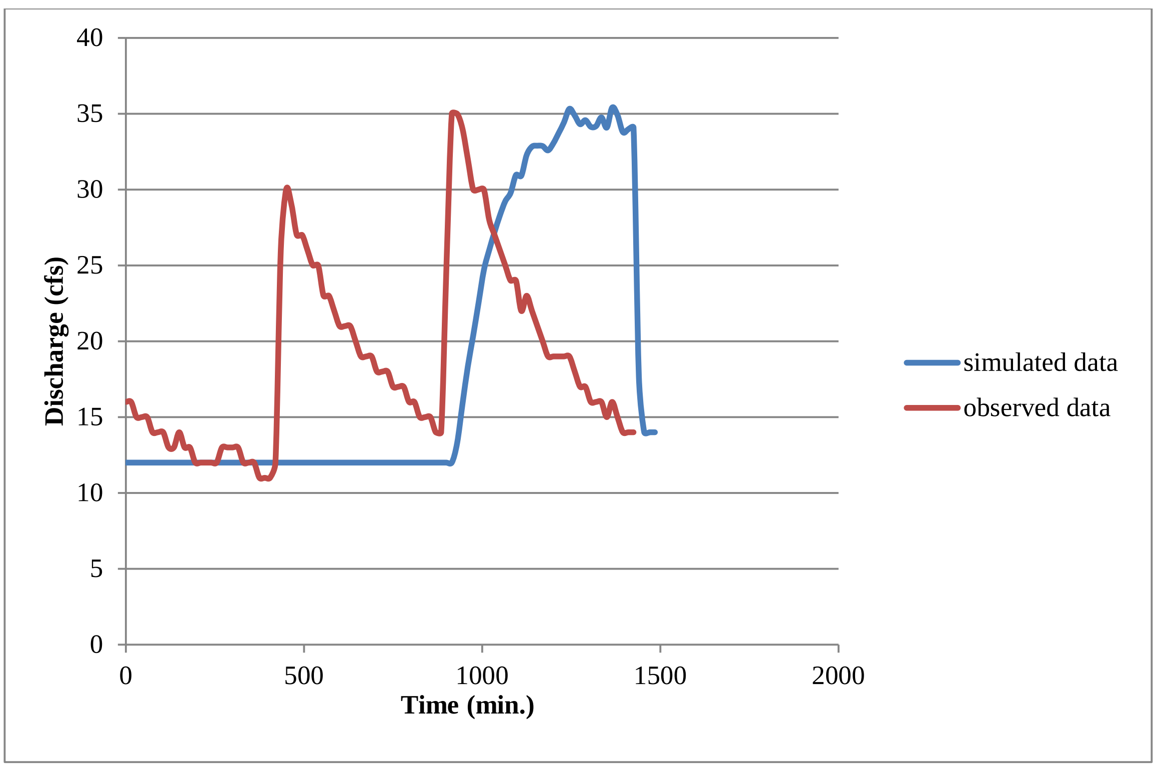

Figure 3.22 Results from new rainfall distribution for 4/27/12 for basin 16345000

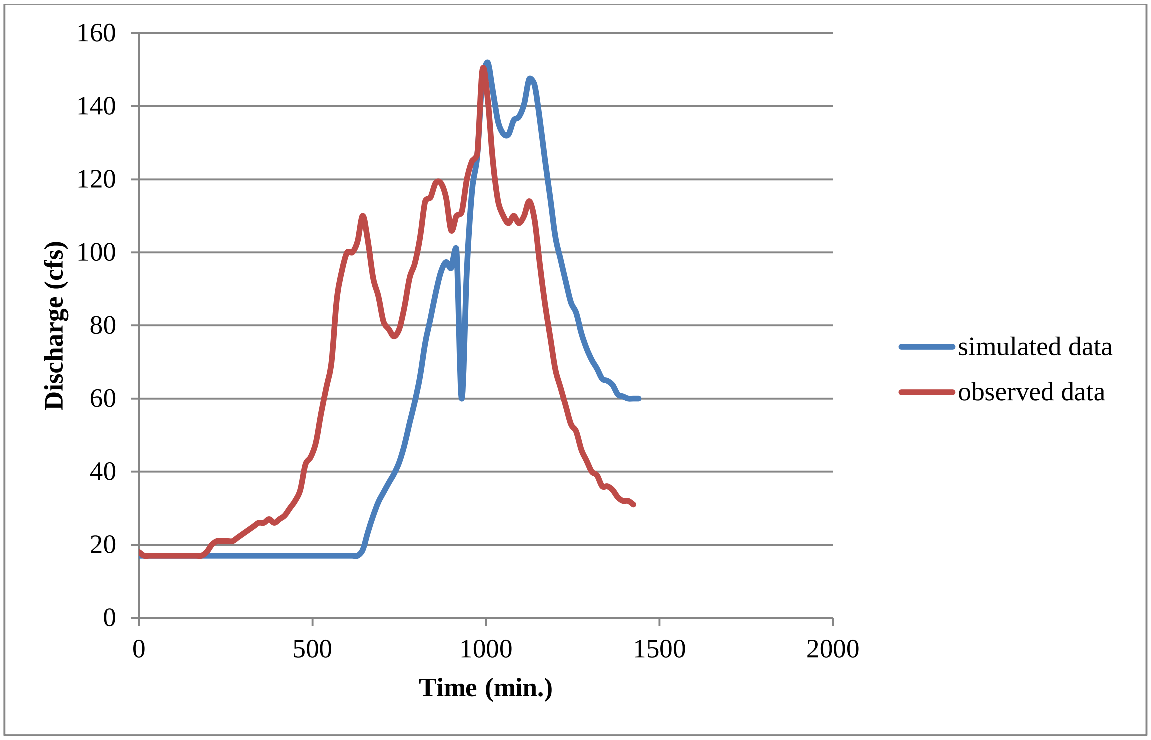

Figure 3.23 Results from new rainfall distribution for 1/5/13 for basin 16200000

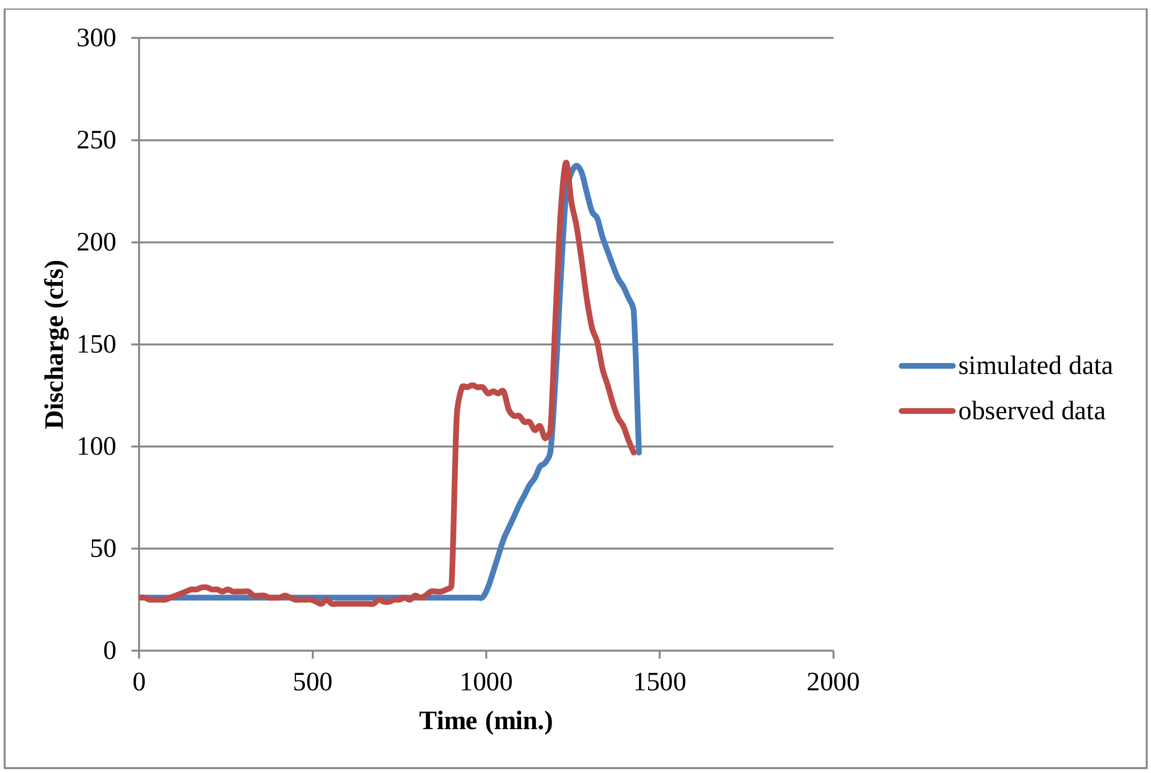

Figure 3.24 Results from new rainfall distribution for 1/5/13 for basin 16345000

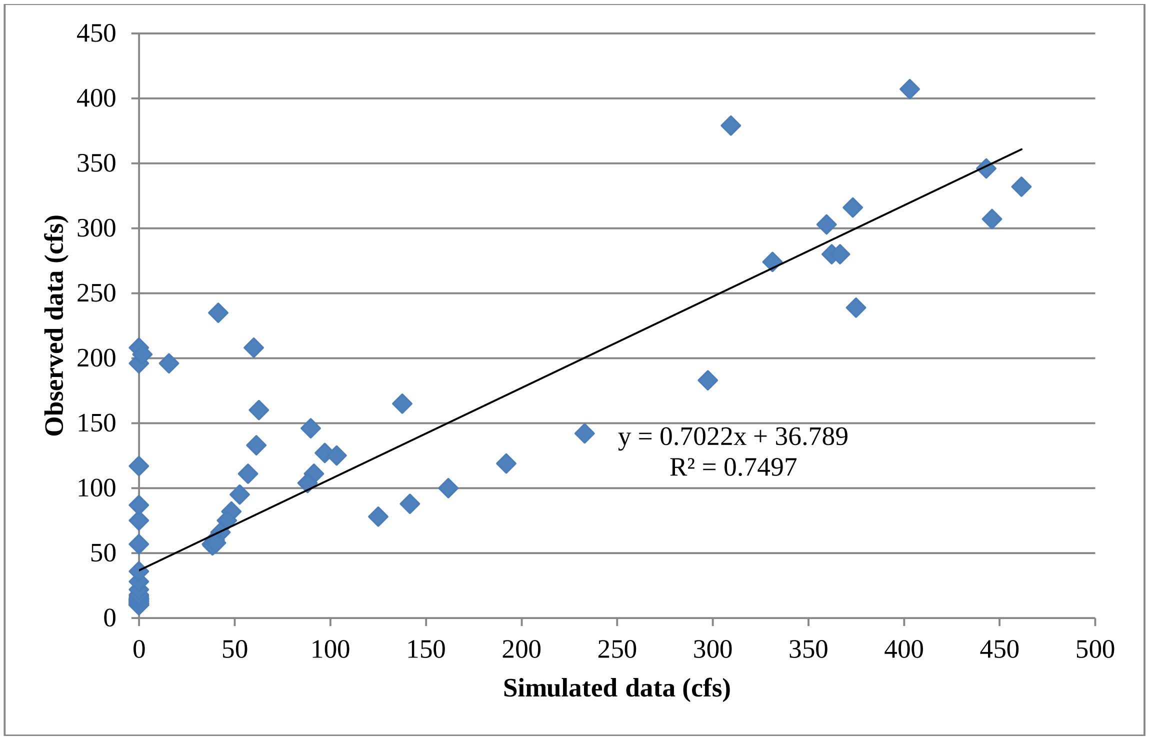

Figure 3.25 Simulated and observed data on 3/2/2012 for basin 16200000 from alternative rainfall distribution

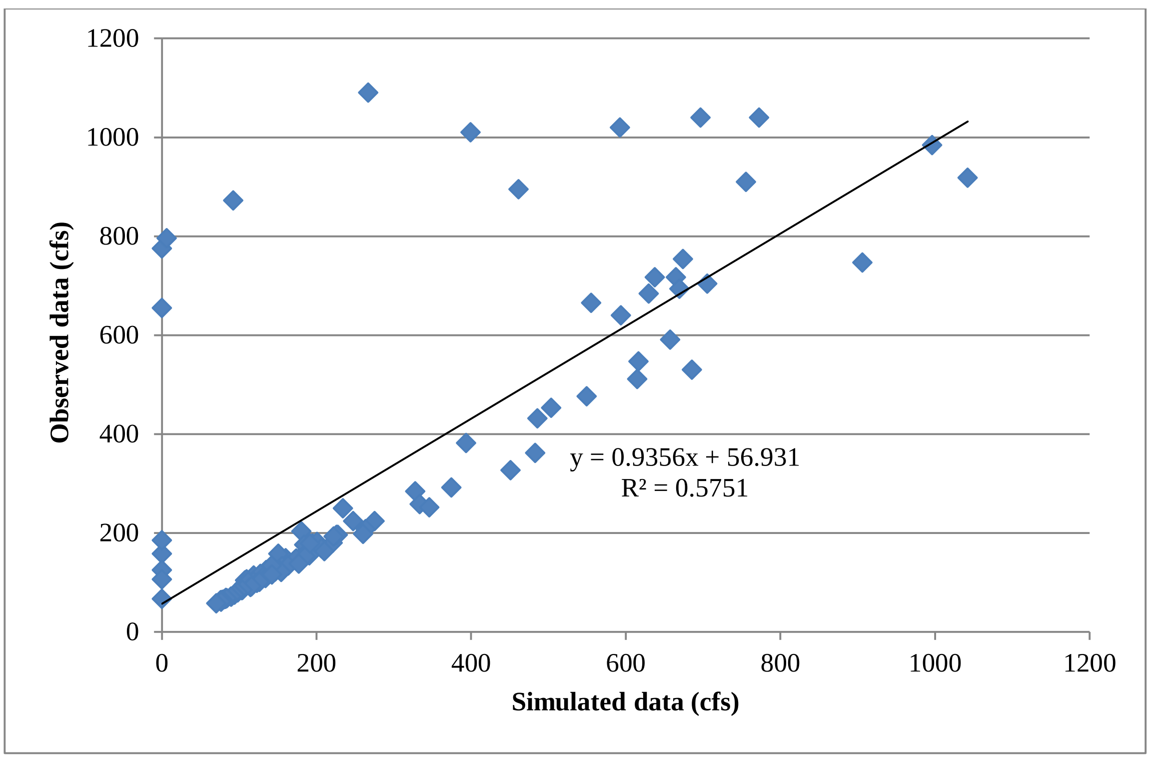

Figure 3.26 Simulated and observed data on 3/4/2012 for basin 16200000 from alternative rainfall distribution

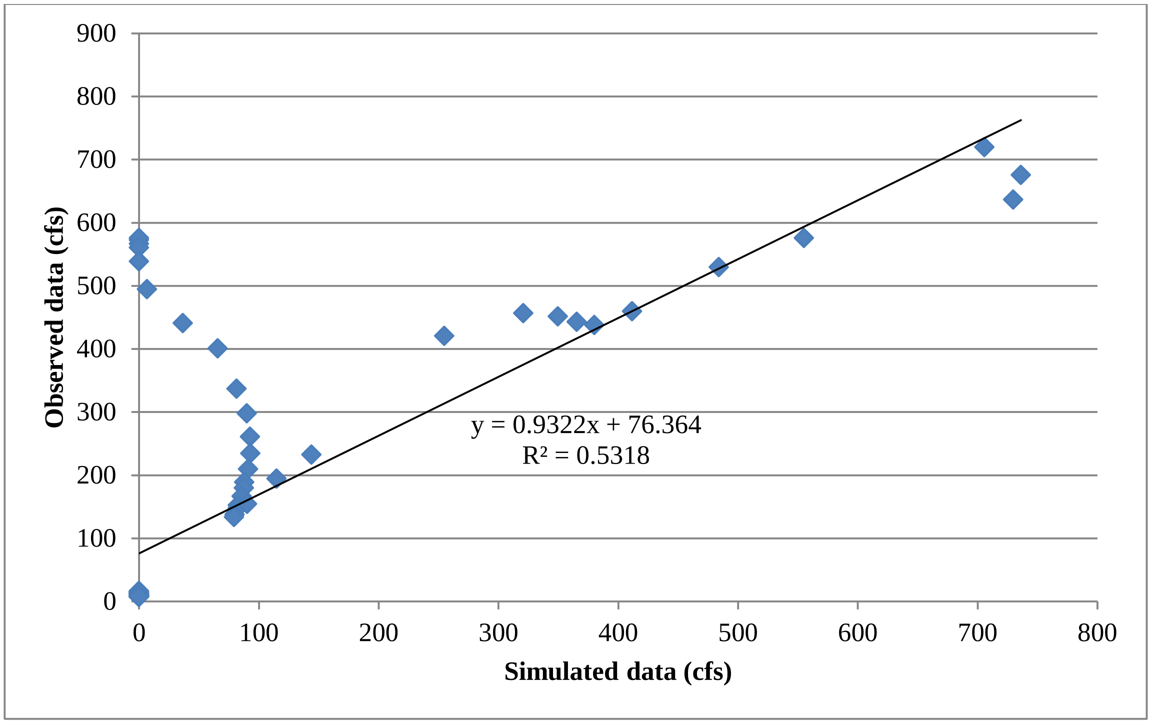

Figure 3.27 Simulated and observed data on 3/2/2012 for basin 16345000 from alternative rainfall distribution

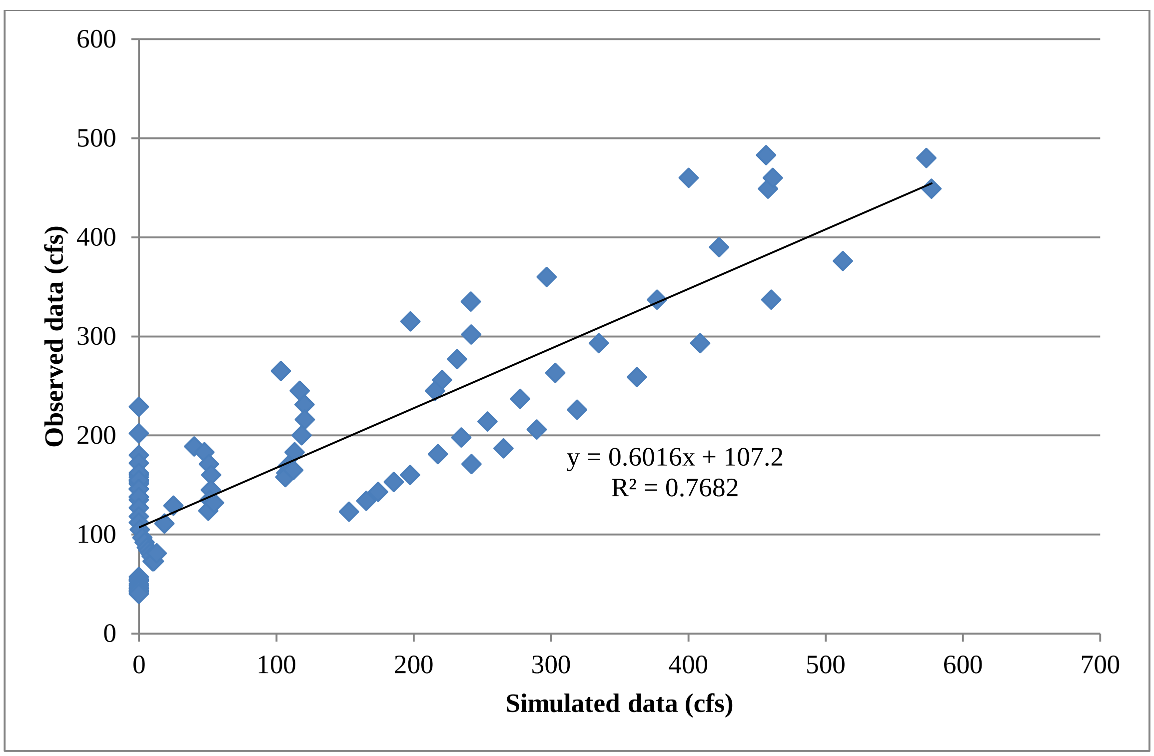

Figure 3.28 Simulated and observed data on 3/4/2012 for basin 16345000 from alternative rainfall distribution

3.2 STREAMFLOW HYDROGRAPHS WITH AND WITHOUT FLOOD BASINS

Figures 3.29 through **3.32** display the hydrographs generated at the outlets at the four hypothetical flood retention basins (R1 through R4, respectively), with and without such basins. **Figure 3.33** displays the hydrographs produced at the existing Lake Wilson/Wahiawa Reservoir (R5). **Figures 3.29** and **3.31** shows the options to have one or two flood retention basins for each outlet, with obviously lower peaks and less flooding potential for the case with two basins. **Figures 3.30** and **3.32**, on the other hand, display the option to have only one basin for each. **Table 3.5** lists the peak discharge values for R1 through R5 before and after the flood retention basins were applied.

Table 3.5 Summary of peak streamflows with and without flood retention basins

Location of outlet	Original peak (without retention basins) (cfs)	Option	Peak (with retention basins) (cfs)	Percent peak reduction
R1	19468	R1	13880	29
		R1+R2	7176	63
R3	4826	R3	4188	13
		R3+R4	2913	40
R2	6101	R2	1587	74
R4	3175	R4	2880	9
R5	15105	R5	12947	14

The discharge values from flood retention basin R1 indicate that each of the highest peak flows differ by approximately 5,000 cfs. In **Figure 3.30**, the first peak flow varies by a rate of roughly 4,000 cfs. **Figure 3.31** illustrates that the peak flow values differ by less than 1000 cfs, while the peak flows in **Figure 3.32** diverge by less than 500 cfs. The simulated flows presented for R5 are consistent with that of the calibration performed previously in the 2008 KBW watershed assessment (Yost et al., 2009).

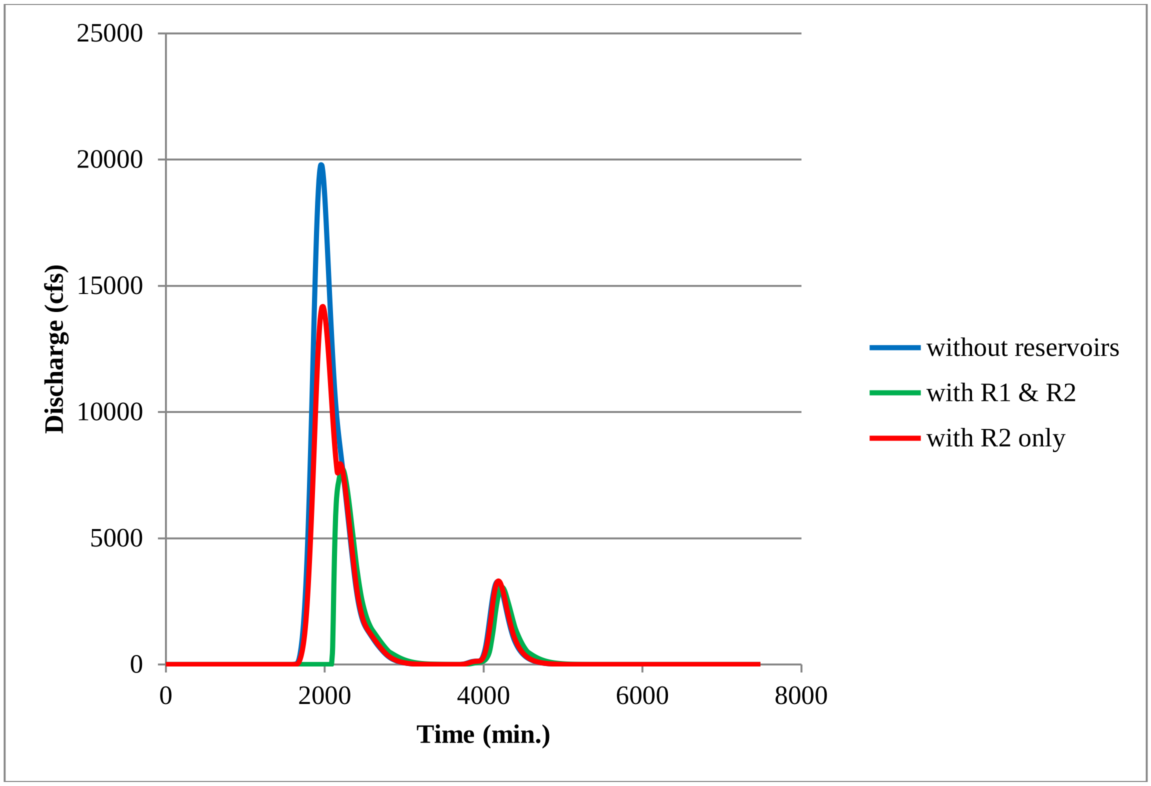

Figure 3.29 Simulated hydrographs at R1

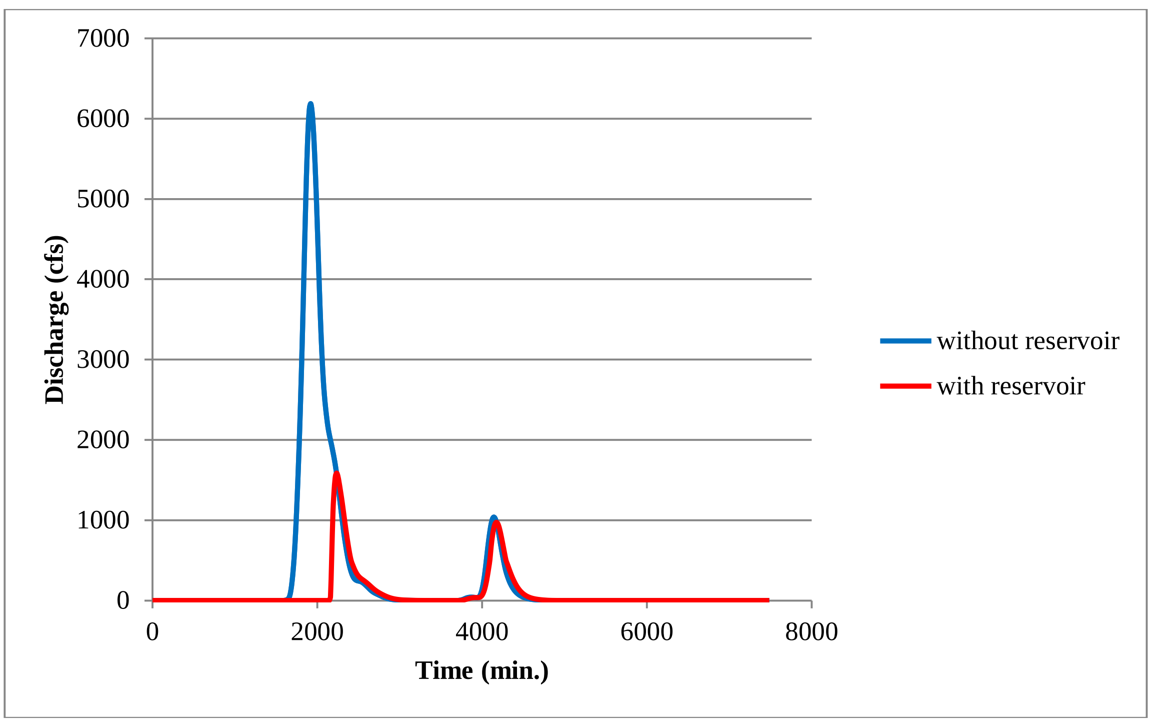

Figure 3.30 Simulated hydrographs at R2

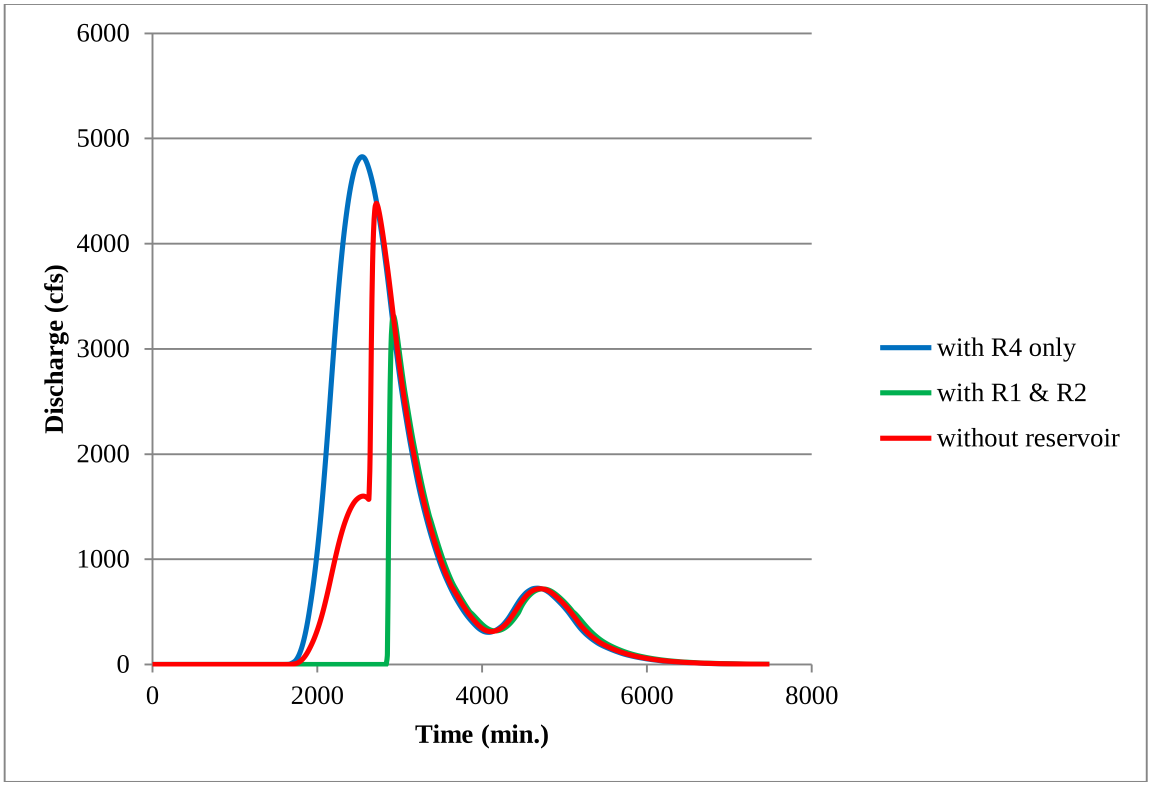

Figure 3.31 Simulated hydrographs at R3

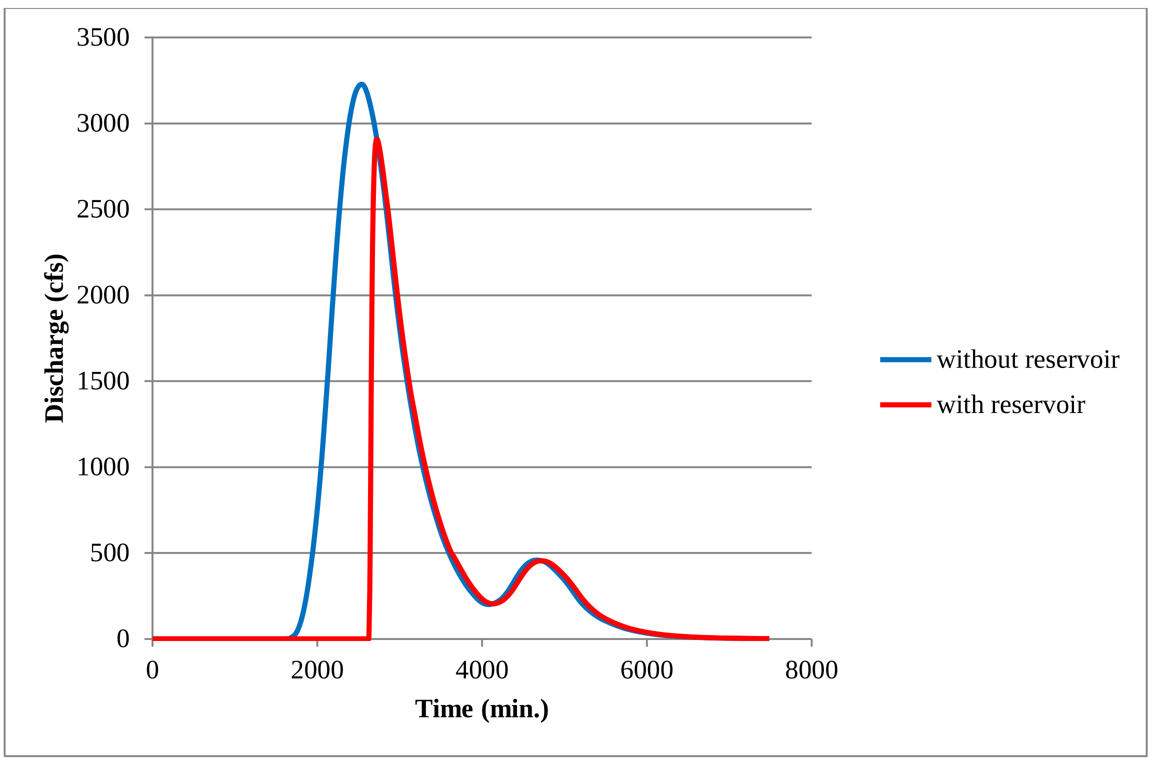

Figure 3.32 Simulated hydrographs at R4

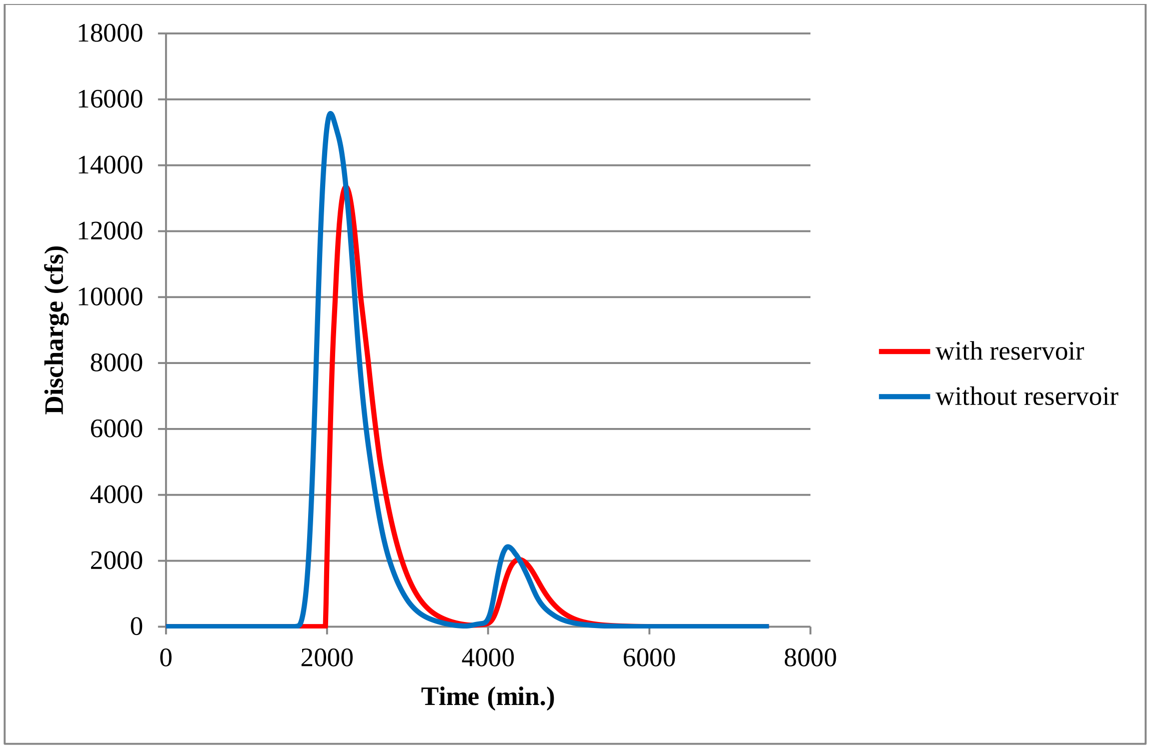

Figure 3.33 Simulated hydrographs at R5

3.3 FLOOD DEPTHS AT DIFFERENT STREAM REACH CROSS-SECTIONS

Figure 2.27 displays the locations of cross-sections for various stream reaches within the floodplain. As described in Section 2.3, the model HEC-RAS was used to assess flooding in the area shown in **Figure 2.26**, based on peak streamflows estimated by HEC-1. HEC-RAS estimates water levels at various sections as well as the extent of the flooding zone. The bar graph in **Figure 3.34** displays the maximum flood depths at each cross-section of the floodplain with and without the flood retention basins R1, R2, R3, and R4. For the case with flood retention basins, the figure also compares the initial flood depths, based on full discharges, against those estimated with discharge values that were reduced by factors of 1/2, 1/3, 1/4, and 1/10 of the peak flows from the initial hydrographs.

As expected, the maximum flood depths at nearly all the cross-sections decreased as discharge values were reduced. The overall maximum flood depth occurred at station 805.570 in reach 8, where the water level was roughly 34 feet. Reach 1 at station 752.158 displayed the lowest average values.

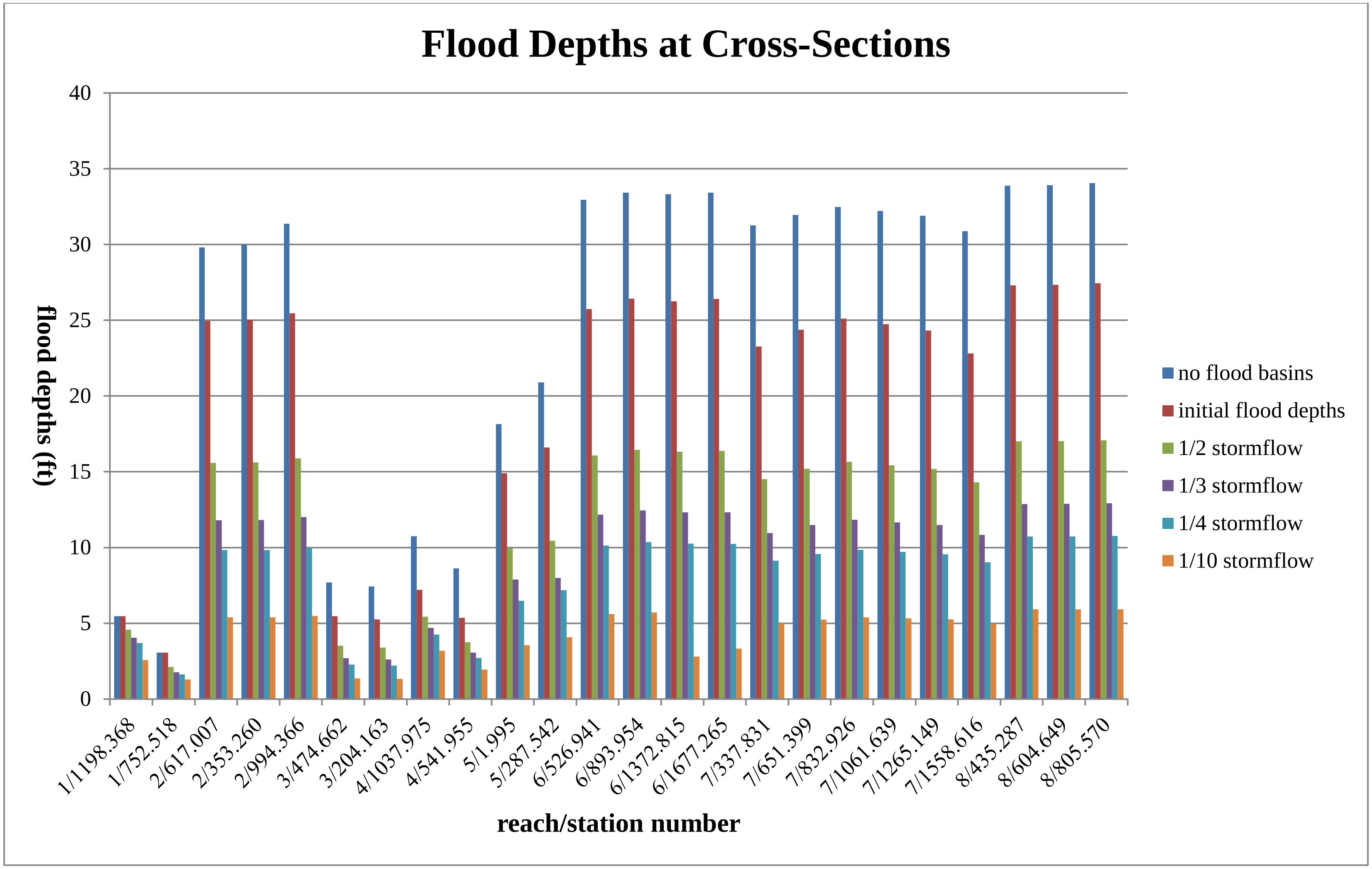

Figure 3.34 Water levels at cross-sections produced from different discharge values. Initial flood depth denotes those estimated by HEC-1 streamflow values. For comparison, others refer to fractions of such streamflow values

3.4 FLOOD ZONE DELINEATIONS

Figures 3.35 through **3.46** illustrate the flood zones within KBW that were delineated by using HEC-RAS for various cases. The maps display different flood zones with water depth contour lines, and with flood boundaries at the 0.1ft contour. For each case, a set of two figures is provided. The first shows detailed contours, while the second superimposes these contours on the geographic area map. These figures include delineations created from scenarios where various values of discharge were used. Obviously, the size of the flooded area is reduced as the discharge value decreases. In the absence of flood basins (Figures 3.35 and 3.36), the majority of the floodplain is subjected to a water level at its maximum height. In comparison with Figures 3.37 and 3.38, a considerable reduction resulted with the four flood retention basins implemented into the HEC-1 simulations, for both the size of the flood zone and values of water levels.

From visually analyzing the results, the greatest level of flooding occurs along the Ki‘iki‘i Stream but is generally concentrated in Kemo‘o Camp (where Ki‘iki‘i Stream ends), just outside of Wahiawa. This area shares the same location with reaches 6 and 8, situated farthest from Kaiaka Bay, and which displayed the greatest overall flood elevations according to the histogram in Figure 3.34. Reach 1 located on the opposite end closer to the Ko‘olau mountains and at the terminus of Paukauila Stream generally exhibited the smallest flood elevations for all scenarios. Based on a topographic map of the floodplain region, the land elevation at reaches 6 and 8 is lower than its surrounding terrain. Reach 1 is positioned where the terrain becomes gradually steeper (see background map in flood depth figures). As expected, and which can also be seen from the following figures, steeper terrain towards the periphery of the floodplain will exhibit less flooding (blue regions) than flat land situated closer to the ocean (green regions).

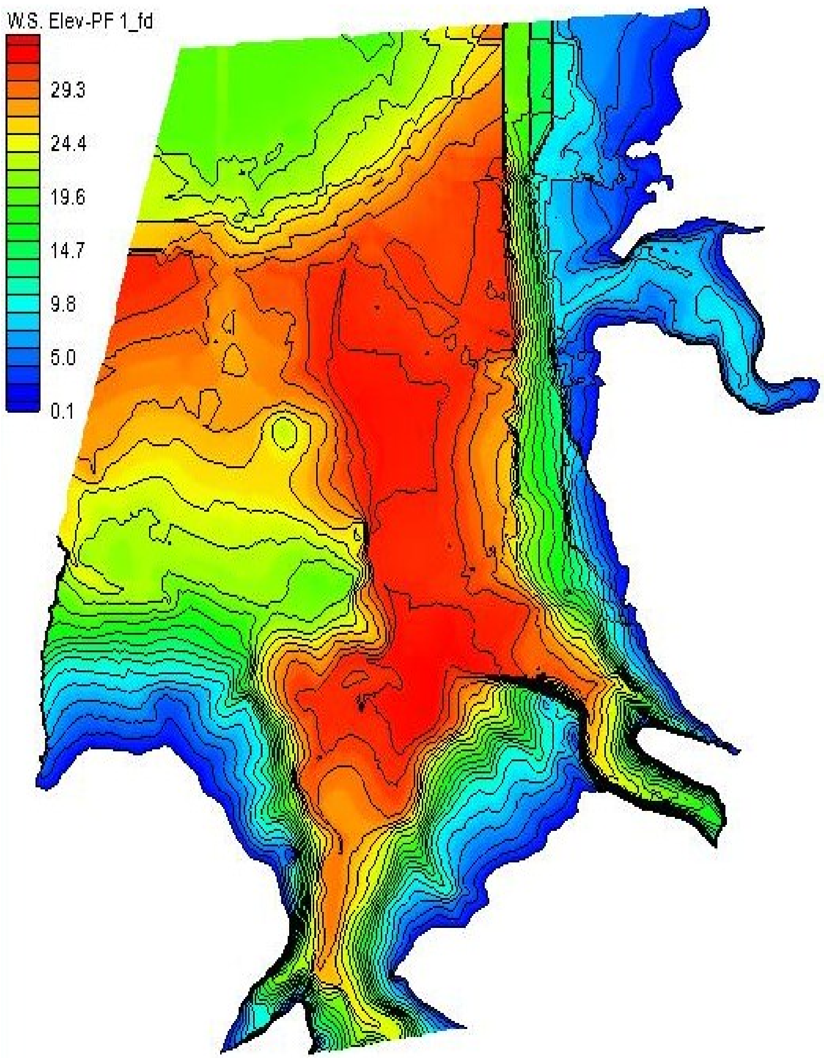

Figure 3.35 Flood depths with no flood basins

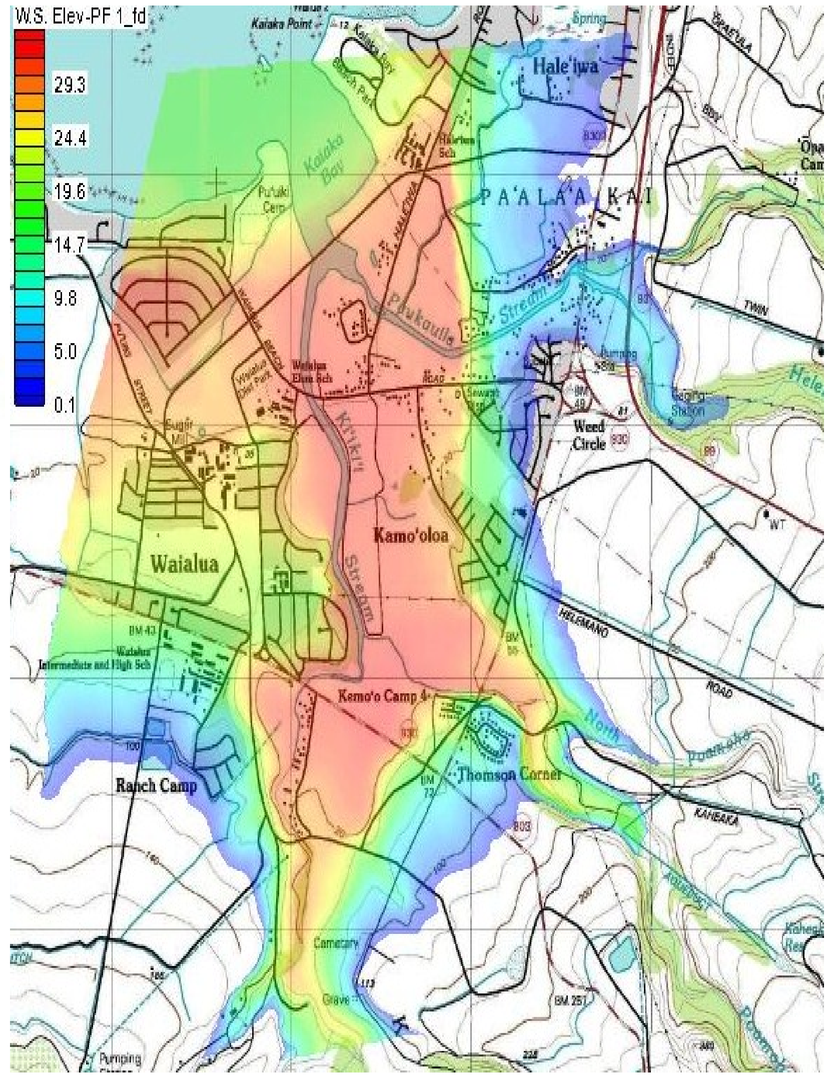

Figure 3.36 Flood depths with no flood basins & background

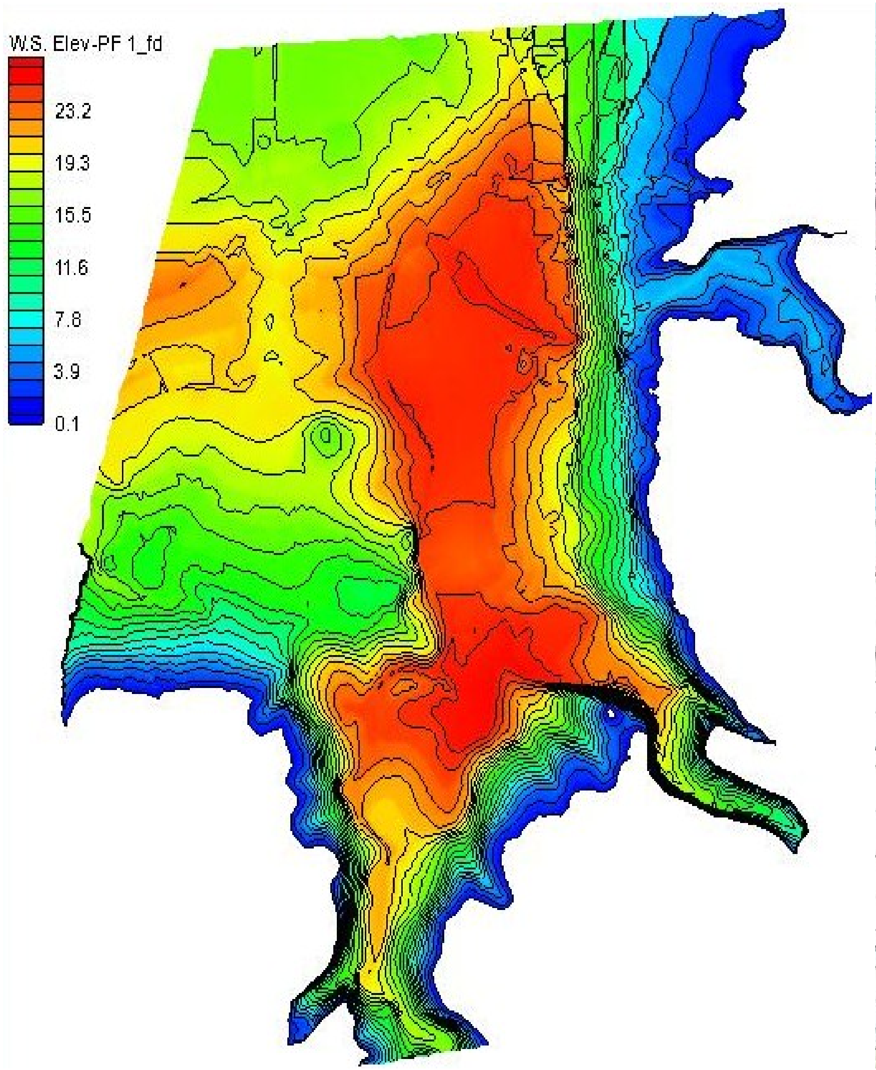

Figure 3.37 Initial flood depths with flood basins

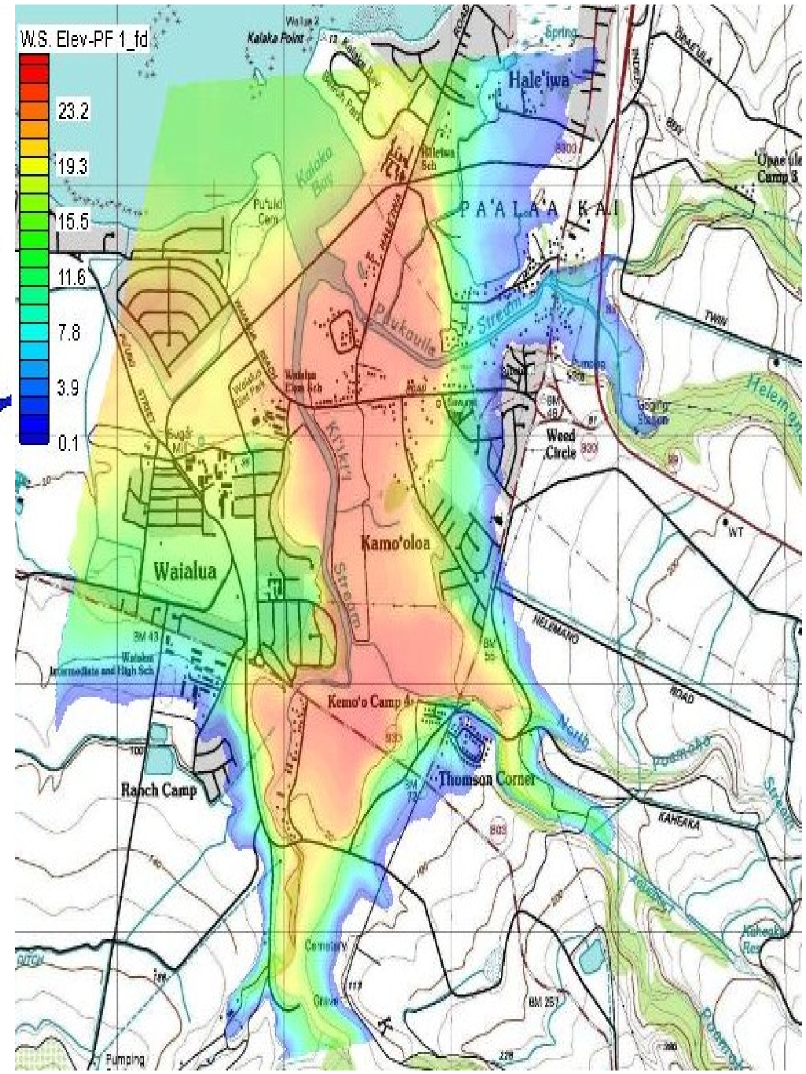

Figure 3.38 Initial flood depths with flood basins & background

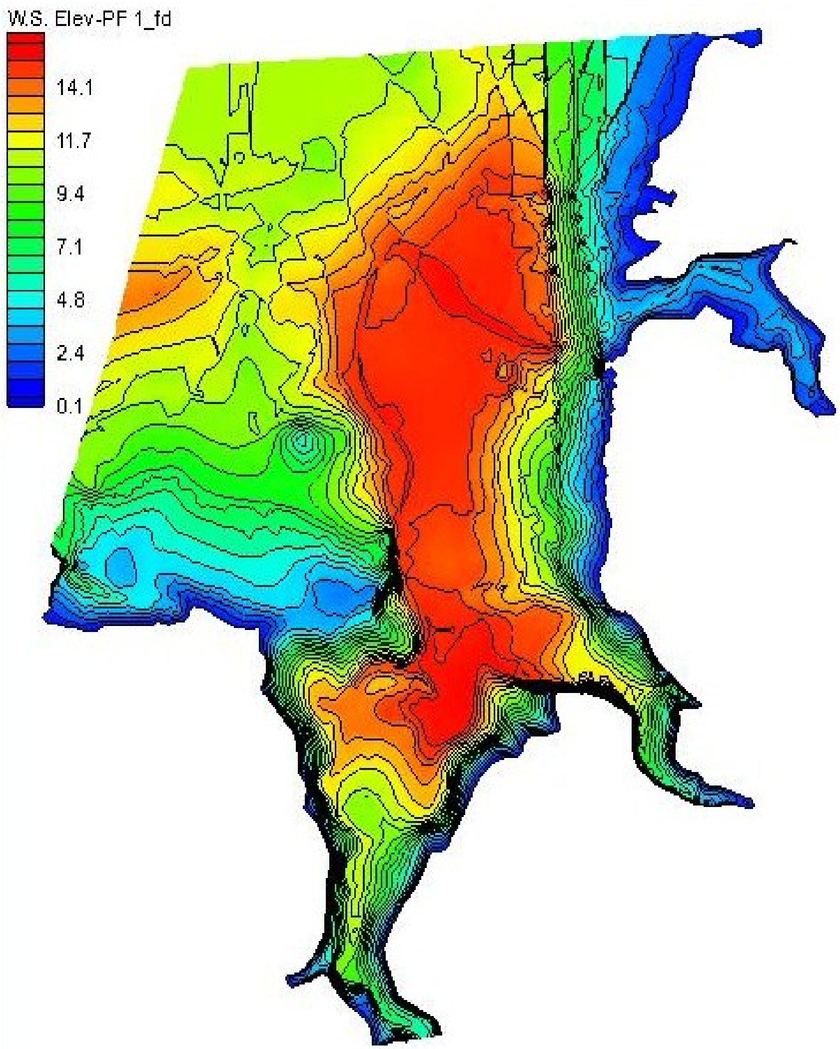

Figure 3.39 Flood depths from 50% of initial peak flow

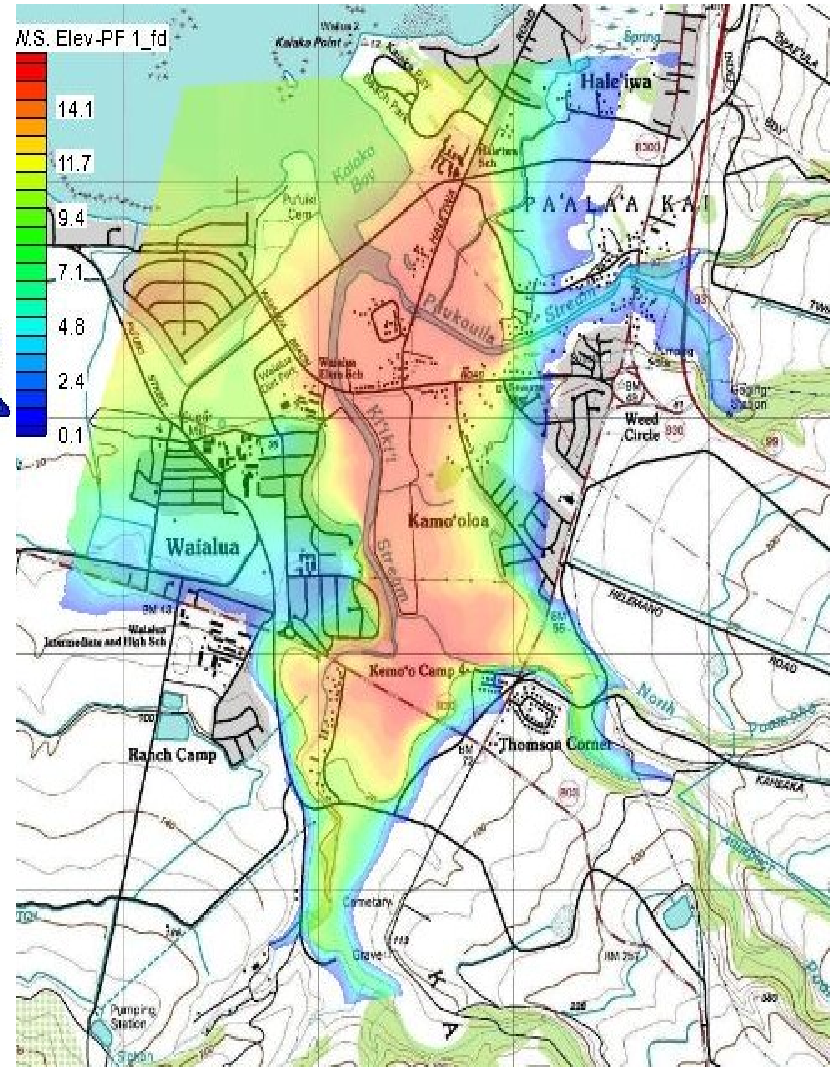

Figure 3.40 Flood depths from 50% of initial peak flow & background

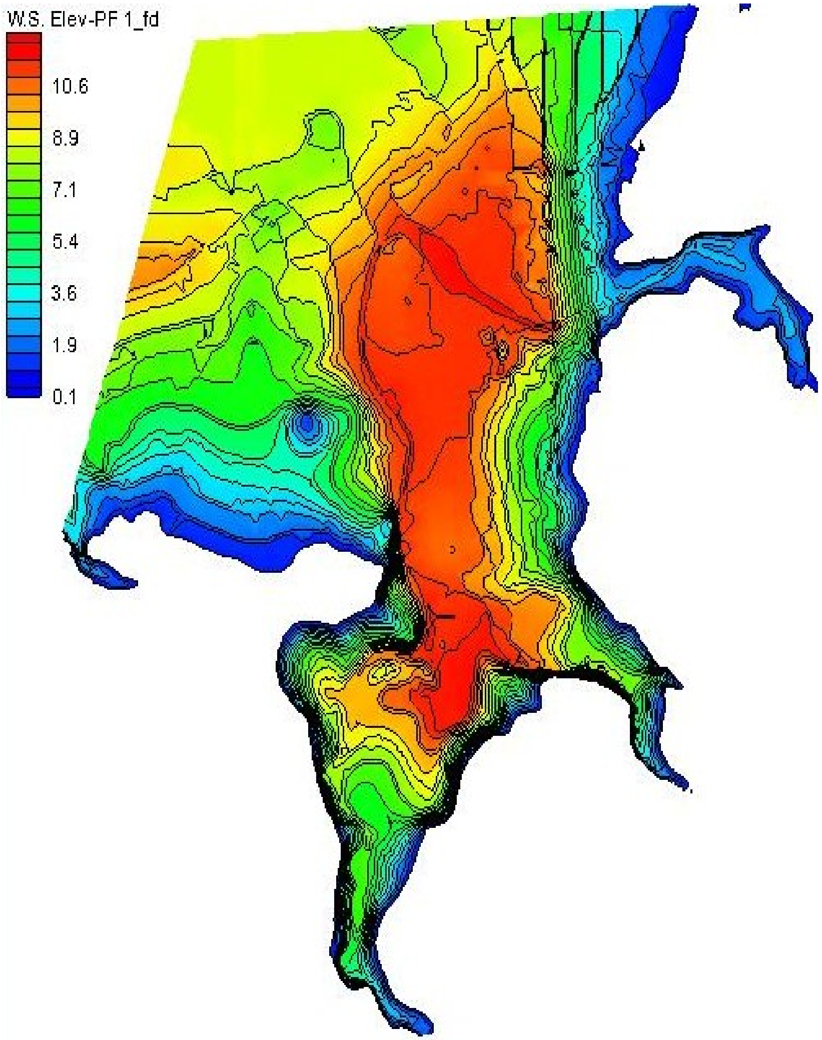

Figure 3.41 Flood depths from 33% of initial peak flow

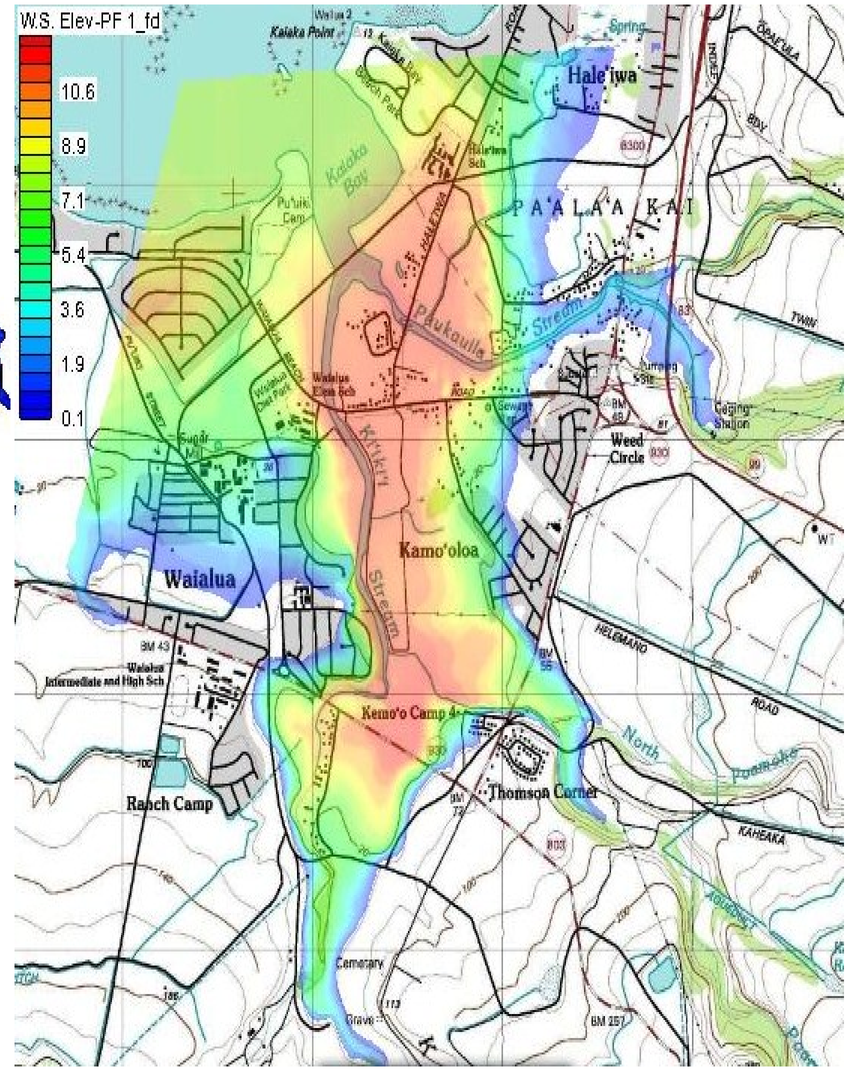

Figure 3.42 Flood depths from 33% of initial peak flow & background

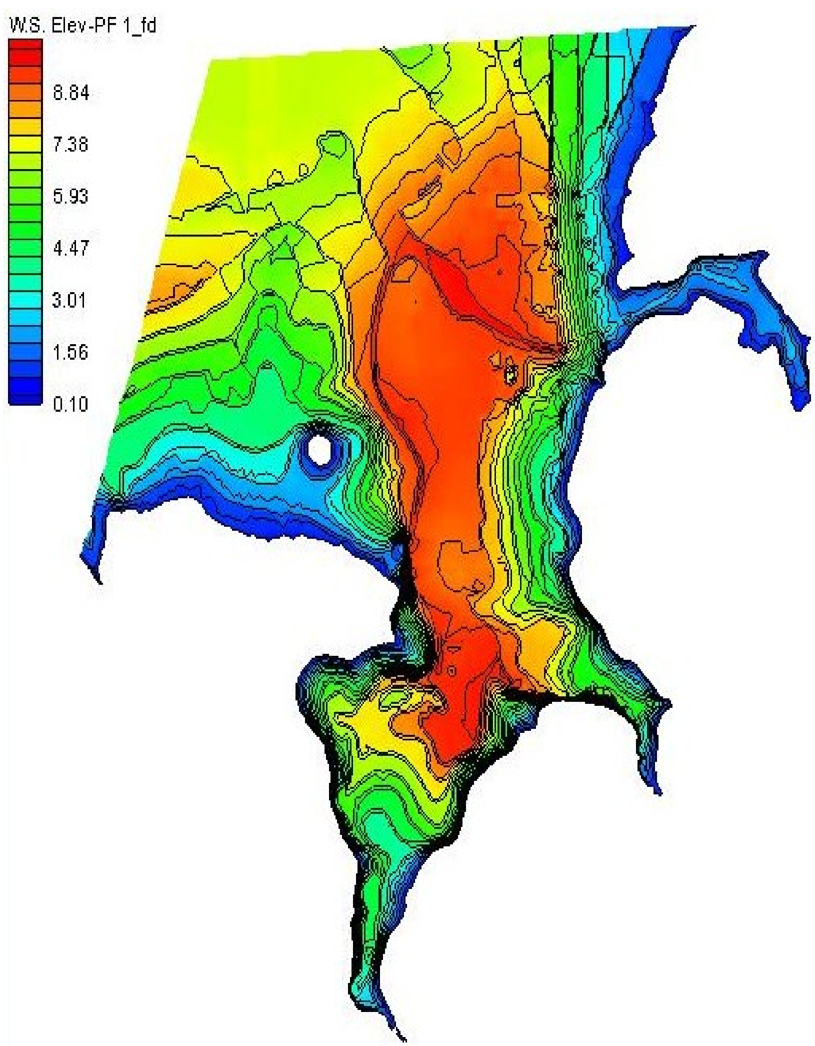

Figure 3.43 Flood depths from 25% of initial peak flow

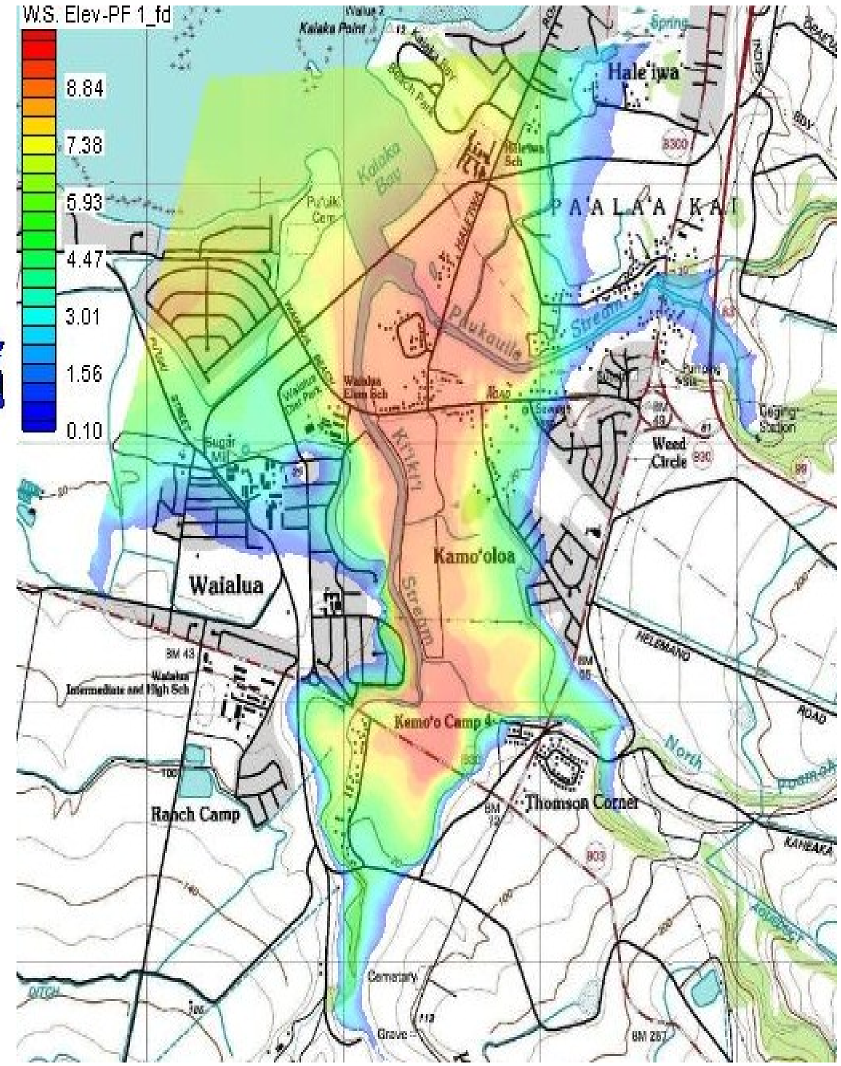

Figure 3.44 Flood depths from 25% of initial peak flow & background

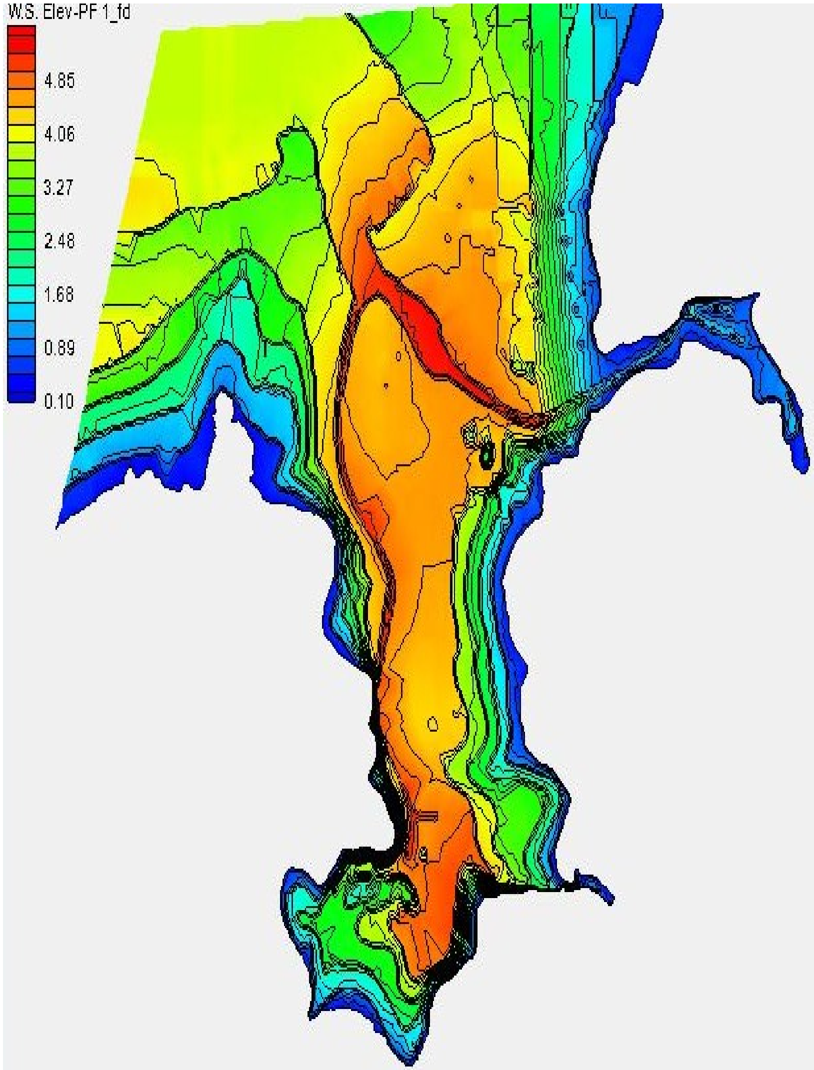

Figure 3.45 Flood depths from 10% of initial peak flow

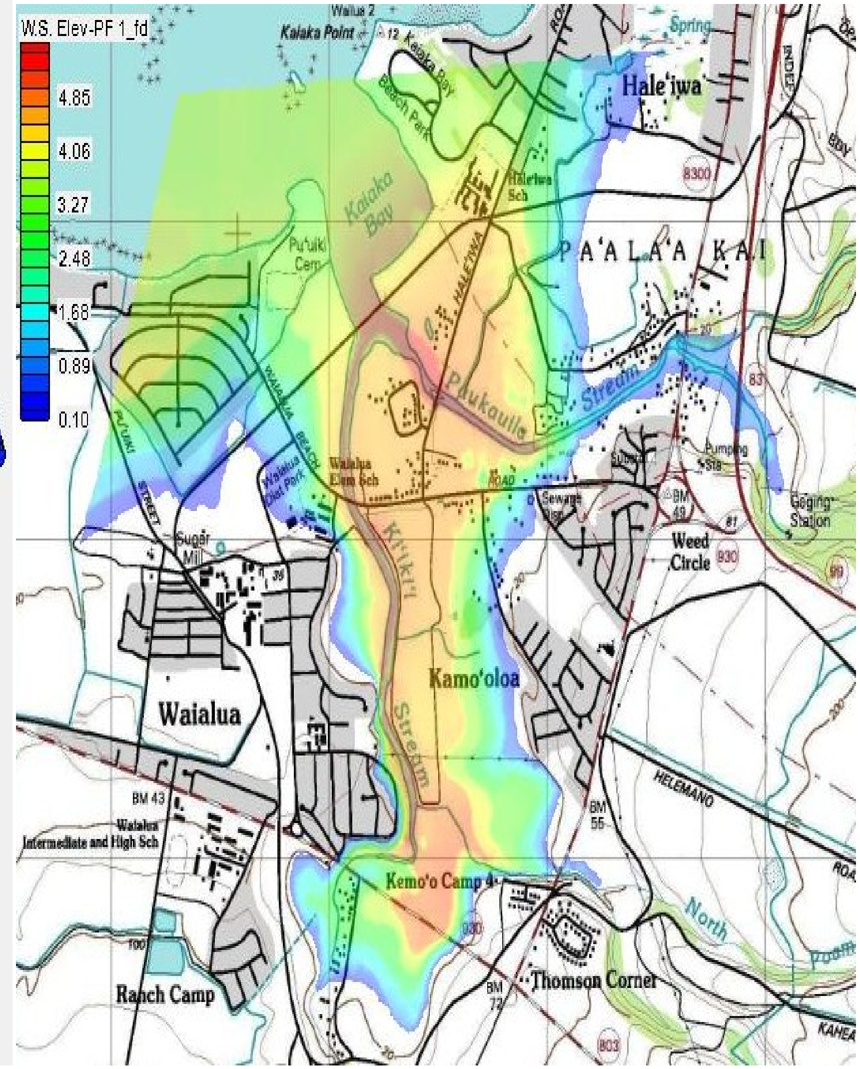

Figure 3.46 Flood depths from 10% of initial peak flow & background

Figure 3.47 displays the reaches in the floodplain region for which flood depths were calculated by HEC-RAS.

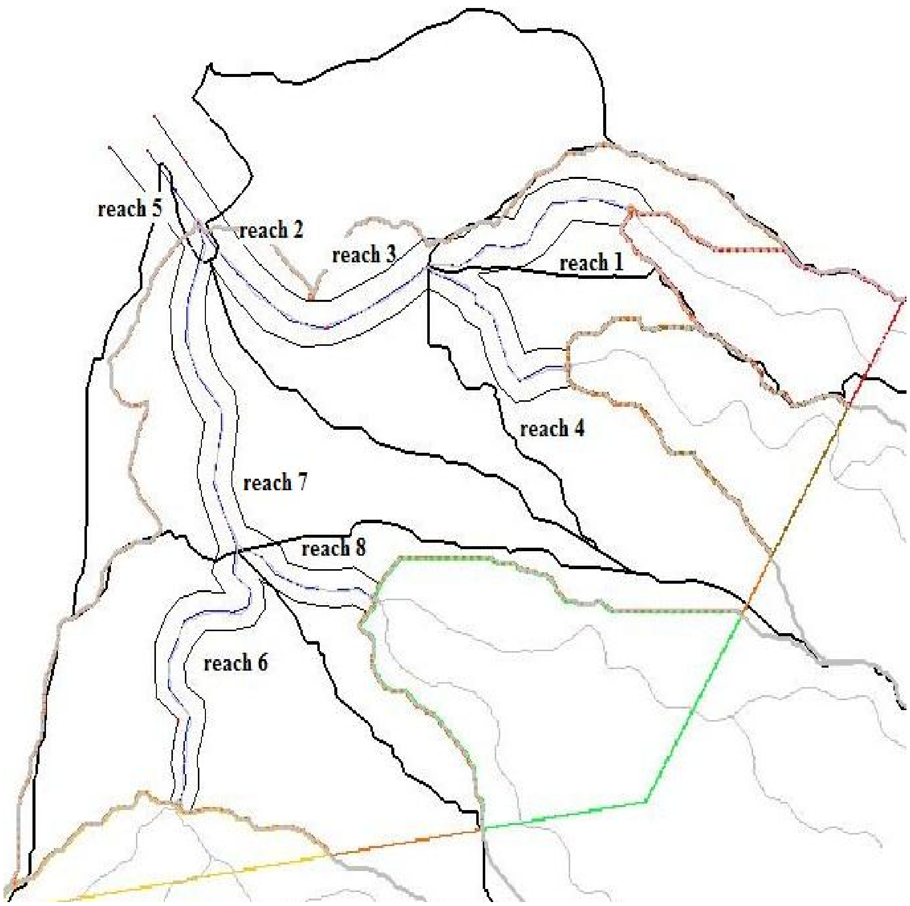

Figure 3.47 Reaches contained within the floodplain

Table 3.6 lists the flow rates for reaches 1 through 8 in **Figure 3.47** under the different scenarios. The table also lists estimated peak streamflows that were calculated by using the USGS Hawai‘i StreamStats application (U.S. Geological Survey, 2013). StreamStats estimated peak flow for 100-year floods for un-gauged stations, or stream outlets, using regression equations. Comparing these estimates against HEC-1's results (labeled as peak flows without flood basins) shows mixed results. HEC-1 overestimates the flow for reaches 2, 3, and 4, and underestimates the values for reaches 1, 5, 6, 7, and 8. **Figure 3.48** depicts the FEMA flood zones color-filled according to a 100-year flood.

The description of each zone in the legend can be viewed in Appendix B, **Table B-2**. **Figures 3.49** to **3.54** show the FEMA flood zones (black lines) compared against the color-filled flood zones generated from the different data sets generated by HEC-RAS. Various streamflows' scenarios are displayed. HEC-RAS overestimates the delineated flood area for the initial peak flows. Apart from the Waialua area, in the north- west side of the map, one third of the initial peak flows seem to produce flood zones that match those provided by FEMA. The results thus indicate that HEC-1 predicts higher estimates for streamflows compared with those used by FEMA. Based on the comparisons in Table 3.6, it seems, however, that StreamStats predicts even higher estimates than HEC-1. In theory, HEC-1 is more accurate considering that it is physically based, yet inaccuracies can result from the lack of accurate input including rainfall. There is a need thus to assess various methods to reconcile these diverse approaches in estimating the 100-year flood peak flows.

Table 3.6 Peak Flow Rates used in HEC-RAS simulations for different stream reaches shown in Figure 3.47

Reach Number	**Reach Station**	**Flow Rates (cfs)**						
		Peak flow with no flood basins	**Peak flows estimated by StreamStats for 100-year flood**	**With flood basins**				
				initial peak flow	**1/2 peak flow**	**1/3 peak flow**	**1/4 peak flow**	**1/10 peak flow**
reach_1	1198.368	3313	8700	3313	1657	1093	828	331
reach_2	994.366	23776	18500	12132	6066	4003	3033	1213
reach_3	474.662	23776	18500	12132	6066	4003	3033	1213
reach_4	1037.975	20463	14400	8818	4409	2910	2205	882
reach_5	287.542	46397	50500	32893	16446	10855	8223	3289
reach_6	1677.26	16902	25600	16440	8220	5425	4110	1644
reach_7	1558.616	22622	32000	20761	10380	6851	5190	2076
reach_8	805.570	5719	13900	4321	2160	1426	1080	432

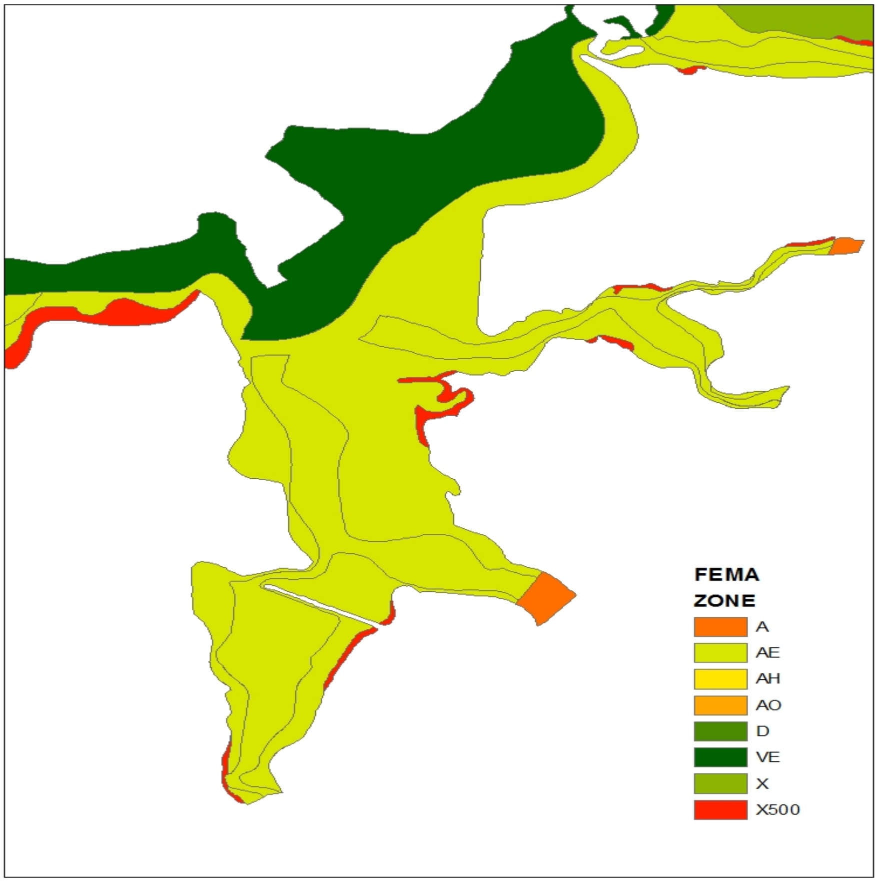

Figure 3.48 FEMA flood zones from 100-year flood

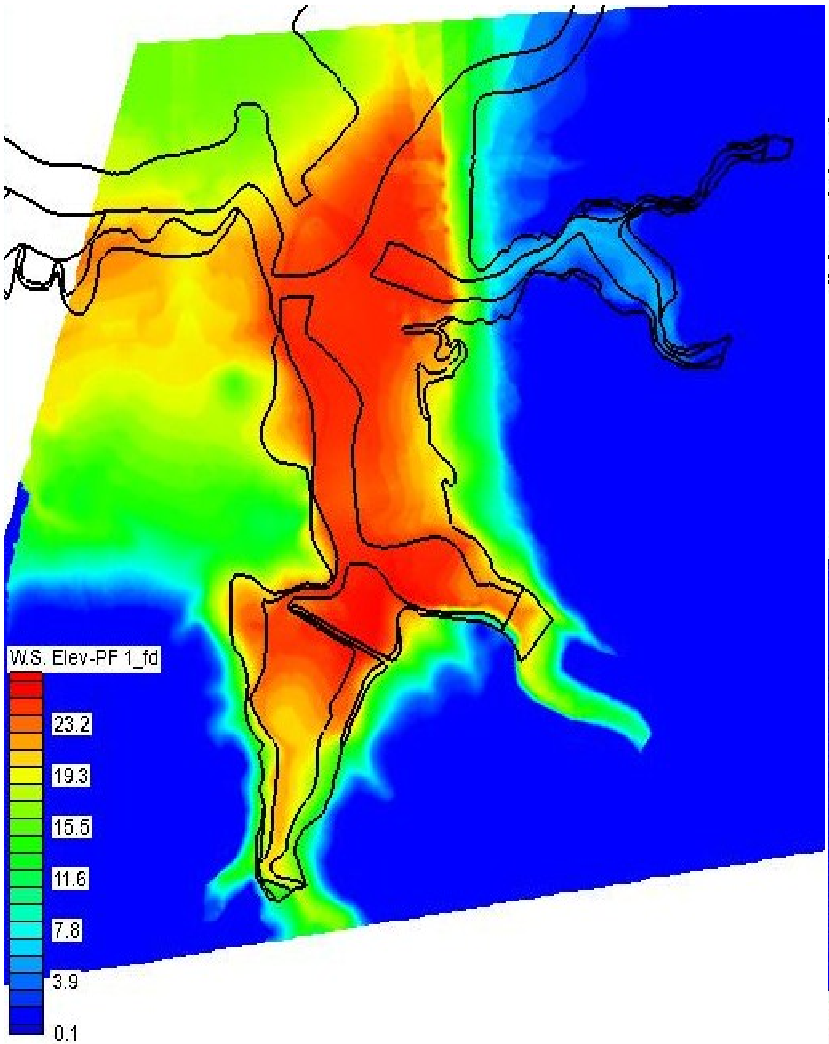

Figure 3.49 FEMA zones & flood depths with no flood basins

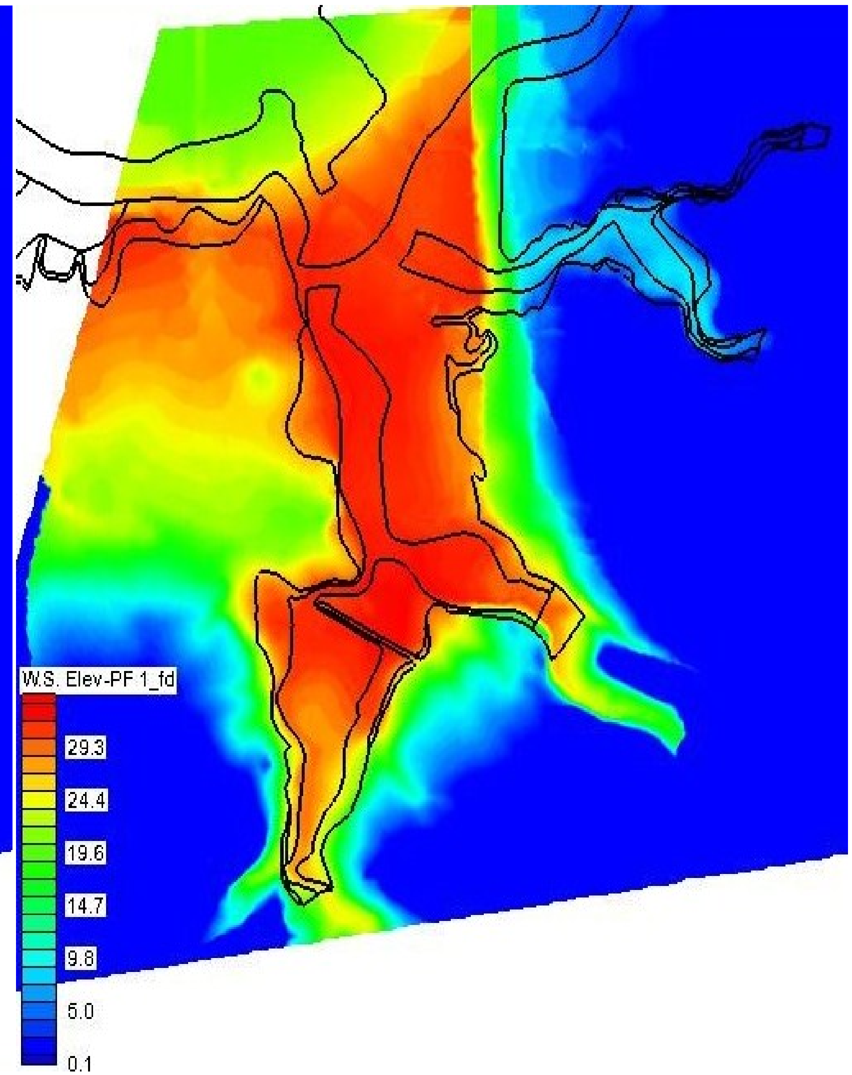

Figure 3.50 FEMA zones & flood depths from initial peak flow with flood basins

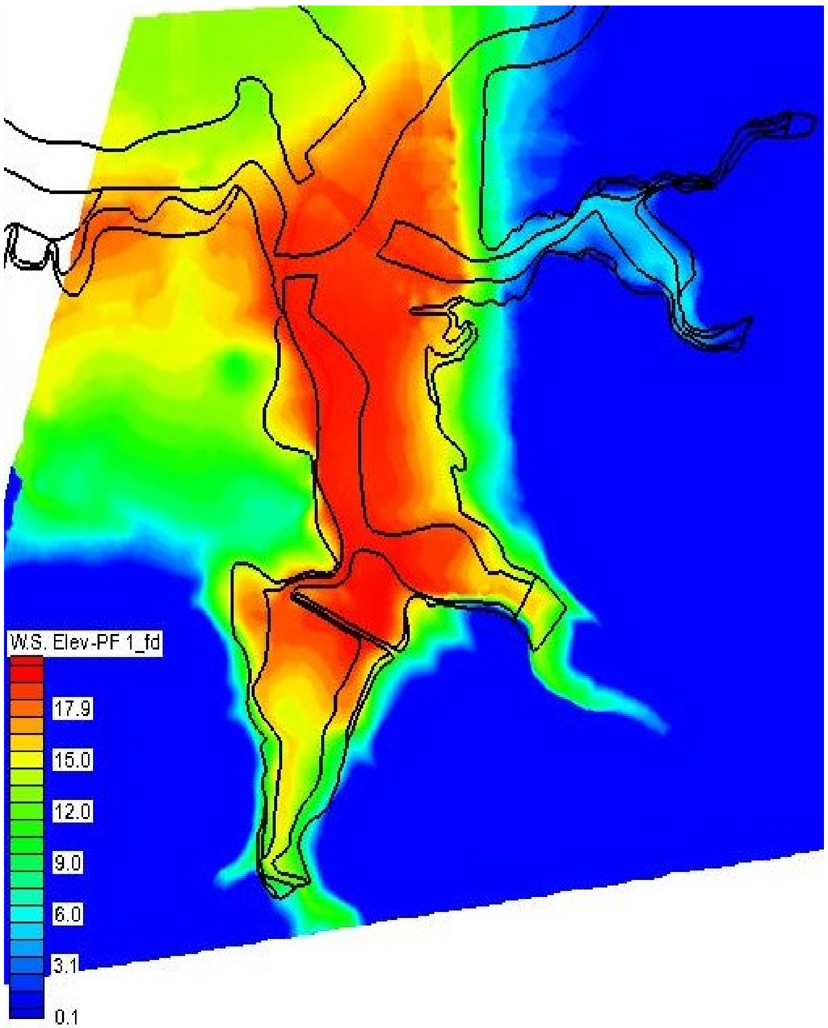

Figure 3.51 FEMA zones & flood depths from 50% of initial peak flow with no flood basins

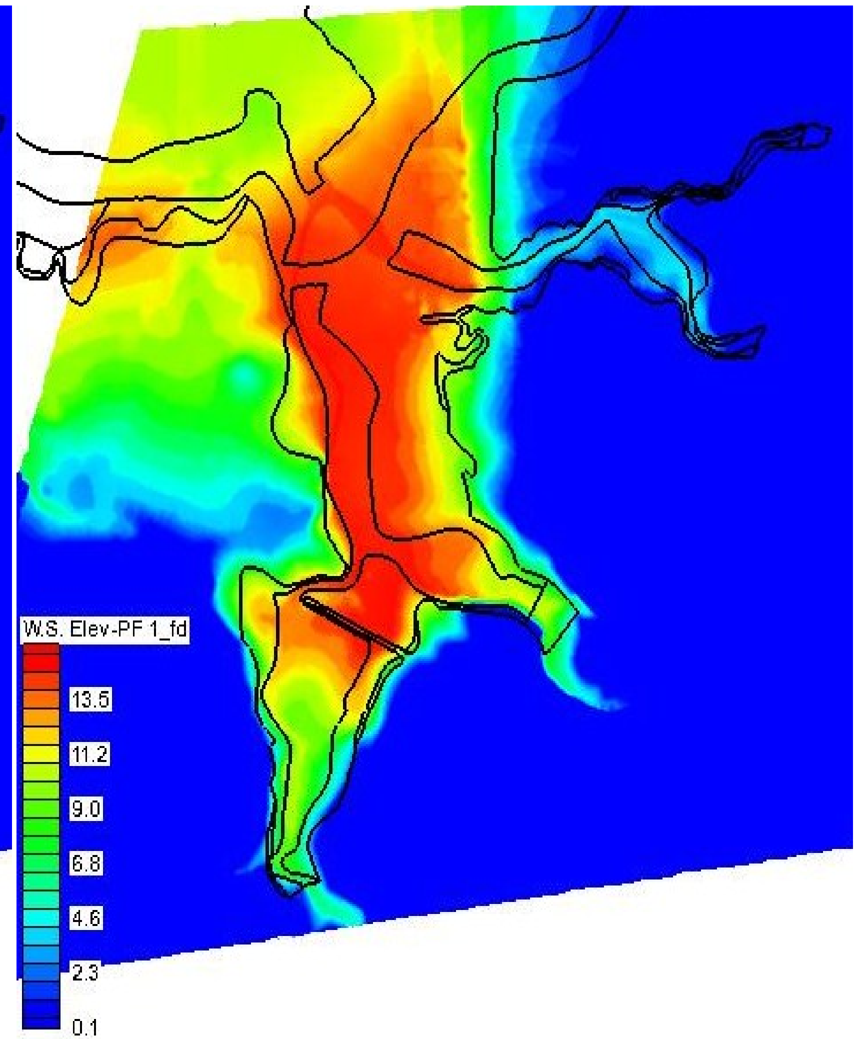

Figure 3.52 FEMA zones & flood depths from 33% of initial peak flow with no flood basins

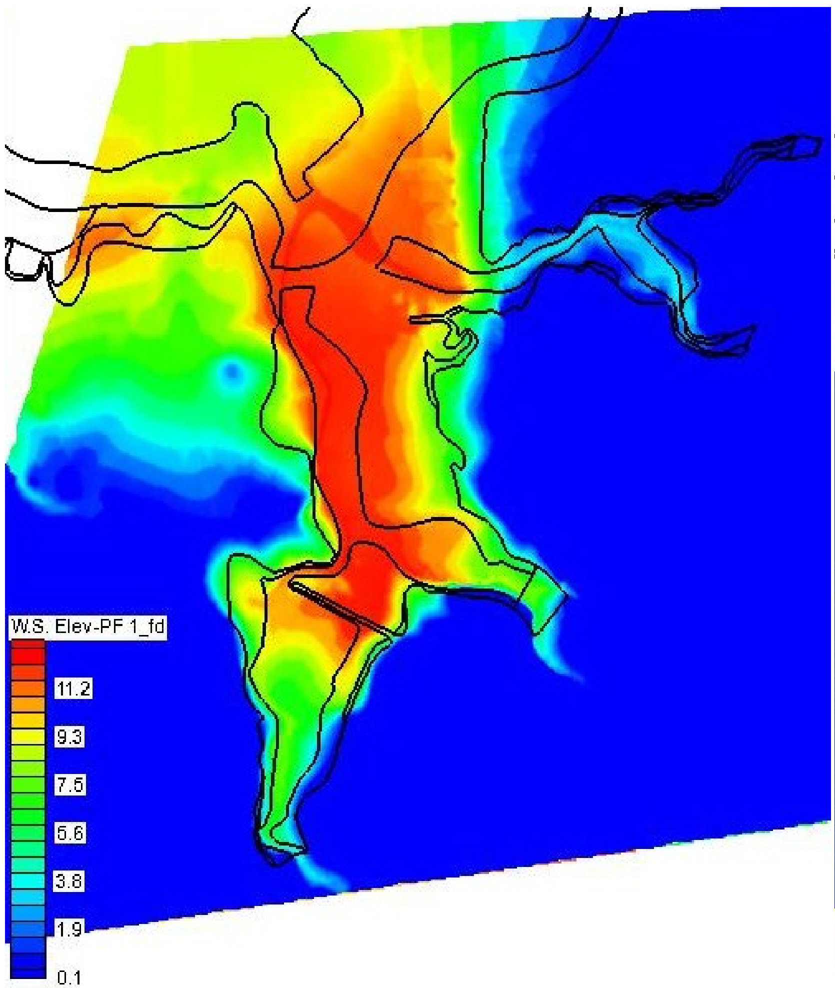

Figure 3.53 FEMA zones & flood depths from 25% of initial peak flow with no flood basins

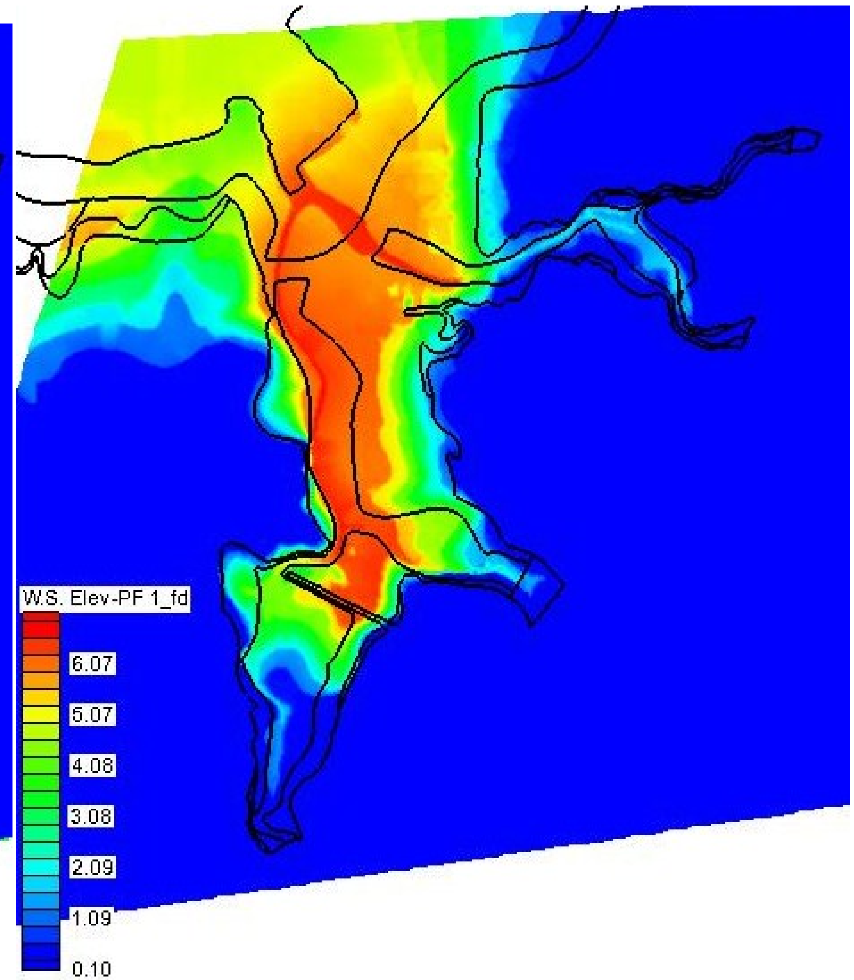

Figure 3.54 FEMA zones & flood depths from 10% of initial peak flow with no flood basins

3.5 WELL RESULTS

Figure 3.55 displays color-filled contour line results from the WELL model and shows the layout of the injection wells in an aerial view. The time for simulation is 2.4 days. The maximum rise of the water table is around the well locations at about 7 ft. The level decreases farther from the wells with an area affected of 3000x3000 ft. The increase in water table elevation is a welcome addition to aquifer storage that helps sustain the area's water resources.

Figure 3.56 displays a graph of the monitoring results, which shows a time series over 2.4 days for the three chosen observation wells, which measures the increase in the hydraulic head. We are assuming that the data produced from the WELL model are not site specific and can be at any of the four hypothetical flood basins.

The first observation well, labeled as curve *1* in graph, located at the coordinates (1100 ft, 1500 ft) in the injection and observation well layout (see **Figures 2.28** and **3.55**) exhibits the water table level with a maximum hydraulic head at roughly 5.5 ft. The second observation well (curve *2* of the graph), located at coordinates (1300 ft, 1500 ft), shows the second largest increase in the water table height at approximately 6.5ft. Results from the third well at (1500 ft, 1500 ft), with values close to the results of the second observation well produced the largest rise of the table, with a maximum value of about 6.7 ft.

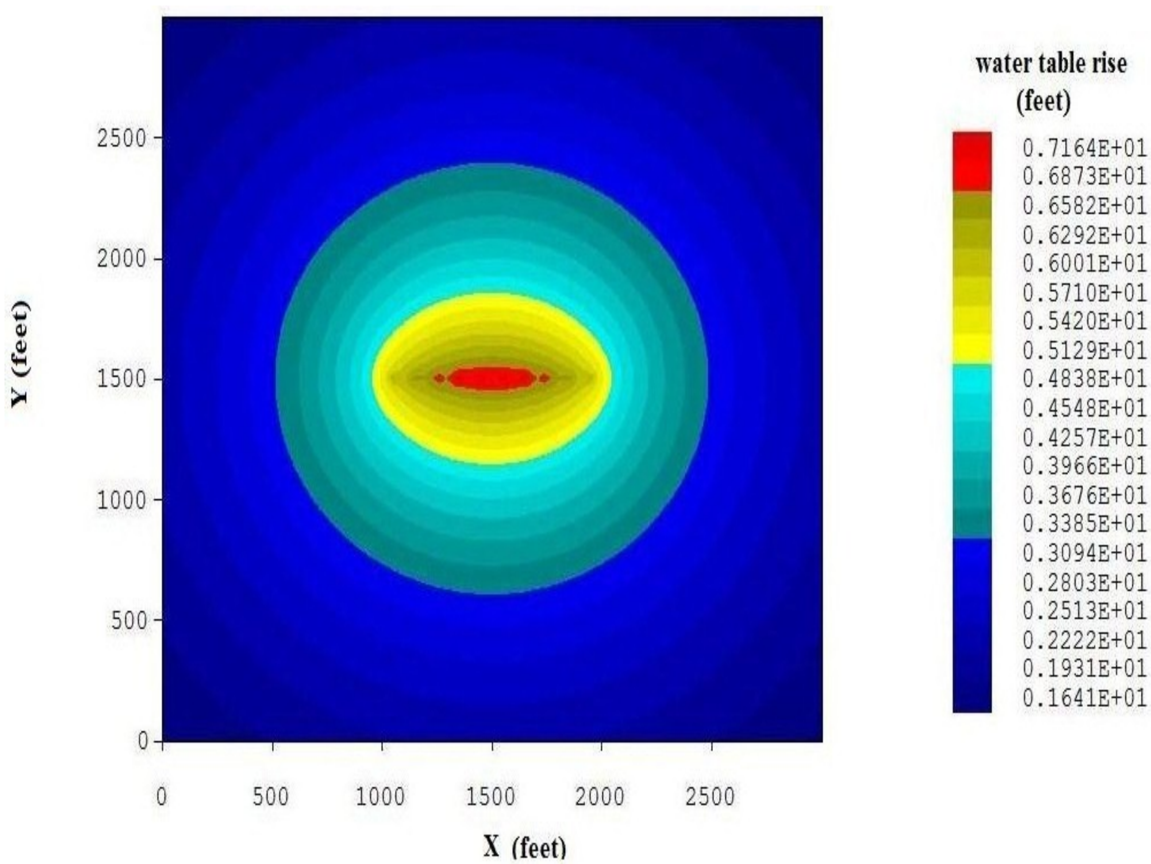

Figure 3.55 Contour lines depicting water table levels

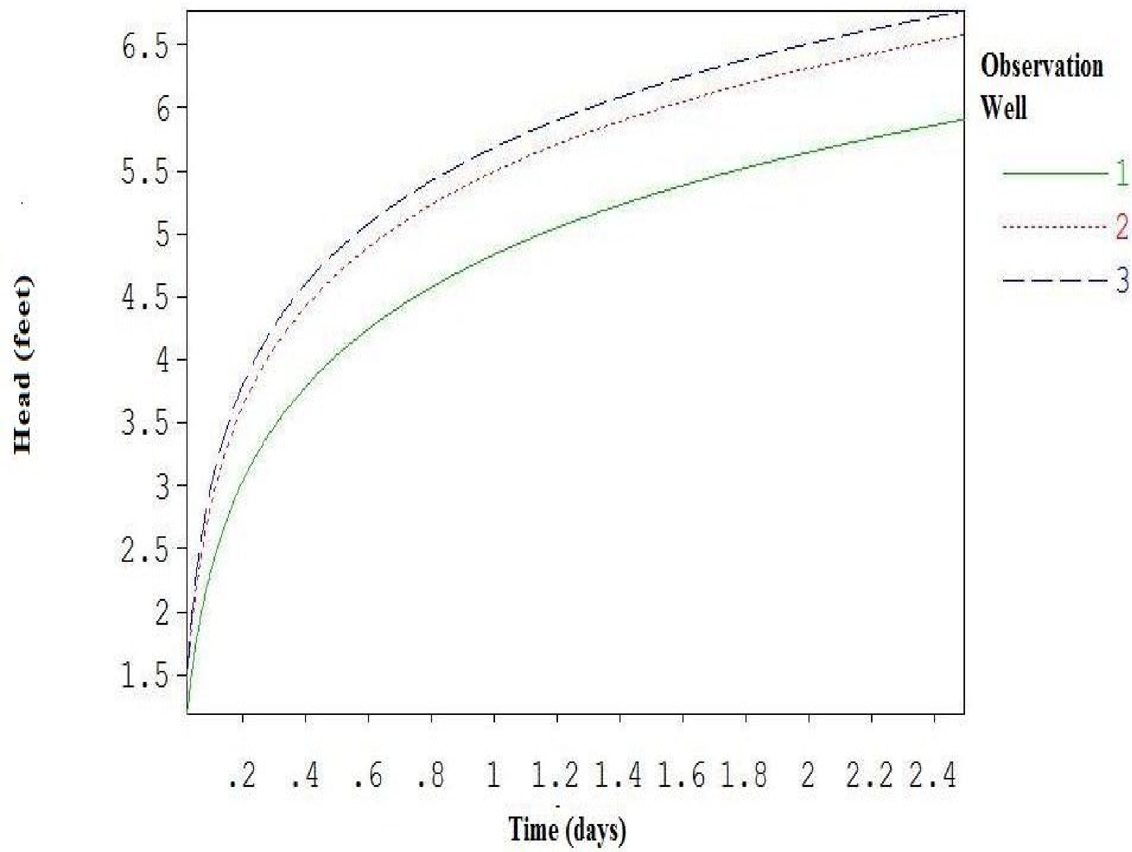

Figure 3.56 Monitoring well results showing the increase in the hydraulic head

4 DISCUSSION

4.1 HEC-1 CALIBRATION

The HEC-1 model calibration was conducted in order to evaluate the model's ability to simulate discharge values. Calibration accuracy was analyzed based on the percent coefficient of variation produced from the root mean square errors reflecting the difference between the simulated and observed hydrographs and scatter plots. Large errors occurred in some cases as evident by the excessive values of the coefficient of variation. The model generally underestimated discharge in the early stages of the storms.

The main cause of the discrepancies was associated with the rainfall distribution curve. Data used to create the first set of distribution curves were acquired from one rain gage station. In this regard, and due to the lack of information, an assumption was made that the data provided from this single rain gage was consistent throughout the entire watershed. If additional precipitation monitoring stations were available within the watershed, the calibration results would have been more accurate. In addition, accuracy of results depends on reliability of values relevant to land use and cover as well as assumptions included in the simulation model. Data imported into the model, such as the land use and soil coverage shapefiles and the estimated SCS curve numbers, were not accurate and detailed enough. Studies have shown that model applications in Hawai‘i are tenuous due to the nature of watersheds regarding mostly to their steep slopes and soil types. Furthermore, the DEM was not in high resolution. Overall, the results of calibration are acceptable as an initial step towards flood management for the study area.

An alternative rainfall distribution was adopted in the study. The assumption was made that such distributions could be derived from the streamflow for each precipitation date. The correlation between the rainstorm and streamflow distributions is justified given that the areas of sub-basins are small with steep terrains. Many of the simulated result sets produced from the alternative rainfall distributions showed improved results compared to the results from the first calibration. For these alternative distributions, the reduction in error was mainly due to the fact that the distributions were more accurate.

4.2 FLOOD RETENTION BASINS & FLOODPLAIN DELINEATIONS

The HEC-RAS model produced results based on hydrographs generated from the flood retention basins in HEC-1. Both cases with and without flood basins were simulated. The simulated hydrographs reflected the application of the flood basins, which resulted in reduced peak flows. However, HEC-RAS seemed to significantly overestimate flood depths in the floodplain region, compared to FEMA's zones. The likely causes can be related to (1) an overestimation of watershed-wide precipitation used as an input to HEC-1 (2) the use of the peak value for streamflow hydrographs as required by HEC-RAS, and (3) errors in HEC-1 calibration. Comparing the delineated flood zone area with FEMA showed that discharges to HEC-RAS should be about one third of our estimate. Another approach would be to use the 100-year flood values instead, which was implemented by using the USGS's StreamStats. However, such values were even higher than HEC-1's at some stream locations. There is a need thus to carefully evaluate the three alternative approaches for better flood zone assessment.

4.3 INJECTION & OBSERVATION WELLS

The model yielded results depicting levels of the water table in the groundwater aquifer as an outcome of harvest-water injection into wells. However, a simplified approach was utilized and the calculations and the results are introduced as demonstration only. A more accurate and site specific model should be utilized for actual design and implementation of the water harvesting technology.

5 SUMMARY & CONCLUSIONS

The objective of this project was to assess the feasibility of using water harvesting to control flooding and conserve water in the Kaiaka Bay Watershed (KBW), which is highly susceptible to flooding. This approach would reduce the risk of flooding and the damages it causes, conserve water, and eventually be utilized in different areas. The software programs WMS and WELL can be a useful resource for flood and well modeling within the watersheds of Hawaiʻi. Modeling provides the tools for predicting future events and setting the appropriate management plans.

Different stages of the project included model calibration, floodplain delineation and assessment, and injection system implementation. While simulated values for the calibration of HEC-1 as well as the flood depths within the final floodplain of KBW diverged from the expected results, the calculations did show that the application of the flood retention basins were efficient in reducing flooding. Accuracy of predictions are sensitive to values of the average precipitation and rainfall distribution and more effort should be utilized in their measurements.

The models HEC-1 and HEC-RAS can be combined to assess current streamflows, predict future values and flooding level, and assist in managing flooding. Accuracy of the models would be enhanced as more data becomes available. The exploratory results from the model WELL demonstrated that the implementation of injection wells would highly support groundwater sustainability within KBW. This project provides an initial assessment for water harvesting for the KBW, and it seems with additional data collection, that the technology can be utilized in this and other areas. Potential problems are mainly related to the availability of land for basin construction, the high cost involved, and the need to meet regulations regarding water injection as well as dam and reservoir operation.

5.1 RECOMMENDATIONS

Additional research is needed for full calibration and validation of the model HEC-1. Furthermore, supplementary data for all models should be obtained in order to minimize the calibration errors. More efforts should be utilized in measuring precipitation data, considering that accuracy of the results is very sensitive to such data. There is a need to evaluate various approaches to estimate the 100-year flood levels in order to accurately predict the extent of the flood zone and the respective flood-water levels. Although many hurdles exist towards implementing a water harvest system in Hawai‘i, it is highly recommended to start a serious effort in this regard. In the long run, the benefits will certainly outweigh the cost.

APPENDIX A: WMS PARAMETERS

Table A-1 Soil Conservation Service Curve Number Table

	Curve Numbers for Hydrologic Soil Group				
ID	A	B	C	D	Land Use Description
11	94	96	98	100	Residential
12	94	96	98	100	Commercial and Service
14	94	96	98	100	Transportation, Communication
17	94	96	98	100	Other Urban
31	58	64	72	77	Herbaceous rangeland
32	52	59	67	74	Shrub and Brush rangeland
33	52	59	67	74	Mixed rangeland
41	61	65	72	78	Deciduous Forest Land
42	63	68	74	79	Evergreen Forest Land
43	63	67	71	74	Mixed Forest Land
75	80	81	85	90	Strip Mines, Quarries, and Gravel Pits

ID: Polygon ID
Hydrologic Soil Group:
Group A Soils have low potential runoff and high infiltration rates. They are mainly made up of drained sand or gravel and have high rates of water transmission.

Group B Soils have average infiltration rates when they are completely wet and consist mainly of soils that are deep and drained on an moderate to extreme scale. These soil textures can be fine to moderately coarse. Their rate of water transmission is average.

Group C soils have low infiltration rates when they are completely wet and are made up soils with a layer that obstructs the downward movement of water and soils that have a moderately fine to fine texture. The rate of water transmission for these soils is low.

Group D soils have high runoff potential. Their infiltration rates are very low when they're completely wet and are mainly made up of 3 types of soils: clay soils with high swelling potential, soils with a permanent high water table, soils with a claypan or clay layer that's at or close to the surface, and shallow soils over material that is almost impervious. The transmission rate of these soils is very low (United States Department of Agriculture, 1986).

Table A-2 Basin Data & Loss Method Parameters

Basin Name	**Basin Data**	**Loss Method**
	Basin Area (mi^2)	**Curve Number**
North Fork Kaukonahua Stream above Right Branch, near Wahiawa	1.375	68
Opaeula Stream near Wahiawa	3.014	68

APPENDIX B: HEC-RAS PARAMETERS

Table B-1 Boundary Condition Location & Types

Reach Number	**Upstream**	**Downstream**
reach_8	Normal Depth slope = 0.025	Junction = 304678
reach_6	Normal Depth slope = 0.025	Junction = 306478
reach_2	Normal Depth slope = 0.025	Junction = 306475
reach_7	Junction = 306478	Junction = 306475
reach_4	Normal Depth slope = 0.025	Junction = 306472
reach_3	Junction = 306472	Normal Depth slope = 0.025
reach_5	Junction = 304675	Normal Depth slope = 0.025
reach_1	Normal Depth slope = 0.025	Junction = 304672

Table B-2 Definition of color-filled FEMA flood zones

Zone	Definition
A	Zone A is the flood insurance rate zone that corresponds to the 100-year floodplains that are determined in the FIS by approximate methods. Because detailed hydraulic analyses are not performed for such areas, no base flood elevations or depths are shown within this zone.
AE	Zone AE is the flood insurance rate zone that corresponds to the 100-year floodplains that are determined in the FIS by detailed methods. In most instances, whole-foot base flood elevations derived from the detailed hydraulic analyses are shown at selected intervals within this zone.
AH	Zone AH is the flood insurance rate zone that corresponds to the areas of 100-year shallow flooding (usually areas of ponding) where average depths are between 1 and 3 feet. Whole-foot base flood elevations derived from the detailed hydraulic analyses are shown at selected intervals within this zone.
AO	Zone AO is the flood insurance rate zone that corresponds to the areas of 100-year shallow flooding (usually sheet flow on sloping terrain) where average depths are between 1 and 3 feet. Average whole-depths derived from the detailed hydraulic analyses are shown within this zone.
A99	Zone A99 is the flood insurance rate zone that corresponds to areas of the 100-year floodplain that will be protected by a Federal flood protection system where construction has reached specified statutory milestones. No base flood elevations or depths are shown within this zone.
V	Zone V is the flood insurance rate zone that corresponds to areas of the 100-year floodplain that will be protected by a Federal flood protection system where construction has reached specified statutory milestones. No base flood elevations or depths are shown within this zone.
VE	Zone VE is the flood insurance rate zone that corresponds to the 100-year coastal floodplains that have additional hazards associated with storm waves. Whole-foot base flood elevations derived from the detailed hydraulic analyses are shown at selected intervals within this zone.
X	Zone X is the flood insurance rate zone that corresponds to areas outside the 500-year floodplain, areas within the 500-year floodplain, and to areas of 100-year flooding where average depths are less than 1 foot, areas of 100-year flooding where the contributing drainage area is less than 1 square mile, and areas protected from the 100-year flood by levees. No based flood elevations or depths are shown within this zone.
X500	0.2% annual chance flood hazard (500 Year Floodplain).
D	Zone D is the flood insurance rate zone that corresponds to unstudied areas where flood hazards are undetermined, but possible.

APPENDIX C: INJECTION & OBSERVATION WELL PARAMETERS

Table C-1 Well information & Parameters

General Parameters		**Well Information**			
Transmissivity	**0.1000E+06**	**Well Number**	**X coordinate (ft)**	**Y coordinate (ft)**	**Well flux rate**
Storativity	0.50000E-1	1	1050.0	1500.0	0.15000E+06
Initial Head	0.0000	2	1150.0	1500.0	0.15000E+06
Minimum X	0.0000 ft	3	1250.0	1500.0	0.15000E+06
Maximum X	3000.0 ft	4	1350.0	1500.0	0.15000E+06
Minimum Y	0.0000 ft	5	1450.0	1500.0	0.15000E+06
Maximum Y	3000.0 ft	6	1550.0	1500.0	0.15000E+06
Time	2.5000 days	7	1650.0	1500.0	0.15000E+06
Number of Contour Lines	20	8	1750.0	1500.0	0.15000E+06
		9	1850.0	1500.0	0.15000E+06
		10	1950.0	1500.0	0.15000E+06
		Observation Points			
		1	1100.0	1500.0	
		2	1300.0	1500.0	
		3	1500.0	1500.0	

.

WORKS CITED

Aquaveo, LLC. 2012. HEC-RAS. http://www.aquaveo.com/hec_ras. Accessed January 24, 2013.

Bennington, Bret. Hydrology Storativity and Transmissivity. http://people.hofstra.edu/j_bennington?.../Storativity_Transmissivity. Accessed February 2, 2013.

Blumenstock, D.I., & P. Saul. 1967. Climates of the States, Hawaii. U.S. Dept. of Commerce, Environmental Science Services Administration, Washington D.C.

Brigham Young University – Environmental Research Laboratory. 2006. Waterhsed Modeling System: WMS v8.0 Tutorials – Vol. 3 Floodplain Modeling.

Brunner, G.W. 2010. River Analysis System Hydraulic Reference Manual (CPD-69). U.S. Army Corps of Engineers, Hydrologic Engineering Center.

Choi, H.M., & J.Y. Lee. 2012. Changes of groundwater conditions on Jeju volcanic island, Korea: implications for sustainable agriculture. Department of Geology, Kangwon National University. African Journal of Agricultural Research. Vol. 7, No. 4: 647-661.

Chu, P.S., Y.R. Chen, & T.A. Schroeder. 2010. Changes in Precipitation Extremes in a Warming Climate. University of Hawai‘i at Manoa. American Meteorological Society. Vol. 23, No. 18: 4881-4900.

Climate Adaptation Knowledge Exchange. 2013. Nonpoint-Source Pollution and Erosion Comparison Tool (N-SPECT). NOAA Coastal Services Center, South Carolina.

Council for Regulatory Environmental Modeling. 2009. Soil and Water Assessment Tool 2000. U.S. Environmental Protection Agency. http://cfpub.dpa.gov/crem/knowledge_base/crem_report.cfm. Accessed April 1, 2013.

Curtis, L.M., M.M. Nelson, & P.L. Oakes. 2001. Estimating Costs of Off-Stream Irrigation Storage Reservoirs. Bulletin 647. Alabama Agricultural Experiment Station. Auburn University.

DeVito, P.A., G.L. Dugan, E.T. Murabayashi, & H.K. Gee.1995. Report Documentation Form. Water Resources Research Center. University of Hawai‘i at Manoa.

Evans, B.M., D.W. Lehning, K.J. Corradini, G.W. Petersen, E. Nizeyimana, J.M. Hamlett, P.D. Robillard, & R.L. Day. 2002. A Comprehensive GIS-Based Modeling Approach for Predicting Nutrient Loads in Watersheds. J. Spatial Hydrology, Vol. 2, No. 2. www.spatialhydrology.com.

Federal Emergency Management Agency (FEMA). 2005. Digital Flood Insurance Rate Map. Scanned and compiled by FEMA from 1:24,000. Digital Flood Insurance Rate Maps (DFIRMs).

Giambelluca, T.W., M.A. Nullet, & T.A. Schroeder. 1986. Rainfall Atlas of Hawaii. Report R76, Department of Land and Natural Resources, Division of Water and Land Development, State of Hawaiʻi (prepared by Water Resources Research Center, University of Hawaiʻi at Manoa).

Haith, D.A. & L.L. Shoemaker. 1987. Generalized Watershed Loading Functions for Stream Flow Nutrients. Water Resources Bulletin, Vol. 23, No. 3: 471-478.

Hawaiʻi Department of Business and Economic Development. 2000. Statistics and Data. State of Hawaiʻi.

Kim, Y., M. Koo, K. Lee, K. Ko, & J.M. Barry. 2008. Application of analysis and modeling for surface water-groundwater system: preliminary study of artificial recharge in Jeju Island, Korea. AGU Fall Meeting, #H31C-0880.

Lee, J.Y., G.S. Lee, & S.H. Song. 2007a. An interpretation of changes in groundwater level and electrical conductivity in monitoring wells in Jeju Island. J. Korean Earth Science Society. Vol. 28: 925-935.

Mike by DHI. 2011. Urban, Coastal, and Riverine Flooding. http://www.dhisoftware .com. Accessed April 1, 2013.

Muirhead, W. 2008. An appraisal of stormwater reclamation and reuse in Hawaii. Proceeding of the Water Environment Federation, Water Environment Federation. 626-649.

Murphy, M.J. & S. Businger. 2011. Orographic Influences on an Oahu Flood. University of Hawaiʻi at Manoa. American Meteorological Society. Vol. 139, No. 7: 2198-2217.

Powell, W.G. 2009. Identifying Land Use/Land Cover (LULC) Using National Agriculture Imagery Program (NAIP) Data as a Hydrologic Model Input for Local Flood Plain Management. MS Thesis. Texas State University.

Richter, B.D., R. Matthews, D.L. Harrison, & R. Winginton. 2003. Ecologically Sustainable Water Management: Managing River Flows for Ecological Integrity. Ecological Society of America. Ecological Applications. Vol. 13, No. 1: 206-224.

Scientific Software Group. 1998. WMS 7. http://www.scisoftware.com/products/wms_ overview/wms_overview.html. Accessed February 3, 2013.

Theis, C.V. 1935. The relation between the lowering of the piezometric surface and the rate and duration of discharge of a well using ground-water storage. Transactions. American Geophysical Union. Vol.16: 519–524.

U.S. Geological Survey (USGS). 2005. USGS seamless data distribution system. http://www.ctahr.hawaii.edu/faresa/workshop/Kaiaka-Waialua%20Field%20Daay/site descript.htm. Accessed January 2, 2013.

U.S. Geological Survey (USGS). 2012. Hawai‘i Precipitation Table: 15-minute precipitation data. http://waterdata.usgs.gov/hi/nwis/current/?type-precip&group_key=NONE. Accessed January 2, 2012.

U.S. Geological Survey (USGS). 2012. Hawai‘i Streamflow Table: 15-minute streamflow data. http://waterdata.usgs.gov/hi/nwis/current/?type=flow&group_key=NONE. Accessed February 3, 2012.

U.S. Geological Survey (USGS). 2013. StreamStats in Hawaii. http://water.usgs.gov/osw/streamstats/hawaii.html. Accessed April 24, 2013.

United States Department of Agriculture. 1986. Urban hydrology for small watersheds. Technical Release 55 (TR-55) (Second Edition ed.). Natural Resources Conservation Service, Conservation Engineering Division.

Weatherford, 2013. WellFlo Well Modeling and Design. http://www.weatherford.com/Products/Production/ProductionOptimization/Software/WellFloSoftware/index.htm. Accessed April 1, 2013.

Yost, R., A. El-Kadi, J. Yanagida, G. Bruland, P. Mills-Packo, C. Unser,… C. Walsh. 2009. Demonstrating Watershed Participatory Assessment and Action, Kaiaka Bay Watershed, Oahu, Hawaii. Departments of Tropical Plant and Soil Science, Geology and Geophysics, Natural Resource and Environmental Management and Resource Systems Management, LLC. University of Hawaii.